

NEAR FIELD AND FAR FIELD SOUND RADIATION FROM Do 31 V/STOL JET
TRANSPORT AND POSSIBILITIES FOR NOISE ABATEMENT IN
FUTURE V/STOL DEVELOPMENT

P. Bartels

NASA-TT-F-15534) NEAR FIELD AND FAR
FIELD SOUND RADIATION FROM Do 31 V/STOL
JET TRANSPORT AND POSSIBILITIES FOR NOISE
ABATEMENT IN FUTURE V/STOL (Kanner (Leo)
Associates) 126 p HC \$9.50

N74-21650

Unclas
37237

CSCL 01C G3/02

136

Translation of "Schallabstrahlung im Nah- und Fernfeld des VSTOL
Strahltransporters Do 31 und Lärminderungsmöglichkeiten bei
zukünftigen VSTOL-Entwicklungen," Dornier-Werke G.m.b.H.,
Friedrichshafen (W. Ger.), BMVg-FBWT-72-23, 1972, 167 pages



1. Report No. NASA TT F-15,534		2. Government Accession No.		3. Recipient's Catalog No.	
4. Title and Subtitle NEAR FIELD AND FAR FIELD SOUND RADIATION FROM Do 31 V/STOL JET TRANSPORT AND POSSIBILITIES FOR NOISE ABATEMENT IN FUTURE V/STOL DEVELOPMENT				5. Report Date April 1974	
				6. Performing Organization Code	
7. Author(s) Peter Bartels, Bonn Bundeswehramt				8. Performing Organization Report No.	
				10. Work Unit No.	
9. Performing Organization Name and Address Leo Kanner Associates Redwood City, California 94063				11. Contract or Grant No. NASW-2481	
				13. Type of Report and Period Covered Translation	
12. Sponsoring Agency Name and Address National Aeronautics and Space Adminis- tration, Washington, D.C. 20546				14. Sponsoring Agency Code	
15. Supplementary Notes Translation of "Schallabstrahlung im Nah- und Fernfeld des VSTOL Strahltransporters Do 31 und Lärm-minderungs-möglich- keiten bei zukünftigen VSTOL-Entwicklungen," Dornier-Werke G.m.b.H., Friedrichshafen (W. Ger.), BMVg-FBWT-72-23, 1972, 167 pages					
16. Abstract Theoretical and experimental near and far field noise studies on the Do 31 V/STOL jet transport aircraft are pre- sented in updated form. Particular significance is also attached to the reduction in noise which the Do 31 has al- ready made possible at existant airports and the problems of noise and noise abatement associated with present and future V/STOL designs. The V/STOL aircraft's flexibility in the selection of flight procedures allows it to adapt well to local conditions. This is important not only militarily but also in terms of optimum economy and noise abatement.					
17. Key Words (Selected by Author(s))			18. Distribution Statement Unclassified-Unlimited		
19. Security Classif. (of this report) Unclassified	20. Security Classif. (of this page) Unclassified	21. No. of Pages 1361	22. Price 9.50		

Table of Contents

	<u>Page</u>
Index of Tables and Figures	v
Notation	x
I. Significance and Effects of the Radiation of Sound from V/STOL Aircraft	1
1. General	1
1.1. Acoustic Near Field	1
1.2. Acoustic Far Field	2
2. Acoustic Studies in the Do 31 Program	2
2.1. Studies in the Near Field	3
2.2. Studies in the Far Field	4
3. Sound Radiation Associated with Future V/STOL Aircraft	6
3.1. Future V/STOL Transport Aircraft/Airliners	6
3.2. Future V/STOL Combat Aircraft	8
II. Sound Radiated by the Do 31 in the Near and Far Fields and Possibilities for Noise Abatement in Future Development	8
Introduction	8
1. Sources of Sound in the Do 31	8
1.1. Sound Components from the Jet Power Plants	9
1.2. Power Plant Parameters Which Affect Sound Radiation	10
1.3. Sound Level Data from the Power Plant Manufacturer	10
1.4. Possibilities for Reducing Sound Radiation	11
2. Sound Level in the Near Field	12
2.1. Theoretical Studies	13

	<u>Page</u>
2.1.1. Method for Calculating Sound Level Contours	13
2.1.1.1. Relationship Between the Reference Sound Field and the Sound Field Which Is To Be Determined	13
2.1.2. Sound Levels in the Airframe	17
2.2. Experimental Studies	18
2.2.1. Preliminary Studies on the Sound Levels To Be Expected	18
2.2.2. Sound Transmission Measurements	19
2.2.3. Cabin Noise Level	19
2.2.4. Noise Levels at the Airframe	20
3. Sound Levels in the Far Field	21
3.1. Theoretical Studies	21
3.1.1. Do 31 Noise Level at a Fixed Distance as a Function of Direction	21
3.1.2. Maximum Levels Along a Line Parallel to the Projected Flight Path of the Do 31	22
3.1.3. Ground Noise Level Contours	23
3.1.3.1. Do 31	23
3.1.3.2. Do 31 As Compared with Conventional Aircraft	24
3.1.3.3. Reduced-Noise Version of the Do 31	24
3.1.4. Maximum Noise Levels as a Function of Power Plant Thrust Components	25
3.1.5. Noise Radiation by Future V/STOL Aircraft	26
3.2. Experimental Studies	26
3.2.1. Peripheral Measurements Performed on the Do 31 E1 and E3	27
3.2.2. Noise Level Measurements During Do 31 E3 Takeoff and Landing Transitions	28

	<u>Page</u>
Tables and Figures	30
References	122

Tables

- 1.2-1. Do 31 E3 power plant data
- 2.1.2-1. Comparison of measured and calculated values of total sound level in airframe of Do 31 E3 (VTO, H = 0 m)
- 2.2.3-1. Do 31 E3 cabin noise levels
- 2.2.4-1. Do 31 E3 sound levels in airframe (overview)
- 2.2.4-2. Do 31 E3 sound levels in airframe. Phase of flight: vertical climb (H = 21 - 23 m)
- 2.2.4-3. Do 31 E3 sound levels in airframe. Phase of flight: cruising II

Figures

- 1. Do 31 E3
- 1.1-1. Sound components from jet power plants
- 1.1-2. Noise components from power plants with different bypass ratios [2].
- 1.2-1. Thrust as a function of rpm (BS Pg 5-2)
- 1.2-2. Hot and cold gas velocities as a function of rpm (BS Pg 5-2)
- 1.2-3. Static nozzle outlet temperature as a function of rpm (BS Pg 5-2)
- 1.2-4. Mass flow as a function of rpm (BS Pg 5-2)
- 1.2-5. Power plant thrust as a function of rpm (RB 162-4D)
- 1.2-6. Jet discharge velocity as a function of rpm (RB 162-4D)
- 1.2-7. Static jet discharge temperature as a function of rpm (RB 162-4D)
- 1.2-8. Mass flow as a function of rpm (RB 162-4D)
- 1.3-1. BS Pg 5-2 peripheral noise level
- 1.3-2. BS Pg 5-2 overall sound level as a function of rpm
- 1.3-3. 1/3-octave spectra for the BS Pg 5-2 at radius of 30.5 m

- 1.3-4. BS Pg 5-2 sound components from hot and cold jets as a function of rpm
- 1.3-5. BS Pg 5-2 jet and machinery noise as function of thrust
- 1.3-6. BS Pg 3 overall near field sound level (cold nozzles)
- 1.4-1. Ejector thrust pod
- 2.1.1-1. AVON reference sound "carpet"
- 2.1.1-2. AVON velocity exponent reference "carpet"
- 2.1.2-1. Increase in noise level due to airframe reflection
- 2.1.2-2. Overall sound-level contours in the airframe of the Do 31 E3 during vertical takeoff (calculated at $H = 0$ m, jet noise with ground reflection only)
- 2.2.1-1. Sound level in a fuselage segment as a function of power plant rpm
- 2.2.1-2. Frequency spectra at microphone position 4
- 2.2.1-3. Arrangement of measurement points
- 2.2.1-4. 1/3-octave spectra of jet noise for various nozzle openings (measurement point 3; $p = 11.1$ technical atmospheres absolute)
- 2.2.1-5. Overall sound level as a function of distance (nozzle opening 100%)
- 2.2.1-6. 1/3-octave spectra of jet noise at different distances from the nozzle opening ($p = 11.1$ technical atmospheres absolute; nozzle opening 100%).
- 2.2.1-7. Sound level of thrust power plants
- 2.2.2-1. Block diagram of measurement instruments
- 2.2.2-2. Do 31 E3 acoustic damping (lining I and II)
- 2.2.3-1. Do 31 E3 microphone positions on airframe
- 2.2.4-1. Microphone installation and measurement setup
- 2.2.4-2. Measured frequency spectrum in Do 31 E3 airframe. Phase of flight: vertical climb ($H = 21 - 23$ m)
- 2.2.4-3. Measured frequency spectrum in Do 31 E3 airframe. Phase of flight: cruising II

- 2.2.4-4. Do 31 E3 flight and power plant parameters (time curves), BS Pg 5-2
- 2.2.4-5. Do 31 E3 flight and power plant parameters (time curves) RB 162-4D. Trial No. 60, Sheet II
- 2.2.4-6. Do 30 E3 flight and power plant parameters (time curves). Trial No. 60, Sheet III
- 2.2.4-7. Do 31 E3 flight and power plant parameters (time curves) BS Pg 5-2. Trial No. 58, Sheet I
- 2.2.4-8. Do 31 E3 flight and power plant parameters (time curves). RB 162-4D. Trial No. 58, Sheet II
- 2.2.4-9. Do 31 E3 flight and power plant parameters (time curves). Trial No. 58, Sheet III
- 3.1.1-1. Do 31 E3 vertical takeoff ($H = 0$). Overall peripheral levels at radius of 100 m.
- 3.1.1-2. Do 31 E3 vertical takeoff ($H = 0$ m). Peripheral octave spectra at 100 m ($0^\circ - 60^\circ$)
- 3.1.1-3. Do 31 E3 vertical takeoff ($H = 0$ m). Peripheral octave spectra at 100 m ($90^\circ - 180^\circ$)
- 3.1.1-4. Do 31 E3 peripheral sound level at 100 m. Hover at $H = 30$ m
- 3.1.2-1. Do 31 E3 takeoff transition
- 3.1.2-2. Do 31 E3 takeoff transition. Octave spectra
- 3.1.2-3. Do 31 E3 landing transition
- 3.1.2-4. Do 31 E3 landing transition. Octave spectra
- 3.1.3-1. Production of a ground level contour during takeoff transition
- 3.1.3.1-1. Do 31 E3 ground noise level distances for vertical takeoff.
- 3.1.3.1-2. Do 31 E3 ground level distances during takeoff transitions
- 3.1.3.1-3. Do 31 ground noise level contours during conventional takeoff
- 3.1.3.1-4. Do 31 E3 ground noise level contours during various takeoff transitions

- 3.1.3.1-5. 95 PNdB ground noise level contours for various Do 31 E3 takeoff procedures
- 3.1.3.2-1. Do 31 E3, Boeing 727 and Boeing 707 ground noise level contours for takeoff from Frankfurt/Main airport
- 3.1.3.2-2. Do 31 E3, Boeing 727 and Boeing 707 ground noise level contours for landing at the Frankfurt/Main airport
- 3.1.3.2-3. Do 31, Boeing 727 and Boeing 707 95 PNdB ground noise level contours during takeoff from Paris/Orly airport
- 3.1.3.3-1. Do 31 (reduced-noise version) ground noise level distances during vertical takeoff
- 3.1.3.3-2. Do 31 (reduced-noise version) ground noise level distances during takeoff transition
- 3.1.3.3-3. Do 31 (reduced-noise version) ground noise level contours during takeoff transition
- 3.1.3.3-4. Do 31 (reduced-noise version) ground noise level contours during various takeoff transitions
- 3.1.4-1. Maximum levels on a parallel line 150 m from runway
- 3.1.5-1. 95 PNdB noise level contours for one version of Do 31 and for the Do 231 during VTO, Berlin/Tempelhof airport
- 3.2.1-1. Plan of measurement points for Do 31 far field sound tests
- 3.2.1-2. Do 31 E1 maximum peripheral noise level [db] at radius of 100 m
- 3.2.1-3. Do 31 E1 maximum peripheral noise level [db (A)] at radius of 100 m
- 3.2.1-4. Measured Do 31 E1 frequency spectrum at radius of 100 m (measurement point 0°).
- 3.2.1-5. Measured Do 31 E1 frequency spectrum at radius of 100 m (measurement point 90°)
- 3.2.1-6. Measured Do 31 E1 frequency spectrum at radius of 100 m (measurement point 225°)
- 3.2.1-7. Measured Do 31 E1 frequency spectrum at radius of 100 m (measurement point 270°)

- 3.2.1-8. Do 31 E3 maximum peripheral noise level contours [dB] at radius of 100 m
- 3.2.1-9. Measured Do 31 E3 frequency spectrum at radius of 100 m (measurement point 0°).
- 3.2.1-10. Measured Do 31 E3 frequency spectrum at radius of 100 m (measurement point 90°)
- 3.2.1-11. Measured Do 31 E3 frequency spectrum at radius of 100 m (measurement point 210°)
- 3.2.1-12. Do 31 E3 maximum peripheral noise level (hovering)
- 3.2.1-13. Measured Do 31 E3 frequency spectrum at radius of 100 m (measurement point 0°), H = 30.5 m
- 3.2.1-14. Measured Do 31 E3 frequency spectrum at radius of 100 m (measurement point 90°), H = 30.5 m
- 3.2.1-15. Measured Do 31 E3 frequency spectrum at radius of 100 m (measurement point 210°), H = 30.5 m
- 3.2.2-1. Do 31 E3 noise level curves vs. time for a takeoff transition (trial 77) (microphone position 150 m to the side of takeoff point)
- 3.2.2-2. Do 31 E3 noise level curves vs. time for a landing transition (trial 77) (microphone position 150 m to the side of the takeoff point)
- 3.2.2-3. Do 31 E3 noise level curves vs. time for a takeoff transition (trial 77) (microphone position 460 m from takeoff point, under flight path)
- 3.2.2-4. Measured Do 31 E3 frequency spectrum at time of maximum noise level (takeoff transition, trial 77) (microphone position 460 m from takeoff point, under flight path; flyover altitude about 210 m).
- 3.2.2-5. Do 31 E3 noise level curves vs. time for a landing transition (trial 77) (microphone position 460 m from landing point, under flight path)
- 3.2.2-6. Measured Do 31 E3 frequency spectrum at time of maximum noise level (landing transition, trial 77) (microphone position 460 m from takeoff point, under flight path; flyover altitude about 180 m).

Notation

BS	--	Bristol Siddeley
c	[m/s]	Jet velocity
D	[m]	Nozzle diameter
F	[m ²]	Nozzle area
f	[Hz]	Frequency
H	[m]	Altitude
H _b	[m]	Elevation of ground above sea level
H.P.	--	High pressure
L.P.	--	Low pressure
HTW	--	Thrust power plant
\dot{m}	[kg/s]	Mass flow
MTW	--	Cruising power plant (old designation for the Pegasus lift-thrust power plant)
n	[rpm]	Engine speed
OASPL	[dB]	Overall sound level
p	[ata]	Pressure [technical atmospheres absolute]
Pg	--	Pegasus (pivoting nozzle power plant by Rolls Royce)
R	[m]	Radius
RF	[%]	Relative humidity
RR	--	Rolls Royce
S	[kp = kg force]	Thrust
SPL	[dB]	Sound level
T	[°K]	Jet temperature
TL	--	Turbine air jet

t	[s]	Time
v	[km/h;m/s]	Aircraft velocity
$x;y$	[m]	Coordinates
ZTL	--	Dual-jet turbine air jet
α	[°]	Nozzle setting
θ	[°]	Angle relative to jet axis
μ	--	Bypass ratio
σ	[°]	Tail nozzle setting

Subscripts

a	Outlet
b	Ground
F	Fan
i	Interior
max	Maximum
N	Rated value
O	Ambient condition
$stat$	Static
tot	Total

NEAR FIELD AND FAR FIELD SOUND RADIATION FROM Do 31 V/STOL JET
TRANSPORT AND POSSIBILITIES FOR NOISE ABATEMENT IN
FUTURE V/STOL DEVELOPMENT

Peter Bartels,
Bonn Bundeswehramt

I. SIGNIFICANCE AND EFFECTS OF THE RADIATION OF SOUND FROM V/STOL /13*
AIRCRAFT

1. General

In studies on the effects of the radiation of sound from aircraft, it is always necessary to distinguish between the acoustic near field and the acoustic far field. Acoustic loads on the airframe are the object of studies in the near field. Problems which occur must be solved by means of suitable design measures.

In the far field, the main concern is aircraft noise, i.e. noise pollution in the vicinity of aircraft and airfields.

1.1. Acoustic Near Field

In the case of vertical takeoff aircraft whose weight is borne only by the engine jets during the takeoff and landing phases, installed thrust is four or five times higher than in the case of comparable conventional aircraft. For similar engines, the radiated acoustic energy is also correspondingly higher. Thus, for V/STOL aircraft, the acoustic near field, i.e. the vicinity of the airframe, is of increased significance relative to conventional aircraft, particularly during the takeoff and landing phases. The following /14 are primarily involved:

-- acoustic strength problems, i.e. the service life of aircraft components subjected to acoustic loads, and

-- cabin noise, i.e. acoustic insulation of the airframe.

In addition, the reliability of certain components (electronics, control units, etc.) under acoustic and vibrational loads must be assured.

In order to be able to counteract the danger of acoustic fatigue and impermissibly high cabin noise by means of measures

* Numbers in the margin indicate pagination in the foreign text.

taken at the proper stage of design, it is necessary to determine the noise level to be expected in the airframe while still in the developmental stage.

1.2. Acoustic Far Field

The problem of aircraft noise (far field) is especially serious for future civilian V/STOL aircraft which are to be employed in the immediate vicinity of populated areas and which are thus subject to much more strict noise requirements than future conventional aircraft.

Behavior which is desirable in terms of the environment is also becoming more and more important with regard to the introduction of new military systems, however.

The most important prerequisite for low noise levels is limited radiation of noise by the engines.

/15

Noise level contours on the ground are a function not only of the radiation of noise by the installed engines, however, but also of the aircraft's flight path. The ground area exposed to a certain noise level can be varied through a suitable choice of approach and departure paths and adjusted to the particular conditions existing in the vicinity of airfields.

The prerequisite for this is that the aircraft be flexible enough in the selection of paths of approach and departure. This flexibility is provided, to a large extent, in the jet-propelled V/STOL design employing lift engines.

2. Acoustic Studies in the Do 31 Program

The suitability of the jet design for a military V/STOL transport aircraft was to be shown or demonstrated in practical terms as part of the Do 31 program.

As dictated by the state of the art in power plant development at that time, it was necessary to equip the Do 31 with single-stage lift power plants and lift-thrust power plants with a low bypass ratio. Other power plants were not available.

Due to their high jet velocities, these power plants are relatively noisy; the sound which they radiate is also highly directional.

Although the Do 31 is thus by no means representative of future V/STOL transport aircraft with regard to noise radiation and frequency composition, very valuable information could nevertheless be obtained for upcoming development.

/16

2.1. Studies in the Near Field

It has already been mentioned that the noise level to be expected in the airframe must be determined at an early point if it is to be possible to promptly counteract problems which arise.

A computer program developed at Dornier was used to calculate the levels to be expected in the airframe and plot them electronically in the form of isacoustic lines. Increases in the noise level due to ground reflection effects could be taken into consideration here and could be confirmed with measurements taken as part of a research contract.

In addition, various preliminary studies provided information regarding the order of magnitude of noise levels at particularly critical locations, regarding sound transmission conditions in shell components of the full-scale Do 31 with and without acoustic insulation, and regarding airframe-reflection components of sound.

Finally, noise levels were measured directly at the surface of the airframe and within the fuselage during various phases of flight in an extensive program of measurements.

During a vertical takeoff, airframe noise levels of more than /17 150 dB were sometimes measured here, as well as levels on the order of 130 dB within the fuselage of the uninsulated experimental aircraft. In a fully equipped, acoustically insulated airframe, such a noise level, for example, would produce internal levels on the order of 110 dB, which are quite comparable to maximum levels in the Boeing 720 during the takeoff phase. In cruising flight and as compared with more comfortable aircraft such as the Boeing 727, the internal level would actually be more than 10 dB higher with approximately the same acoustic insulation.

The external levels were compared for an example using re-worked computed results. In addition, the dependence of airframe reflection upon the rigidity of the skin fields, fan noise components from Rolls Royce measurement results and noise level increases caused by the jet deflection cascades of the pivoting nozzles on the lift-thrust power plants were taken into consideration in the computed results.

Agreement was extraordinarily good for this case, which to a large extent was affected by ground reflection. Deviations of more than 2 dB occurred only at a few locations.

Due to the typical directional characteristic of sound radiation associated with intact exhaust jets from single-jet power plants (lift power plants, on the Do 31), for which the maximum noise levels occur between 30° and 45° relative to the axis of the jet, the noise components of the highest intensity are reflected close to the ground. Their effect can, as indicated by

large-scale tests performed at Dornier, dominate up to heights which amount to more than 30 times the diameter of the jet (e.g. up to a height of more than 15 m for a jet nozzle diameter of 0.5 m).

In addition, these reflected noise components are particularly undesirable for a conventional skin/stringer mode of construction, since the maxima in their frequency composition coincide approximately with the natural frequencies of the skin, i.e. amplified vibrational excitation occurs.

/18

A considerable reduction in these unfavorable effects could be achieved, in the case of unmodified power plants and modes of construction, for example, by the use of low-reflection grates as takeoff and landing platforms.

Additional improvements described in the principal report which would also have favorable effects with regard to far field noise include mixing nozzles for dividing the power plant jet. A thrust loss could be avoided through an additional ejector action on suitably designed lift pods.

In the direction of maximum sound radiation, it is possible to achieve noise reductions of more than 10 dB by means of mixing nozzles; this can mean reductions of 6-12 dB in the airframe close to reflecting ground.

2.2. Studies in the Far Field

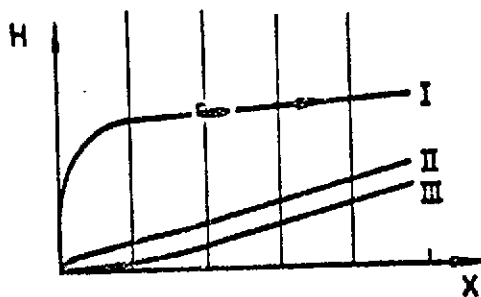
The far field level and the curves of noise level versus time for the Do 31 were determined on the basis of experience obtained in the use of the computer program for determining near field levels, making use of various auxiliary methods.

The good agreement between calculations and available measurement results confirmed the usability of the computational methods and permitted relatively realistic determinations of ground noise level contours (contours of equal noise level which enclose an area exposed to higher levels).

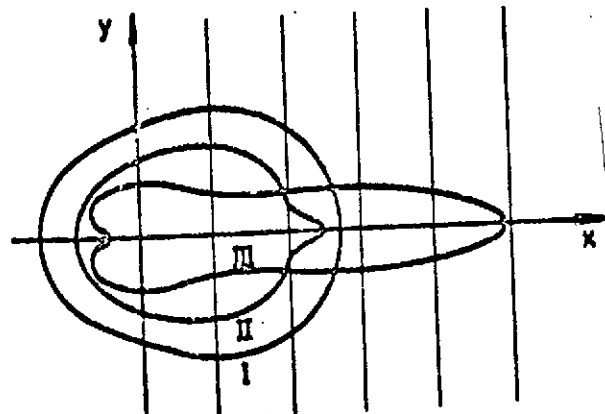
In addition to assumed flight paths which were basically feasible (e.g. vertical climb to a relatively high altitude), ground levels to be expected in takeoff and landing transitions actually flown were also calculated.

/19

A more comprehensive noise measurement program for confirming the computed results and studying jet interference and shielding effects could unfortunately not be carried out.



Flight paths



Ground noise level contours

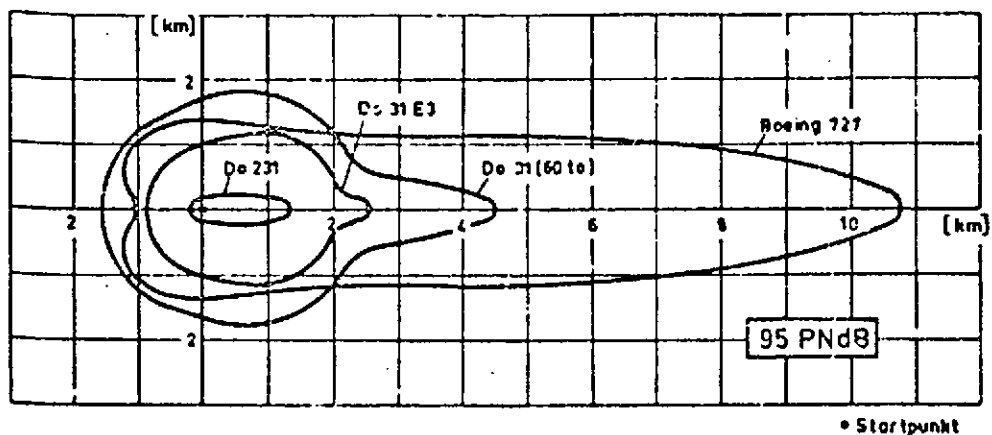
An almost optimum flight profile, in terms of noise, i.e. a flight procedure in which the smallest ground area is exposed to noise, was obtained for the Do 31 from the ground noise level calculations. The possibility cannot be ruled out here that, depending upon local conditions, another flight profile, e.g. one which yields a narrower yet longer ground noise level contour, would cause less noise pollution (e.g. over a river or over a railroad yard).

For the optimum flight procedure, in terms of noise, the ground /20 levels of the Do 31 models with relatively high takeoff weights and/or relatively large payloads were determined and compared with the ground noise level contours of conventional jet aircraft of comparable size now being used.

The results indicate impressively (fig., p. 6) the feasibility of a considerable reduction in the noise from present medium range air traffic at existant airports even with the obsolete generations of Do 31 power plants. The ground noise level contour which has been added to the figure for the Do 231 V/STOL jet clearly indicates the advances which could be achieved with future lift fan power plants and noise-reducing measures by the beginning of the 1980s.

The use of mixing nozzles on the lift power plants in conjunction with a design for the lift pod as an ejector was studied /21 as one possibility for reducing the noise level of the Do 31. Reference to these studies has already been made in Section 2.1 regarding the near field.

Reductions in noise of about 10 PNdB by these measures could be expected on the basis of earlier assumptions. This value was actually sometimes exceeded in large-scale tests -- to be sure,



Ground noise level contours

Key: • Takeoff point

only in the direction of the jet maximum for the unmixed jets, i.e. within a region between about 30 and 45° relative to the jet axis. Depending upon the observer's distance, increases relative to the noise levels of circular jets can even occur laterally with respect to the jet axis. For these reasons, and because of the continually more pronounced trend toward low-noise dual-stage power plants, the use of the ejector lift pod with single-stage lift power plants was not pursued further. Only a particularly prominent result from among those listed in the principal report will be covered.

A comparison of the maximum levels for the Do 31-E3 and the Do 31 version equipped with quieter lift power plants shows, as a function of the power plant thrust components, that carefully tuning the noise components from the lift power plants and the cruising power plants (lift-thrust power plants) operating with them during the VTOL phases is very important -- a significant result which can also be applied to future versions. In the case of the Do 31-E3, the dominant role of lift power plant noise, which determines overall noise over almost the entire thrust range, is clearly apparent. Overall noise from the quieter version, on the other hand, is relatively independent of the ratio of thrust components of both propulsion groups; this also facilitates the pilot's task.

3. Sound Radiation Associated with Future V/STOL Aircraft

/22

3.1. Future V/STOL Transport Aircraft/Airliners

The results of extensive work performed in the V/STOL transport sector during recent years show that the future V/STOL

transport aircraft/airliners will be equipped, like the successfully tested Do 31, with jet power plants.

For future V/STOL aircraft, it has become necessary that a noise level of 95 PNdB not be exceeded at a distance of 150 m. In England, for example, a level of 90 PNdB is required at a radius of 1500 ft or is specified as the maximum noise level with which the populus may be burdened.

This noise level is in some cases 30 EPNdB¹ or more below that of aircraft presently in use or about 20 EPNdB below the FAA requirements for conventional aircraft.

The strict noise requirements led to the installation of low-noise dual-stage lift power plants with a high bypass ratio, as planned for Dornier project Do 231. They have the following consequences:

- the power plant jets aimed at the ground possess only a small jet noise component;

- a reduction in laterally radiated fan and turbine noise components must be accomplished by means of noise-absorbing elements in the inlets and outlets of the power plants and by means of noise-absorbing designs for certain airframe components.

Due to the noise-reducing measures, conditions in the near field will be considerably more favorable than in the case of the Do 31. Particular attention is required only for noise-absorbing airframe components.

/23

In establishing final noise requirements for future V/STOL transport aircraft, it is necessary to consider that available traffic noise arteries, railroad yards at principal railroad stations or ports and waterways can be utilized for the aircraft's transition phases. A prerequisite for this is that the equipment be flexible enough in the selection of approach and departure paths and be able to maintain the most favorable flight path, in terms of noise, under all conditions, even with strong side winds, for example.

This requirement is satisfied in the case of an aircraft with jet propulsion such as the Do 31 and Do 231.

¹ EPNdB = Effective perceived noise level
= Unit of noise which takes the effect of individual tones and the curve of noise level versus time for the moving sound source upon human perception into consideration.

3.2. Future V/STOL Combat Aircraft

For V/STOL combat aircraft, performance requirements are more important than environmental aspects in the selection of power plants.

Accordingly, the near field problems described in Section 2.1 will also have to be considered.

This does not mean, however, that we should not attempt to achieve the lowest possible level of noise radiation in the installation of power plants.

II. SOUND RADIATED BY THE Do 31 IN THE NEAR AND FAR FIELDS AND POSSIBILITIES FOR NOISE ABATEMENT IN FUTURE DEVELOPMENT

/24

Introduction

To an increasing extent, the introduction of new means of transport and transportation is becoming dependent upon the burden on the environment which is thereby to be expected.

In addition to air pollution, the magnitude of noise radiation is of decisive importance, particularly for future civilian V/STOL aircraft to be flown directly out of and directly over inhabited municipal areas. But military aircraft will also be subject to environmental protection requirements in the future; a reduction in the noise pollution which affects those located near an airfield plays an important role here.

The aim of this report is to go beyond a comprehensive documentation of results from theoretical and experimental acoustic studies within the framework of Do 31 development and point out significant possibilities which are opened up by jet-supported V/STOL aircraft for reducing present and future aircraft noise problems.

1. Sources of Sound in the Do 31

/25

The power plants and other sources of noise of an aircraft are decisive factors in the generation of noise and possibilities for reducing it, as well as in the effects of sound radiation in the near and far fields.

The Do 31 E3 (Fig. 1-1), for which the testing of V/STOL engineering stood in the foreground during development, is equipped with a total of 10 power plants. On the right and left, next to the fuselage, on the underside of each wing: one Pegasus 5-2 (BS Pg 5-2) in-flight or cruising power plants by Rolls Royce-Bristol; at the end of each wing, in so-called lift pods: four RB 162-4D lift power plants by Rolls Royce.

The nozzles of the cruising power plants, two cold (front) and two hot (rear) nozzles, can be pivoted between 10° and 120° relative to the horizontal, with 10° representing the cruising position. During the V/STOL phases, for example, the entire thrust of the cruising power plants can be employed for the generation of lift.

The lift power plants are installed rigidly in the lift pods at an angle of 15° relative to the vertical, but are equipped with pivoting nozzles for control about the aircraft's vertical axis that can be moved $\pm 15^\circ$ relative to the longitudinal axis of the power plant.

In addition to these power plants, whose contribution to noise is described in 1.1 or in connection with the power plants and aircraft design, the following are some more sources of sound in the Do 31: the jet deflection cascades of the pivoting nozzles on the lift-thrust power plants, which increase the jet noise component by about 3 dB, and the tail control nozzle, which can be opened to a greater or lesser degree to control the aircraft about the transverse axis during V/STOL phases.

1.1. Sound Components from the Jet Power Plants

/26

The components of noise from the Do 31 E3 important in determining overall noise are jet sounds from the hot gas jets of the lift and cruising power plants which result from the turbulent mixing of the jets with the surrounding medium.

In the VTOL phases, the noise of the lift power plants prevails (Section 3.1.4), from which the gas jets exit at velocities between 500 and 550 m/s, as opposed to the cruising power plants, for which velocities of only about 300 m/s occur in the secondary stream (cold nozzles) or between 350 and 430 m/s in the primary stream (hot nozzles).

In the case of the BS Pg 5-2 cruising power plant (indicated at the top of Fig. 1.1-1), typical features of sound radiated by dual-stage power plants are already recognizable in spite of the bypass ratio of 1.4 (ratio of the mass throughputs of the cold secondary and hot primary streams), which is low compared to present power plant generations.

Favorable energy conversion is achieved through the withdrawal of energy from the hot gases to generate a cold secondary stream of low discharge velocity, and the high hot gas discharge velocities responsible for the jet noise are reduced. On the other hand, high-frequency noise contributions from the fan or secondary flow propeller are created which are operant on the inlet and outlet ends of the power plant and are heard above the jet noise. Compressor noise components are operant toward the front, moreover

(in the case of the Pegasus power plant, the "fan" is identical to the three-stage low pressure compressor, Fig. 1.1-1). In addition to the fan and jet noises, turbine noise is generated on the outlet end which can outweigh jet noise under partial load conditions (Fig. 1.1-2).

With a suitable reduction in fan noise, which is being achieved more and more in recent and future power plants and is being striven for to an increasing degree, the turbine component /27 can even determine overall noise.

Since turbine noise is based on the same mechanism of origin as fan or compressor noise, it can be combatted in a similar manner, although this is made difficult by the high temperatures and short duct lengths behind the turbine (Section 3.1.5).

1.2. Power Plant Parameters Which Affect Sound Radiation

The essential data required, among other things, for determining the jet noise components in Section 2.1 are compiled in Table 1.2-1 and Figs. 1.2-1 through 1.2-8 for the power plants in the Do 31 E3. They were obtained from power plant literature provided by Rolls Royce and could be largely confirmed by measurements.

The large number of power plant parameters which affect the so-called machinery noise components (fan/compressor, turbine and combustion chamber noise) cannot be covered in greater detail within the scope of this report. In addition to indicating their effects on the basis of measurements (Section 1.3), it must suffice here to refer to publications such as [1-3] and to basic studies by the firm of Dornier on fan noise in the dual-jet power plants program [4, 5], in which additional references are cited.

1.3. Sound Level Data from the Power Plant Manufacturers

Sound measurements were performed on various versions of the Pegasus pivoting nozzle power plant by the power plant manufacturer, Rolls Royce-Bristol, primarily as part of development of the Hawker Siddeley "Harrier" V/STOL combat aircraft (precursor: "Kestrel"). On the other hand, RR had no measurement results for /28 the lift power plants of the Do 31 E3.

A number of acoustic data characteristic of power plant performance in the Do 31 E3's V/STOL phases are plotted in Figs. 1.3-1 through 1.3-6 from the results of studies reported in [7-10].

Aside from very large distances from a power plant, which were not studied here, maximum noise (e.g. in the physiological

noise level unit PNdB [6]) is radiated at 100° polar or about 110° linear, i.e. parallel to the power plant; discussion here is therefore limited to these angles.

The following trend, diagrammed in Fig. 1.1-1, for example, is confirmed in Fig. 1.3-1: even for a low bypass ratio, the fan and/or machinery noise and jet noise components typical of dual-jet power plants become evident in the rearward area.

As a supplement to the above, the change in noise level with rpm is plotted in Fig. 1.3-2 for an angle of 100° relative to the inlet.

Fig. 1.3-3 shows hardly any difference, as was to be expected, in the frequency spectra for angles of 100° and 110° , aside from deviations beyond about 4000 Hz, which can apparently be attributed to installation effects (shielding by the Kestrel fuselage).

Even at an angle of 70° relative to the jet outlet axis (corresponding to 110° relative to the inlet), the noise component of the hot jet predominates, as Fig. 1.3-4 shows, over the noise component of the cold jet, which primarily includes "machinery noise," above 80% rpm. In noise level units of PNdB, on the other hand, machinery noise predominates over the entire power range along a line parallel with the power plant (Fig. 1.3-5).

Finally, an interesting result from near field studies on a /29 Pegasus 3 power plant is shown in Fig. 1.3-6. Since this version of Pegasus has the same fan/compressor component as the BS Pg 5-2, the results from the cold stream can be transferred directly to the cruising power plant of the Do 31 E3. The contours of equal sound radiation include only the sound coming from the cold nozzles of the power plant and that generated by the cold jet (fan, compressor and jet components); all remaining components have been masked off and led away.

1.4. Possibilities for Reducing Sound Radiation

Information on the unfavorable sound distributions, total noise radiation and ground erosion effects caused by the lift power plants on the Do 31 E3 resulted in various proposals for reduced-noise V/STOL transport aircraft, of which a particularly interesting advanced development of the Do 31, called the Do 31 D for short, will be described.

In a feasibility study between Hawker-Siddeley Aviation and Dornier, a mixing nozzle - ejector combination for the Rolls Royce RB 162-81 single-jet thrust power plants (rated thrust about 2500 kp), representing the state of the art at that time, was proposed on the basis of results of theoretical studies and measurements performed on models and full-scale power plants ([11-13] and others).

Fig. 1.4-1 shows one version of an ejector thrust pod possible on the Do 31, representing a practical compromise to an ideal ejector design and size.

The essential aim here was to approach the ideal effect, possible only with considerably larger ejectors, as closely as feasible by intensifying jet mixing with the aid of mixing nozzles /30 (consisting of 9 or 12 segments).

The ejector effect which was striven for is based on the fact that almost complete mixing of the primary and secondary streams results in a mixed jet of higher mass throughput, lower temperature and lower jet velocity and thus not only in a reduction in noise but an increase in thrust.

Due to the nonideal ejector design in the Do 31 D, an increase of just a little less than 15% in thrust was assumed which would be quite sufficient to compensate for the overall increase in weight and the thrust losses due to the mixing nozzle.

To reduce the noise level in the airframe, reducing the maximum level, oriented 30-45° relative to the jet axis, of the undivided power plant jets, particularly while close to reflecting ground, made it possible to achieve noise level reductions between about 6 and 12 dB.

For the far field level of the Do 31 D, a total noise reduction of about 10 PNdB was assumed for about the same takeoff weight as in the case of the Do 31 E3, resulting in considerable reductions in the ground areas exposed to noise and in interesting shifts in the thrust-dependent maximum level (Sections 3.1.3 and 3.1.4).

According to more recent information [14], it does appear difficult to achieve an appreciable reduction in noise to the sides from mixing nozzle / ejector combinations without special measures (e.g. sound-absorbing components or much longer mixing chambers). Underneath the flight path, that is primarily in the direction of the maximum in jet noise, however, relatively large reductions in noise level can be expected; this is particularly /31 important for use over inhabited areas. For such a reduced-noise V/STOL design, for example, just 1/4 of the climb altitude for the Do 31 E3 would be sufficient to produce the same ground noise level at about 2/3 of the distance to the sides.

2. Sound Level in the Near Field

/32

In the acoustic near field or the airframe area, the principal consideration is acoustic strength, i.e. the acoustic fatigue strength of acoustically loaded components, and cabin

noise, i.e. the transmission of sound. In addition, the reliability of instruments, control units, linkages, etc. exposed to noise and vibration is of important, although subordinate in the case of jet propelled aircraft; this aspect cannot be covered in detail here.

2.1. Theoretical Studies

In order to be able to counteract the hazard of acoustic fatigue and that of impermissible cabin noise at the proper time, it is necessary to predetermine the noise levels to be expected in the airframe, approximately during the drafting stage and relatively accurately during the developmental stage.

In a Federal Ministry of Defense study contract, a computational method for determining sound level contours in the near fields of jet power plants was developed as a joint project by the firms of Dornier and Hawker Siddeley Aviation [15], the fundamentals of which are given in 2.1.1 and the principle of which has remained the same even after the reworking and improvement which has taken place in the meantime.

2.1.1. Method for Calculating Sound Level Contours

With the aid of excerpts from [15], which have been reworked and to which important material has been added for this documentation, it is possible to mathematically determine the "jet noise" components for subcritical jets at "arbitrary" points in the aircraft and the surrounding near field for any configuration and any number of gas jets or jet powerplants. /33

Much more complex principles, still not completely understood at present, apply to machinery noise components (fan, compressor, turbine, combustion chamber) and dipole noises, e.g. from flow about rigid objects, which in the Do 31 E3 occur only on the cruising power plant at certain power levels. These components are thus best obtained from empirical data or measurements for the near field (Section 1.3) and must be superimposed on the "jet noise" components in the applicable areas.

2.1.1.1. Relationship Between the Reference Sound Field and the Sound Field Which Is To Be Determined

According to Lighthill [16], the following formula gives the acoustic power of jets:

$$P = K \cdot \rho_0^2 \cdot V^8 \cdot a_0^{-5} \cdot L^2 \quad \left[\frac{\text{cmkg}}{\text{s}} \right] \quad (2.1.1)$$

where V = mean jet velocity
 L = characteristic length.

Sound intensity is

$$I = P/F \left[\frac{\text{kg}}{\text{s cm}} \right] \quad (2.1.2)$$

where F = surface area of sphere = $4\pi r^2$.

In addition

/34

$$I = \frac{\overline{p^2}}{\rho_o a_o} \left[\frac{\text{kg}}{\text{s cm}} \right] \quad (2.1.3)$$

where ρ_o = density of surrounding medium
 a_o = sonic velocity in surrounding medium
 $\overline{p^2} = p_{\text{max}}^2/2$ = mean square of acoustic pressure amplitudes.

After introducing a new Lighthill constant \overline{K} , we obtain

$$I = \overline{K} \frac{\rho_1^2 V^4 L^2}{\rho_o a_o^5 r^2} = \frac{\overline{p^2}}{\rho_o a_o} \quad (2.1.4)$$

and, from this,

$$\overline{p^2} = \overline{K} \frac{\rho_1^2 L^2 a_o^4}{r^2} \left(\frac{V}{a_o} \right)^4 \left[\frac{\text{kg}}{\text{cm}^2} \right]^2 \quad (2.1.5)$$

According to [26], the exponent of Mach number V/a_o generally varies within the sound field. The exponents "N" were determined mathematically from sound fields measured for different jet velocities.

Introduction of the logarithmic scale, due to the large intensity range, covering about eight orders of magnitude, and the decibel constants yields the familiar relationship according to which two intensities differ by the following on the decibel scale:

$$10 \log \frac{I_1}{I_2} \cong 10 \log \frac{\bar{p}_1^2}{\bar{p}_2^2} \quad (2.1.6)$$

where \log = logarithm base 10.

I.e. the difference in sound intensity for a sound field point j /35
is the following between power plant K under study and the reference
power plant B for power plant K (subscript B_K)²

$$L_{j_K} - L_{j_{B_K}} = 10 \log \frac{\bar{p}_K^2}{\bar{p}_{B_K}^2} \quad (2.1.7)$$

$$L_{j_K} - L_{j_{B_K}} = 10 \log \left[\frac{\bar{K}_K \rho_K^2 L_K^2 a_{o_K}^4 r_K^{-2}}{\bar{K}_{B_K} \rho_{B_K}^2 L_{B_K}^2 a_{o_{B_K}}^4 r_{B_K}^{-2}} \cdot \right. \quad (2.1.8)$$

$$\left. \cdot \frac{\left(v_K / a_{o_K} \right)^{N_{j_K}}}{\left(v_{B_K} / a_{o_{B_K}} \right)^{N_{j_{B_K}}}} \right]$$

On the basis of the important assumption, verified experimentally, that the velocity exponents, referred to length/diameter ratios, are the same for all jets, we find that the sound fields are similar for jets of the same exit velocity.

I.e.,

$$N_{j_K} = N_{j_{B_K}} \quad \text{and} \quad L_K / r_K \cong D_K / r_K = D_B / r_B$$

In addition, it can be assumed that

$$\bar{K}_K \approx \bar{K}_B.$$

² This is to allow for the possibility of using different reference sound fields for different power plant generations.

It then follows from Eq. (2.1.8) that

$$L_{j_K} = L_{j_{B_K}} + 20 \log \rho_K / \rho_{B_K} + 40 \log a_{o_K} / a_{o_{B_K}} + N_{j_{B_K}} \cdot 10 \log \frac{v_K / a_{o_K}}{v_{B_K} / a_{o_{B_K}}} \quad (2.1.9)$$

The level L sought at $j_K(\theta, r/D)$ for power plant K is found from level L for reference power plant B associated with power plant K at point $j_{B_K}(\theta, r/D)$ and corrections for jet density, sonic velocity in the surrounding medium, and jet exit velocity.

With the abbreviations

$$f_K = 20 \log \rho_K / \rho_{B_K} \quad (2.1.10)$$

$$h_K = 40 \log a_{o_K} / a_{o_{B_K}} \quad (2.1.11)$$

$$g_K = 10 \log \frac{v_K / a_{o_K}}{v_{B_K} / a_{o_{B_K}}} \quad (2.1.12)$$

we can write the following simplified form:

/37

$$L_{j_K} \left(\theta_{j_K}, r_{j_K} / D_K \right) = L_{j_{B_K}} \left(\theta_{j_K}, r_{j_K} / D_{j_K} \right) + N_{j_{B_K}} \left(\theta_{j_K}, r_{j_K} / D_K \right) \cdot g_K + f_K + h_K \quad (2.1.13)$$

Sound reflection components which cause a rise in noise level at certain points and which cannot be determined, for example, by means of sound sources with mirror-inversion effects (such as rigidity-dependent airframe reflection components; see Section 2.1.2) are not included in Eq. (2.1.13), above.

The superposition of noise level components from all power plants effective for j results in the overall sound level at point j :

$$L_j = 10 \log \sum_K 10^{\frac{L_{jK}}{10}} \quad (2.1.14)$$

These relations, in conjunction with the reference quantities (Figs. 2.1.1-1 and 2.1.1-2), were employed for computer determination of near field noise levels in a program expanded for the determination of θ_{jK} and r_{jK}/D_K between points in space and arbitrarily oriented power plants. The program can be augmented with available supplementary programs and subroutines which, for example, permit the loading of complexes of data (such as reference field parameters), electronic plotting of contours of equal noise level (program ISOPLO), and far field calculations extending beyond the near acoustic field.

The program is written in such a manner that in addition to overall noise levels, up to 30 reference fields for 1/3-octave levels can be loaded and processed for each reference power plant for the calculation of frequency spectra. /38

2.1.2. Sound Levels in the Airframe

Sound levels in the airframe of the Do 31 E3 were calculated by the method described in 2.1.1 with an improved reference sound field developed in the course of other assignments.

In addition, the effect of ground reflection, fan and machinery noise components of the Pegasus power plant (see 1.3), increases in noise level from the jet deflecting cascades of the Pg 5-2 and increases due to the rigidity of the corresponding fuselage fields have been taken into consideration for this case, flown with the Do 31 E3 and supported with measurements.

These rigidity values, as the reciprocals of the flexure of panels subjected to point loads at the microphone positions, were calculated with the versatile COSA program system developed at Dornier, by the method of finite elements; this was also done for specimens in which increases in noise level had been measured in earlier tests [17]. The effect of rigidity upon the increases in noise level could be confirmed by measurements (Fig. 2.1.2-1). Fig. 2.1.2-2 shows the results of the first computational step in accordance with [15], i.e. the "jet noise" component, including ground effect.

Table 2.1.2-1 shows the results -- corrected for the effects mentioned -- obtained at the points which could be compared with measurement results from the studies described in 2.2.4.

2.2. Experimental Studies

/39

The experimental studies on the acoustic near field of the Do 31 E3 began at the end of 1963 with preliminary studies on a Pegasus 2, predecessor to the BS Pg 5-2, and ended in the first half of 1968 with measurements performed on the airframe surface and within the Do 31 E3 during different operations.

It was not possible to carry out extended measurements, particularly for the purpose of characterizing interference and shielding effects, as planned in a program proposed on the basis of accumulated experience for the purpose of goal-oriented augmentation of the near and far field results.

2.2.1. Preliminary Studies on the Sound Levels To Be Expected

In collaboration with the Bristol Engine Div. of Rolls Royce, sound measurements were performed on a Do 31 fuselage segment [18], in addition to other preliminary studies.

The weaker version of the Pegasus, Pg 2, which developed a thrust of about 5400 kp at the maximum rpm at which it was operated, was available as a source of sound. This thrust is achieved by the Pg 5-2 of the Do 31 at about 85% rpm, which was exceeded by the Do 31 only for brief intervals during a few phases of operation, i.e. the measured maximum levels on the surface of the fuselage segment are likewise hardly exceeded on the Do 31 E3 by the cruising power plant alone, without ground reflection.

The results in Fig. 2.2.1-1 indicate a practically linear increase in noise level above 60% rpm and a typical shift in the level maxima toward higher frequencies with decreasing rpm (shift from jet noise to machinery noise) in the frequency spectra for measurement point 4 plotted in Fig. 2.2.1-2.

In addition, sound level measurements were carried out by Dornier as a part of the testing of Do 31 tail control nozzles at the DVL [German Laboratory for Aeronautics and Astronautics], Porz-Wahn. The relations involved in the near field computation method (Section 2.1.1) no longer apply to the supercritical conditions occurring at this nozzle. The Do 31 control surface assembly (Fig. 2.2.1-3), for which expected acoustic loads were to be determined, is located within the immediate vicinity of the outlet and in the same plane as the jet. The major results of these studies [19], in which a microphone was set up in the "free field"

/40

(without control surface assembly) at positions 1-4 shown in Fig. 2.2.1-3, are compiled in Figs. 2.2.1-4 through 2.2.1-6.

In addition to structural and temperature studies, sound level measurements were made in the vicinity of the lift pods during operation of the lift power plants in testing of the large-scale hover frame of the Do 31 [20]. The results (Fig. 2.2.1-7), in conjunction with later measurements (Section 2.2.4), confirm the favorable configuration of the pods, with which no structural components close to the pods were endangered by acoustic effects even at relatively high rpm levels -- up to 95% -- occurring in V/STOL operation, although 157 dB was measured close to the pods at just 80%.

2.2.2. Sound Transmission Measurements

Information concerning acoustic damping of the unlined airframe is an important component of an assessment of the cabin lining required for a given cabin noise level with an insulating material which, while offering high acoustic damping, thermal insulation, insensitivity to moisture, etc. is supposed to be especially light -- a requirement which primarily opposes the reduction of low-frequency sounds.

In the acoustic laboratory of Dornier AG, sound transmission measurements were performed on a fuselage segment of the Do 31 [21, 22]. A microphone in front of and one behind the segment made it possible to determine the reduction in noise level during passage through the component. A frequency spectrum between 50 Hz and 6.3 kHz was covered here in 1/3-octave increments. Fig. 2.2.2-1 shows the test setup; the results are plotted in Fig. 2.2.2-2 for two lining thicknesses and the unlined airframe.

/41

2.2.3. Cabin Noise Level

As part of the test program described in 2.2.4 [23], several microphones were installed within the fuselage of the Do 31 E3, and maximum overall noise levels were recorded during three different operations.

The microphones were installed in the cockpit and in the center section of the fuselage at four locations over a length of about 7 m at window height, at a distance of about 0.5 m from the fuselage skin (positions 7_i through 11_i in Fig. 2.2.3-1).

The results (Table 2.2.3-1) show the significant effect of the cruising power plants on cabin noise levels above 80% rpm; if the airframe is lined in the same manner as up-to-date aircraft (similar to 2.2.2, Mat. II), these are comparable to the

maximum levels in the Boeing 720 [24], although in cruising flight they will exceed its interior cruising noise levels.

2.2.4. Noise Levels at the Airframe

/42

In addition to the cabin levels described above, noise levels were measured at 12 positions right at the surface of the airframe of the Do 31 E3 in an extensive program in the field of V/STOL engineering which has so far been unexcelled.

The results were of wide interest, e.g. for comparative studies with other V/STOL equipment, for checking and expanding existant computational methods (Section 2.1.1), for determining different power plant noise components and ground effects, and for evaluating the danger of acoustic fatigue.

Fig. 2.2.4-1 shows microphone installation and the measurement provisions which were used. The noise levels were recorded on tape from a total of nine flight phases, including not only typical takeoff and landing transitions, but also vertical climbs and conventional operations. Parallel to the above, as in all tests with the Do 31, a large number of measured values were automatically recorded, such as power plant conditions, flight performance, etc., with the associated time code so that an exact correlation between noise levels and the associated power plant and flight parameters was possible upon evaluation of the data.

Table 2.2.4-1 provides an overview of the total noise levels measured in the nine operational phases, with the associated main power plant data and trial numbers; microphone malfunctions or the use of existant microphones (e.g. 7-11) for internal level measurements are indicated by blank spaces in the table. The presentation of two noise level values per measurement point was chosen to indicate the effects of acoustic pressure fluctuations during the time interval analyzed (see Fig. 2.2.3-1 for microphone positions). Maximum levels of 157 dB were measured at the under-side of the center section of the wing (measurement point 5) and 152 dB at the fuselage in approximately the inlet plane of the cruising power plants (measurement point 8).

As an example, the 1/3-octave band spectra are shown in Tables 2.2.4-2 and 2.2.4-3 for the vertical climb II and cruising II operations and are also plotted in Figs. 2.2.4-2 and 2.2.4-3 for fuselage measurement point 8.

/43

Finally, the time curves of the power plant and flight parameters affecting noise levels in trials 60 and 58 provide an impression of the short-term variations in sound-influencing factors in a jet-supported V/STOL aircraft based on the Do 31 design. The time intervals excerpted from the overall

recordings for the acoustic analyses are shown on the time axes of Figs. 2.2.4-4 through 2.2.4-9.

3. Sound Levels in the Far Field

/44

In the far field, the problem is flight noise, i.e. the immersion of noise due to aircraft, for which the radiation of sound by power plants and the flight procedure are of primary significance.

Going beyond the results of theoretical and experimental far field noise studies within the framework of Do 31 development, particular importance is given in this chapter to the reduction in flight noise problems at existant airports which is already possible with V/STOL engineering, to the effects of noise abatement, and possible improvements through V/STOL development in the future.

3.1. Theoretical Studies

Check calculations were performed for various Do 31 E3 operations for which noise measurements were available. In addition, the maximum noise levels, dependent upon the thrust components of the power plant groups, and the directional characteristic of Do 31 E3 noise radiation were calculated as a basis for the noise level contours which result on the ground during operational utilization. These calculations were also made for the reduced-noise version of the Do 31 and the future Do 231 jet V/STOL aircraft.

To the extent possible, the theoretical results are compared directly with the measured results in the following. All other results apply, if not otherwise noted, to ISA conditions, $H = 0$ m and 70% relative humidity.

3.1.1. Do 31 Noise Level at a Fixed Distance as a Function of Direction

/45

The noise levels around the Do 31 E3 at a radius of 100 m were calculated for the case of a vertical takeoff, shortly before the aircraft leaves the ground [25], and have been compared with the measured levels in Fig. 3.1.1-1. The fan noise components which dominate at some angles were determined empirically, among other things, with the aid of measurement results obtained on the Pegasus 3 (Section 1.3) and were superimposed on the jet noise components. The dispersion band for the measured results is due to the different noise level values at measurement points which are symmetrical relative to the longitudinal axis of the aircraft (Section 3.2.1).

The calculated and measured frequency spectra are compared in Figs. 3.1.1-2 and 3.1.1-3. The values measured at two points symmetrical with respect to the aircraft's longitudinal axis are again included here. The spectra, which are relatively broadband for all positions around the circumference, indicate high fan and turbine noise components for the power plants which predominate vis-a-vis the jet noise components, particularly at the 90° and 120° positions.

An additional case (Fig. 3.1.1-4), for a hover altitude of just $H = 30$ m above ground, no longer shows a pronounced directional character. The radiation of sound is almost circular. The sound level at the perimeter of a 100 m circle averages 122 dB. The calculated values fall in the dispersion band of the measured results.

3.1.2. Maximum Levels Along a Line Parallel to the Projected Flight Path of the Do 31

The maximum levels along a line parallel to the projection of the flight path at a distance of 150 m were calculated for a typical V/STOL operation flown by the Do 31 E3 (takeoff and landing transition) [25].

The noise levels during operations by the Do 31 E3 were plotted at 150 m to the side of the takeoff point and at an additional measurement point directly under the flight path (Section 3.2.2). The calculated overall noise levels and frequency spectra could thus be compared directly in two cases (TO1, VL3) and with restrictions in two cases (TO4 and VL2). /46

The curves of total noise level versus time (calculated at times TO1 through TO6 and VL1 through VL5) are plotted in Figs. 3.1.2-1 and 3.1.2-3 with the associated operating states. Figs. 3.1.2-2 and 3.1.2-4 show a comparison of calculations and measurements in the form of octave spectra. Particularly in the case of VL2, noise components in the high-frequency range are conspicuous here which explain the difference between calculations and measurements in terms of attitude and the position of the check point relative to the aircraft. As the following table shows, such differences affect physiological noise level units in particular (e.g. PNdB).

Time	TO1		VL3		TO4		VL2	
Noise level unit	dB	PNdB	dB	PNdB	dB	PNdB	dB	PNdB
Calculated	90.2	98.4	110.4	118.2	120.2	126.7	114.8	120.8
Measured	91.6	98.6	110.1	119	117.8	125.1	117.6	125.4

3.1.3. Ground Noise Level Contours

Ground noise level contours provide information concerning the size of the ground areas exposed to sound from a particular aircraft for a particular flight pattern. Higher noise levels do not occur outside the area enclosed by contours of equal noise level.

The origin of a ground noise level contour is shown in simplified form in Fig. 3.1.3-1 in the example of the takeoff transition of a Do 31 type V/STOL aircraft. After a vertical takeoff, the transition phase is primarily initiated by rotating the lift-thrust power plant jets away from the vertical. The maximum distance of the noise level under consideration for the rearward portion of the contour (arc about P_I) occurs when aircraft is at point I on its flight path. At point II on its flight path, aerodynamic lift is sufficient to allow the lift power plants to be cut out; a final circular noise level contour is obtained about P_{II} . During the subsequent climb, only the lift-thrust or cruising power plants remain in operation, as in conventional jet aircraft, and narrow noise level contours typical of CTOL aircraft are then produced, if the noise level under consideration is still exceeded at the ground. /47

3.1.3.1. Do 31

Ground noise level contours were determined for the Do 31 on the basis of the measurement results and calculations from [25-28] described in this report for various flight paths and flight sequences which were flown or are feasible.

So-called ground noise level distances were first determined for perceived noise levels of 90 to 105 PNdB during purely vertical takeoff and for various takeoff transitions which were flown as V/STOL airport traffic patterns by the Do 31 E3 (Figs. 3.1.3.1-1 and 3.1.3.1-2). In addition, the ground noise level curves for different conventional flight phases were obtained which in most cases determine the maximum extent of the contours in the direction of flight. One example of ground noise level contours during conventional Do 31 takeoff is shown in Fig. 3.1.3.1-3.

The ground noise level contours for the three different flight paths are shown together in Fig. 3.1.3.1-4. In all three flights, forward speed was developed while just a few meters above the ground and the transition phase thereby initiated. Trial 75/27 (center figure) yielded the smallest enclosed area for the 95 PNdB contour and was therefore used in parallel with the likewise favorable pattern 72/24 for subsequent consideration. /48

Fig. 3.1.3.1-5 shows this "optimum noise level" contour along with a contour which results from vertical climb by the Do 31 E3

to high altitudes (I), and a contour (III) for conventional take-off (with the cruising power plants only). It is found from this that, for the noise conditions associated with the Do 31 E3, the more economical flight pattern II is more favorable with regard to the noise zone on the ground than vertical climb to high transition altitudes. Under some circumstances, moreover, a conventional takeoff can lead to a lower level of noise pollution; this exception can be attributed to the unfavorable noise component of the Do 31 lift power plants, which is covered in detail in Section 3.1.4.

3.1.3.2. Do 31 As Compared With Conventional Aircraft

The advantages of V/STOL engineering with respect to existant aircraft noise problems due to conventional jet aircraft can even be shown very impressively with the "loud" Do 31 E3 just on the basis of its V/STOL characteristics, using the example of the Frankfurt/Main airport (Figs. 3.1.3.2-1 and 3.1.3.2-2).

The 90 and 95 PNdB takeoff and landing noise level contours for the Do 31 E3 were compared with those for the Boeing 727 [29] and the Boeing 707 [30]. As a first approximation, the same sizes were assumed here for the Do 31 landing noise level contours as for takeoff. The two conventional aircraft were selected as representative of noise pollution caused by short/medium-range and long-range aircraft presently being used. The seating capacity of the Boeing 727 corresponds approximately to that of future civilian V/STOL aircraft. The Boeing 707 generates approximately the same takeoff thrust as the Do 31 E3, with turbofan power plants of low bypass ratio but with primary velocities similar to those of the single-jet thrust power plants of the Do 31 E3. /49

The advantages resulting from V/STOL engineering are shown even more clearly in the example of the Paris/Orly airport [31], at which the populated areas extend to within a very small distance from the airport. Even a version of the Do 31 which has been rendered obsolete by the state of the art in power plant engineering, with a takeoff weight of about 60 t and without noise-abatement measures, would expose only the airport grounds to noise levels above 95 PNdB (Fig. 3.1.3.2-3).

3.1.3.3. Reduced-Noise Version of the Do 31

As has already been described in Section 1.4, the possibility exists for improving the unfavorable noise distribution on the Do 31 E3 by using mixing nozzles on the thrust power plants in conjunction with a design for the lift pods in the form of ejectors.

In addition, a reduction in noise from the lift-thrust power plants during takeoff, by about 4 PNdB (at a distance of 150 m), through the use of mixing nozzles has been assumed for the reduced-noise version of the Do 31 being considered here. For an overall reduction in noise of 10 PNdB in the vertical takeoff phase, the noise level distances and ground noise level contours plotted in Figs. 3.1.3.3-1 through 3.1.3.3-4 would be obtained for /50 such a reduced-noise version.

As compared to the Do 31 E3, the maximum extents of the contours transverse to the direction of flight would thus be only about half as large for the same takeoff profiles, and they would amount to about 70% in the direction of the flight paths.

Since the planned noise-abatement measures can be considered to have been rendered obsolete by the present state of the art in dual-stage power plant engineering, they will not be considered further within the scope of this report, except for a particularly interesting comparison (Section 3.1.4).

3.1.4. Maximum Noise Levels as a Function of Power Plant Thrust Components

In the Dornier V/STOL designs, separate lift and thrust units, which represent different noise sources and noise directions, are also being planned for future projects. The cruising power plants contribute to the generation of lift here with a lesser or greater amount of power and noise during the takeoff and landing transitions.

The theoretically possible thrust combinations for the Do 31 E3 power plants and the reduced-noise version of the Do 31, whose thrust power plants have 25% higher rated thrust, result in the so-called noise "carpets" (Fig. 3.1.4-1). The lines of constant takeoff weight which are obtained for 7% excess thrust for takeoff are plotted in the "carpets."

The illustration shows, for example, that the Do 31 E3 at a takeoff weight of 19.5 t would have to take off with a combination of 40% lift power plant and 92% cruising power plant thrust in order to produce a minimum of noise, in this case 119 PNdB. With the percentages reversed in the thrust combination, maximum noise level would be 128 PNdB at 150 m parallel to the takeoff path. This means that the aircraft is not optimally design with regard to noise. The noise levels are determined almost exclusively by the lift power plants. /51

On the other hand, the reduced-noise version of the Do 31 is considerably more favorable with regard to the change in noise accompanying the change in the percentages of thrust of the two power plant groups. The curves of constant takeoff weight exhibit

minima, e.g. 114 PNdB at 19.5 t takeoff weight, that cannot be achieved with the Do 31 E3. Of particular importance, however, are the limited effects of changes in the thrust combinations upon the noise levels, which even in the extreme case amount to no more than 3 PNdB and would vary by only about 1 PNdB within practical ranges.

This aircraft would thus be practically independent of the ratio of power plant thrust components with regard to noise radiation, something which would considerably reduce the burden on pilots in the adaptation to local requirements which is possible with V/STOL aircraft, thereby increasing safety.

3.1.5. Noise Radiation by Future V/STOL Aircraft

/52

As bid requests, designs [32] and evaluations during recent years have shown, turbofan and liftfan power plants are being given preference for future V/STOL aircraft.

On the basis of experience with the Do 31 and advanced studies, the Do 231 V/STOL aircraft has been proposed by Dornier as a V/STOL aircraft of this future type. In this short- and medium-range aircraft, designed for about 100 passengers, cruising power plants and lift power plants (liftfans) with bypass ratios of about 6 and 10 are planned in which the predominant noise is generated by the fans. Of the 12 liftfans (RR project RB 202-31), four each are housed in outboard wing lift pods and two each are housed in the nose and tail of the fuselage. The two cruising power plants (RR project RB-220) are installed between the lift pods and the fuselage, similar to those in the Do 31 [33].

Through the use of noise contours for a Do 31 version with a takeoff weight of 60 t, for which no reduction in noise from the lift and cruising power plants has been assumed, and for a Do 231, Fig. 3.1.5-1 shows the significant reduction in noise which might be made possible by intensive R & D work in the power plant and aircraft sectors over a period of about 20 years.

The studies required for this would have to be intensified in close collaboration between the aircraft and power plant industries and city and traffic planners with regard to future structuring of the environment.

3.2. Experimental Studies

/53

An extensive study program was worked up and proposed for the Do 31 E3. The studies were to help primarily to experimentally demonstrate the noise radiation characteristics of the Do 31 E3 in various flight patterns for different thrust components from the power plant groups and to help determine the jet interference

effects of the thrust power plants on the radiation of sound and determine the influence of shielding effects.

These basic studies, of importance for future V/STOL development, could only be started within a very modest scope, for financial reasons, and had to be terminated after just a few measurements.

3.2.1. Peripheral Measurements Performed on the Do 31 E1 and E3

Measurements in a circle of radius 100 m were performed on the Do 31 E1 and Do 31 E3 during various operations at the Dornier factory airfield, Oberpfaffenhofen/Munich [34, 35].

A total of 12 microphones were set up at angular intervals of 30°. This interval between measurement points was halved by rotating the aircraft 15° in two trials run in succession under equivalent conditions (Fig. 3.2.1-1).

The maximum values of overall sound levels for a static run with the Do 31 E1 -- this aircraft is equipped only with the BS Pg 5-2 lift-thrust power plants for testing conventional characteristics -- are plotted in Fig. 3.2.1-2 in dB (or dB (1in)) and in Fig. 3.2.1-3 in the weighted unit dB (A), and the frequency spectra in 1/3-octave band widths are plotted in Figs. 3.2.1-4 through 3.2.1-7 for four angular positions. Five of the 24 measurement points malfunctioned. Intermediate values have been interpolated. The causes of the asymmetry in the radiation of sound against the direction of the wind, which is particularly conspicuous in the frequency spectra transverse to the aircraft (Figs. 3.2.1-5 and 3.2.1-7), remains unexplained. A typical "jet noise" spectrum was measured for the 225° direction (Fig. 3.2.1-6). Large dB (A) values occurring against the inlet direction indicate higher-frequency noise components of the fan and compressor stages (see Fig. 3.2.1-4). /54

The noise levels at a radius of 100 m about the Do 31 E3 were measured in the setup shown in Fig. 3.2.1-1 for a typical vertical takeoff transition and hovering at an altitude of about 30.5 m (100 ft) above the ground [35].

The peripheral overall noise levels which were measured immediately prior to vertical liftoff of the aircraft from the ground platform are plotted in dB in Fig. 3.2.1-8; these are the maximum values of the frequency-dependent pressure or noise level fluctuations (see frequency spectra). The frequency spectra are shown in 1/3-octave bands in Figs. 3.2.1-9 through 3.2.1-11 for the directions of interest 0°, 90° and 210° (0° = in front of aircraft). A particularly conspicuous feature is the shape of the peripheral noise level contours, which exhibit a pronounced /55

constriction at the sides of the aircraft which apparently cannot be attributed just to a shielding of noise components by the fuselage of the aircraft. A consideration of the frequency spectrum for 90° confirms the suspicion that other noise components than "jet noise" must be decisive factors in this direction. Nothing of the jet noise maxima at about 200 Hz can be seen in the spectrum; the overall noise level is determined unequivocally by peaks at about the 2000 Hz band. In addition to the shielding effects mentioned above, the causes of this might be the reflection of jet noise components by the ground, the noise components of the jets transverse to the jet axis -- with about 2 to 3 times higher frequencies -- and "machinery noise components," particularly from the Pegasus dual-stage power plant (cf. spectrum of Pg 5 alone in Fig. 3.2.1-7).

The direction of the power plant jets at about 15° from the vertical, to the rear, and the configuration of the power plants cause machinery noise components from the inlet and outlet to be operant in front of the aircraft and only components from the outlet to be operant behind the aircraft, but unshielded by the fuselage, with a correspondingly higher noise level (Figs. 3.2.1-9 and 3.2.1-11).

In contrast to the noise level conditions at $H = 0$ m, Fig. 3.2.1-12 shows an almost circular curve for the peripheral noise level for the Do 31 E3 hovering at an altitude of 100 ft, expressed both in the linear or unweighted noise level in dB and in the physiological noise unit PNdB [6]. Accordingly, the frequency spectra exhibit no relatively large differences (Figs. 3.2.1-13 through 3.2.1-15).

3.2.2. Noise Level Measurements During Do 31 E3 Takeoff and Landing Transitions

/56

During a takeoff and a landing transition by the Do 31 E3 (trial 77), the curves of noise level versus time were taken at a measurement point 150 m to the side of the runway at the altitude of the takeoff and landing point, and at a measurement point 460 m away from the takeoff and landing point, under the flight path.

The results of the measurements [36, 37], partly reworked and augmented with sample point calculations, are shown in Figs. 3.2.2-1 through 3.2.2-6. In addition to the curves of noise level versus time, the essential flight parameter data describing the transition processes are plotted in Figs. 3.2.2-1 and 3.2.2-2.

It is particularly interesting that, in spite of the low thrust level, approximately the same maximum value in noise level (in PNdB) is obtained for the two control points during landing as

during takeoff. For the measurement point to the side, this can probably be attributed to the differences in the noise characteristic and distance; for the point under the flight path, to approximately equivalent flight parameters at the time at which the noise level maximum occurred (cf. frequency spectra in Figs. 3.2.2-4 and 3.3.2-6).

The curves of noise level versus time in Figs. 3.2.2-3 and 3.2.2-5 were converted to 15°C (ISA value) and 60% humidity and to the PNdB noise unit by two different methods [38, 39] included in the computer program [28]. The differences between dB and PNdB, about 7 to 10 units, are on the same order of magnitude as predicted mathematically in Section 3.1.2 along a line parallel to the takeoff path at 150 m.

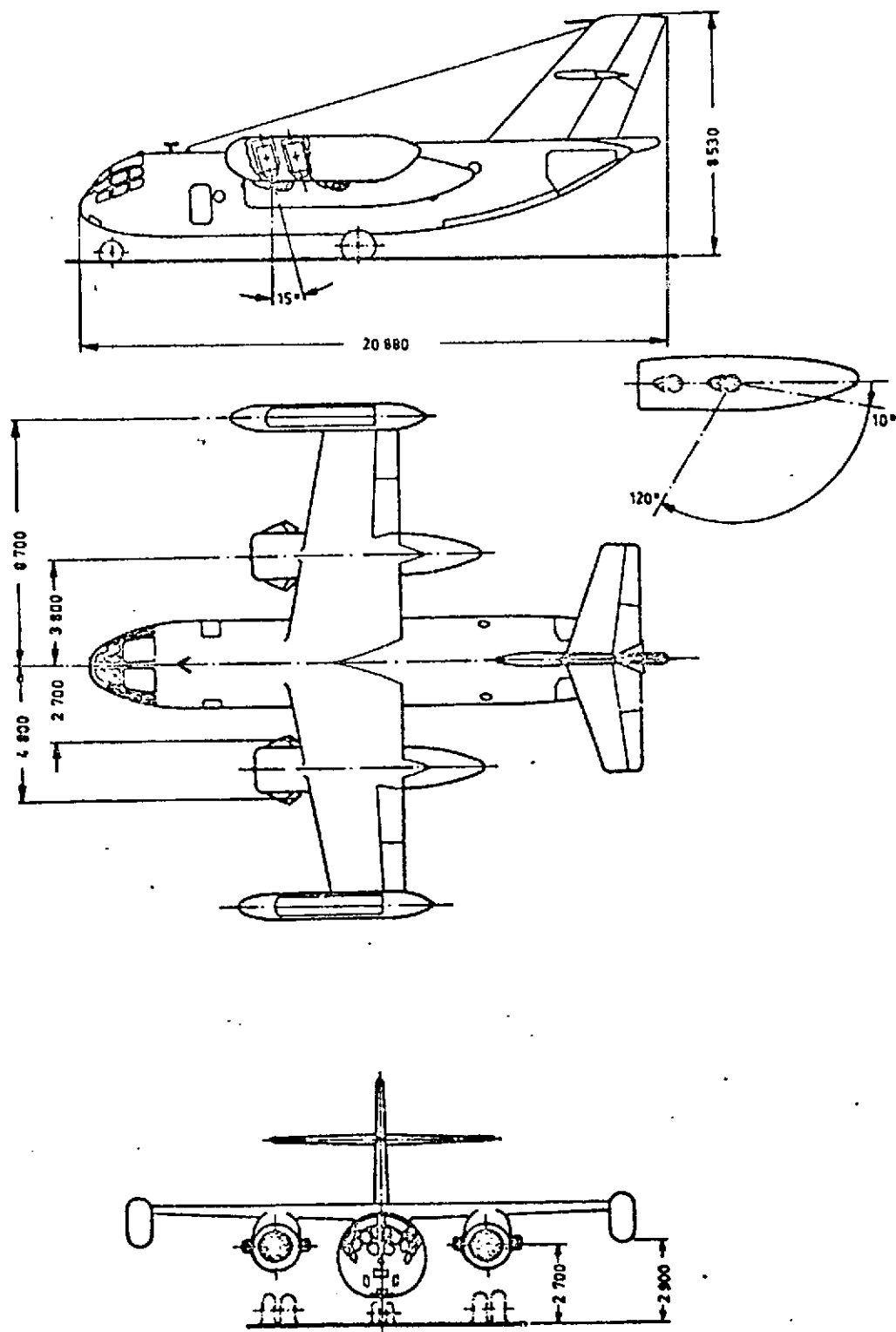
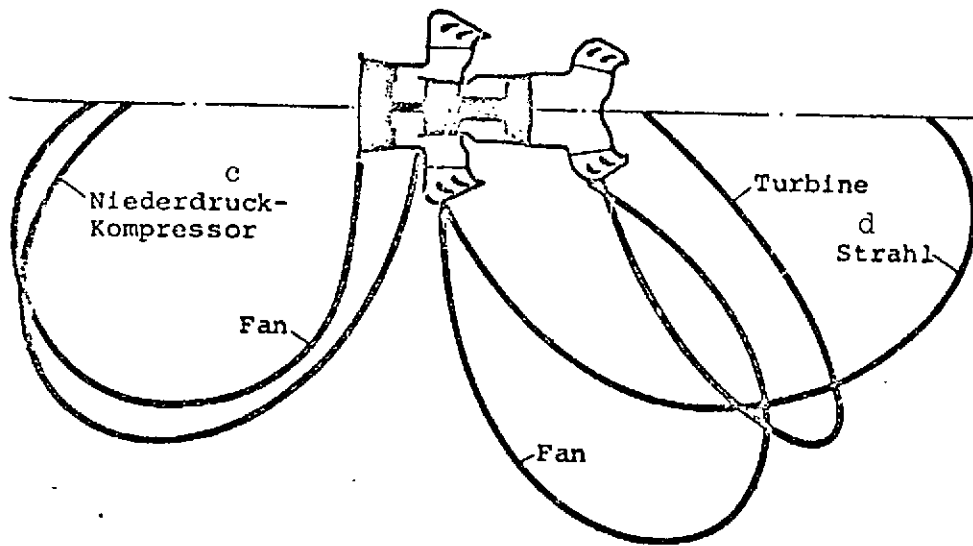


Fig. 1-1. Do 31 E3.

a Zweistrom - Triebwerk (ZTL)



b Einstrom - Triebwerk (TL)

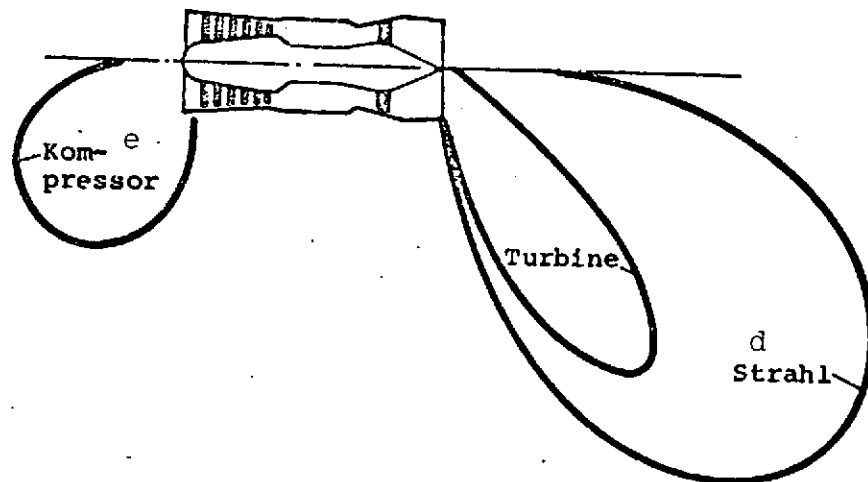
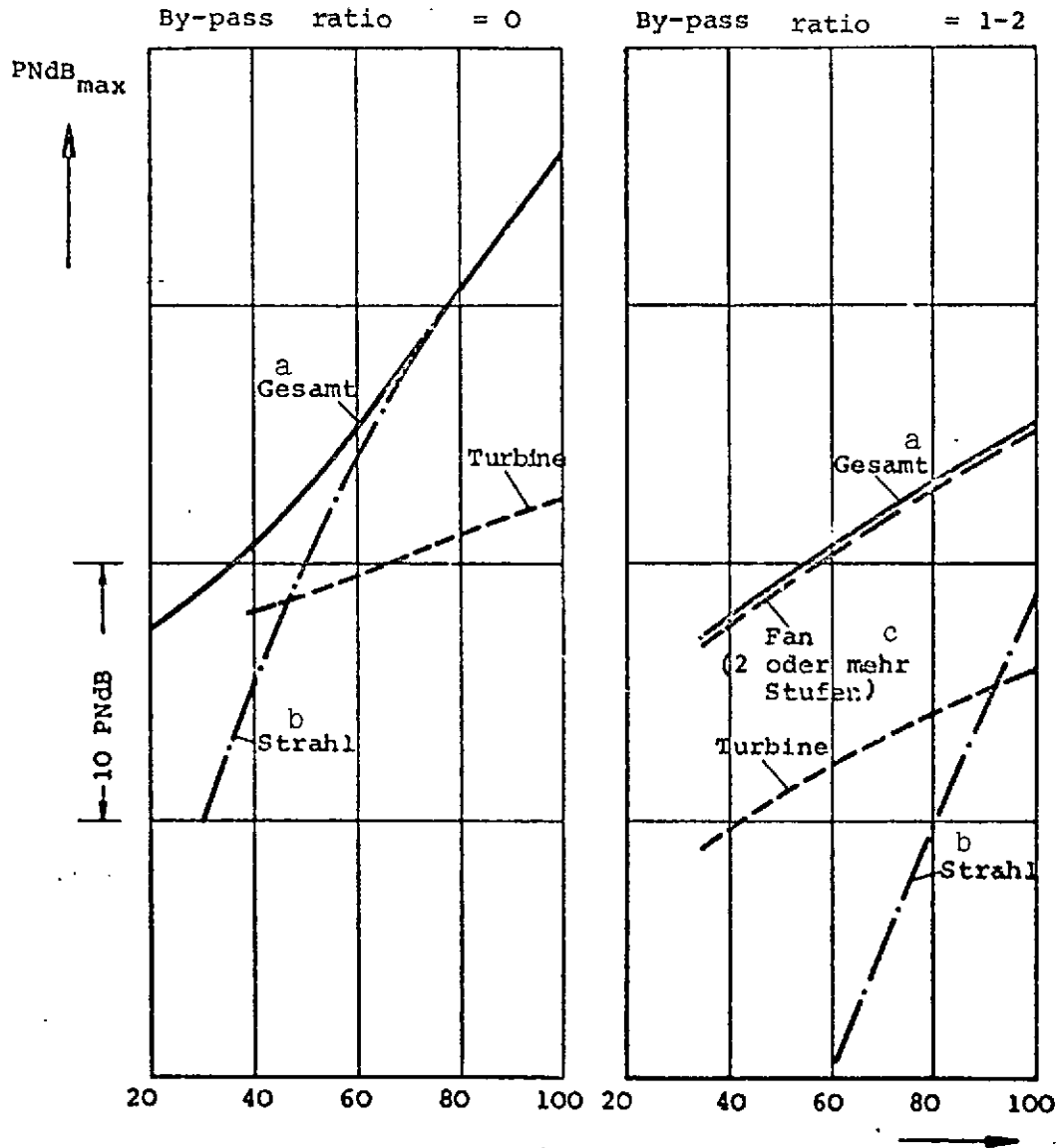


Fig. 1.1-1. Sound components from jet power plants.

Key: a. Dual-jet power plant; b. Single-jet power plant;
c. Low-pressure compressor; d. Jet; e. Compressor

All power plants referred to the same thrust

/65



Percentage of available maximum net thrust

Fig. 1.1-2. Noise components from power plants with different bypass ratios [2].

Key: a. Overall
b. Jet
c. (Two or more stages)

TABLE 1.2-1. Do 31 E3 POWER PLANT DATA

/66

Model	BS Pg 5-2	RB 162 - 4D
Function	Lift-cruise power plant	Lift power plant
Rated thrust S_N [kp]	Cold: 3770 Hot: 4150	2000
Rated speed n_N [rpm]	Fan: 6500	12,500
Nozzle area F [m^2]	Cold: 0.242 Hot: 0.291	0.147
Nozzle diameter D [m]	Cold: ca. 0.42 Hot: ca. 0.46	0.432
Max. jet Vel. c_a [m/sec]	Cold 350 Hot 540	620
Max. jet tem. T_{stat} [K]	Cold: 308 Hot: 780	1100
Max. mass flow \dot{m} [kg/s]	Cold: 105 Hot: 76	31.5
Bypass ratio μ	1.4	
Compressor/turbine stages	L.P.3, H.P.8/H.P.2, L.P.2	6/1

ISA, $H = 0 \text{ m}$, $v = 0 \text{ m/s}$

$n_{FN} = 6500 \text{ rpm}$

/67

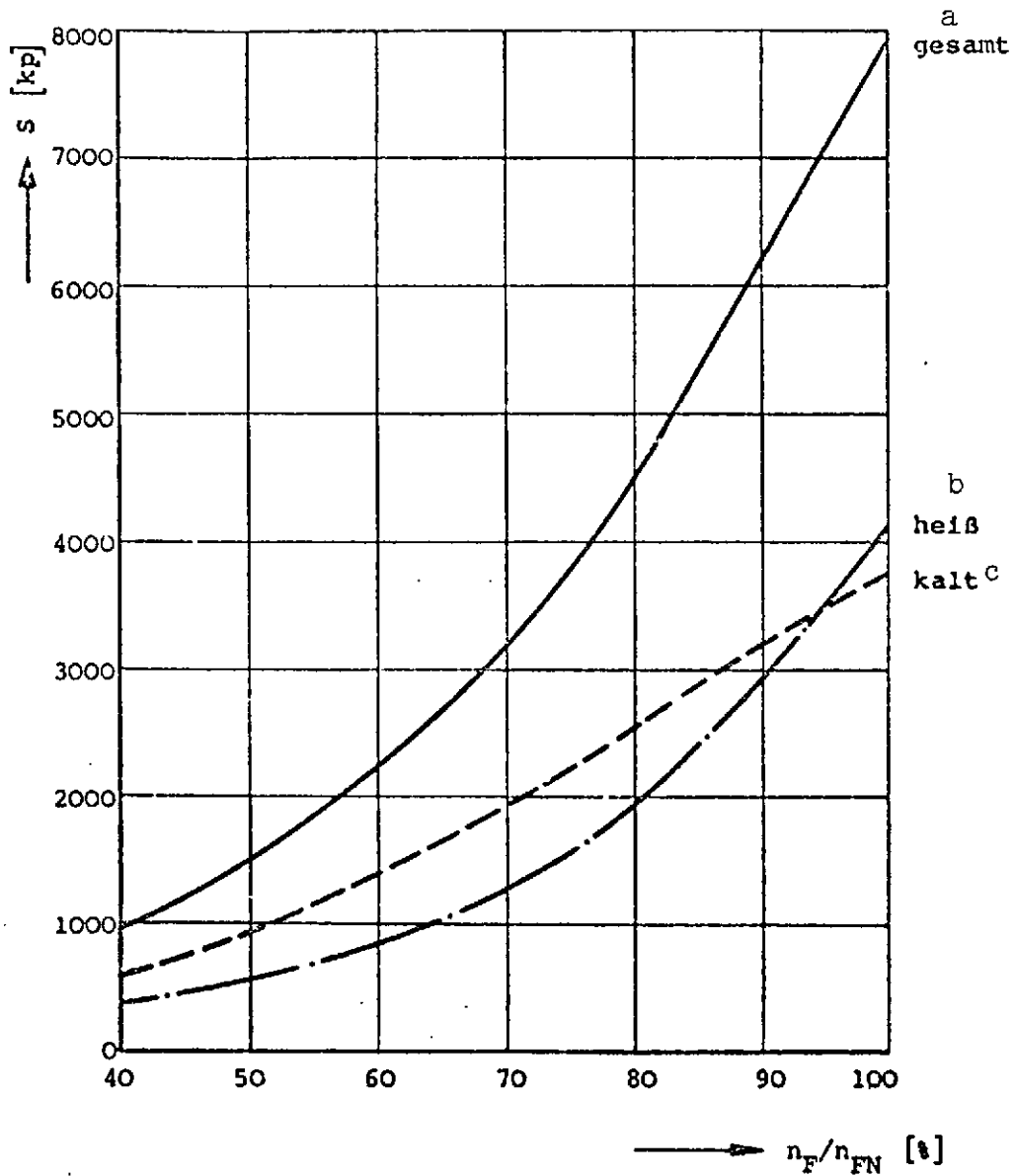


Fig. 1.2-1. Thrust as a function of rpm
(BS Pg 5-2)

Key: a. Overall
b. Hot
c. Cold

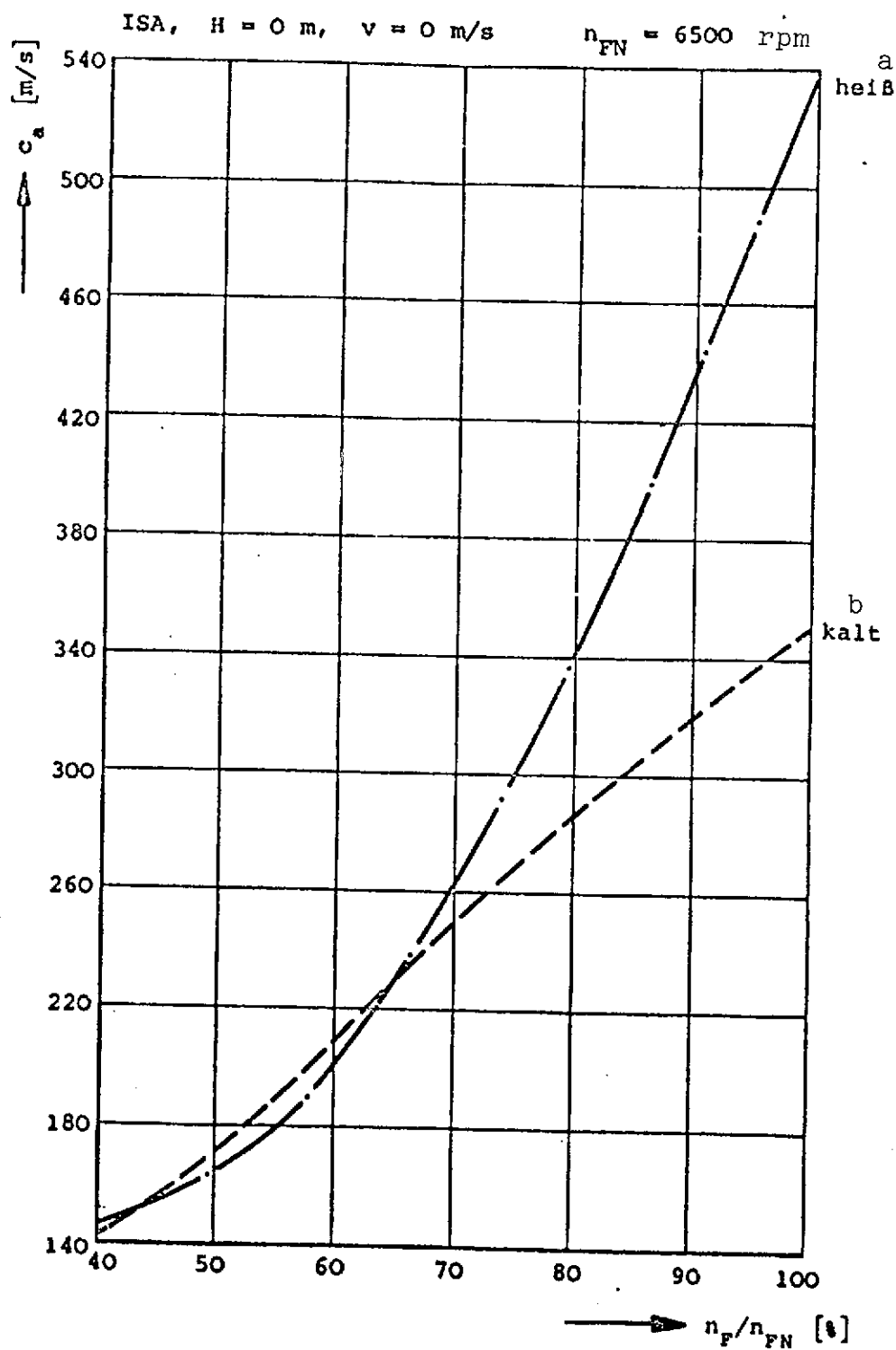


Fig. 1.2-2. Hot and cold gas velocities as a function of rpm (BS Pg 5-2).

Key: a. Hot
b. Cold

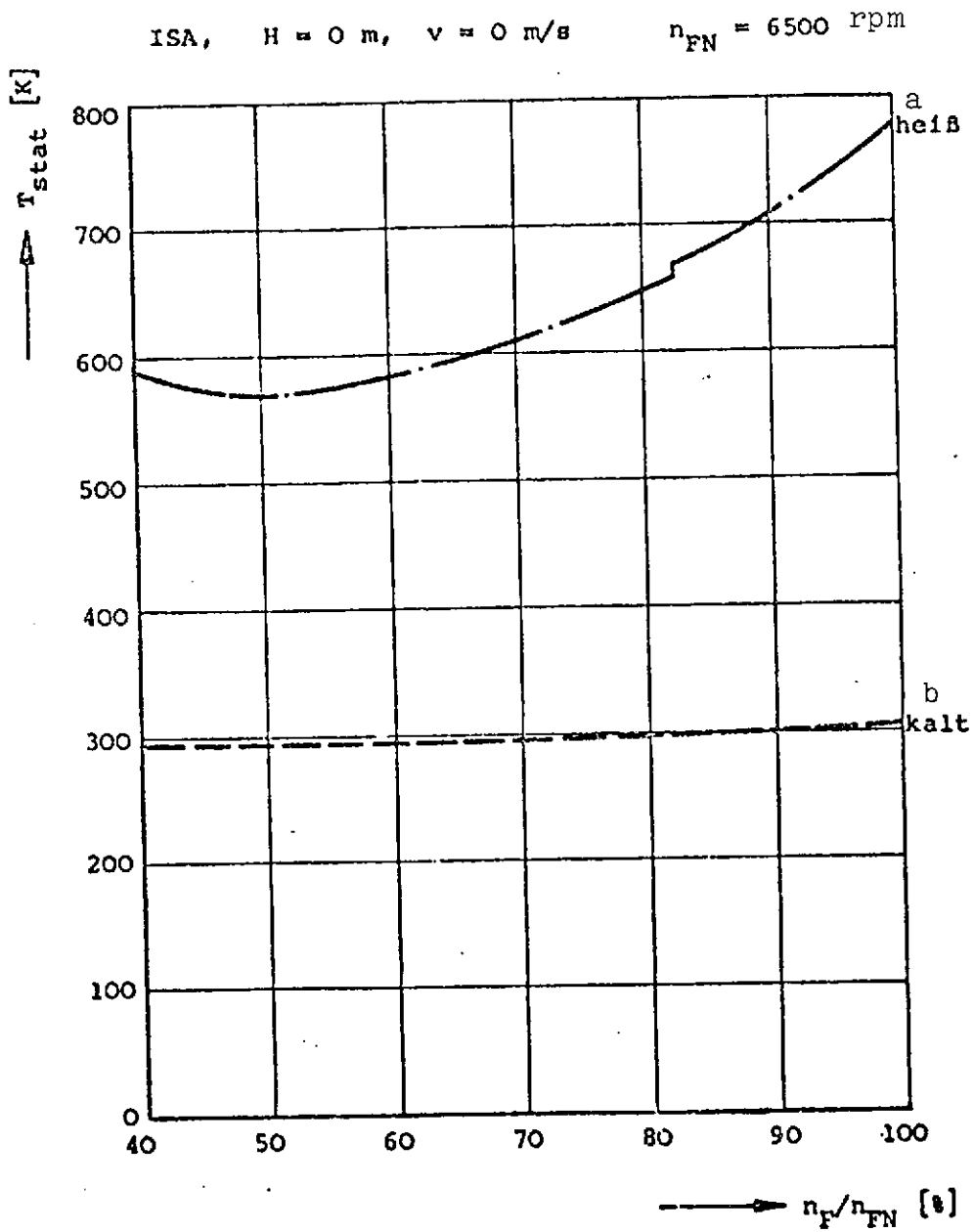


Fig. 1.2-3. Static nozzle outlet temperature as a function of rpm (BS Pg 5-2).

Key: a. Hot
b. Cold

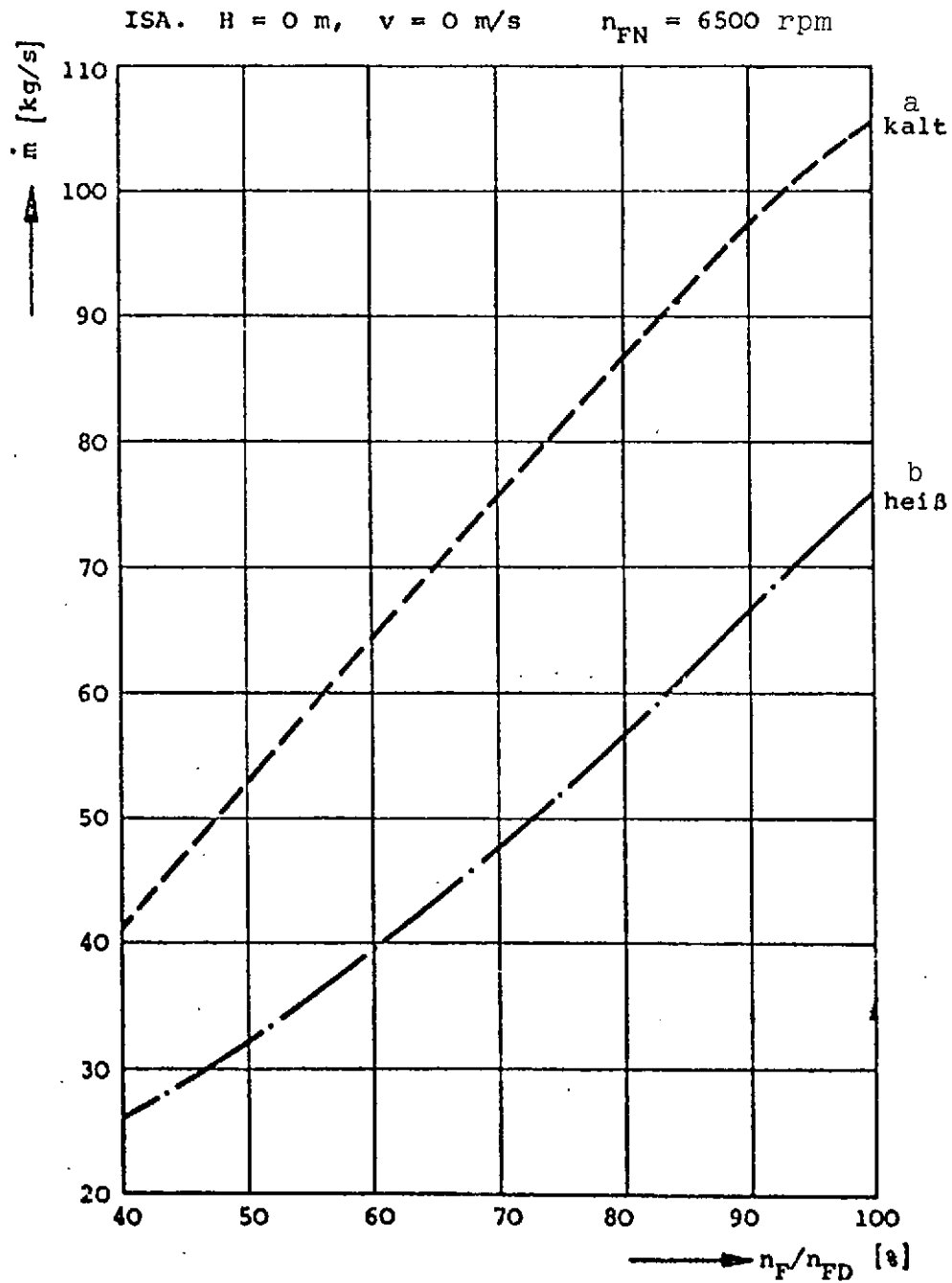


Fig. 1.2-4. Mass flow as a function of rpm
(BS Pg 5-2).

Key: a. Cold
b. Hot

ISA, $H = 0$ m, $v = 0$ m/s $n_N = 12\,500$ rpm

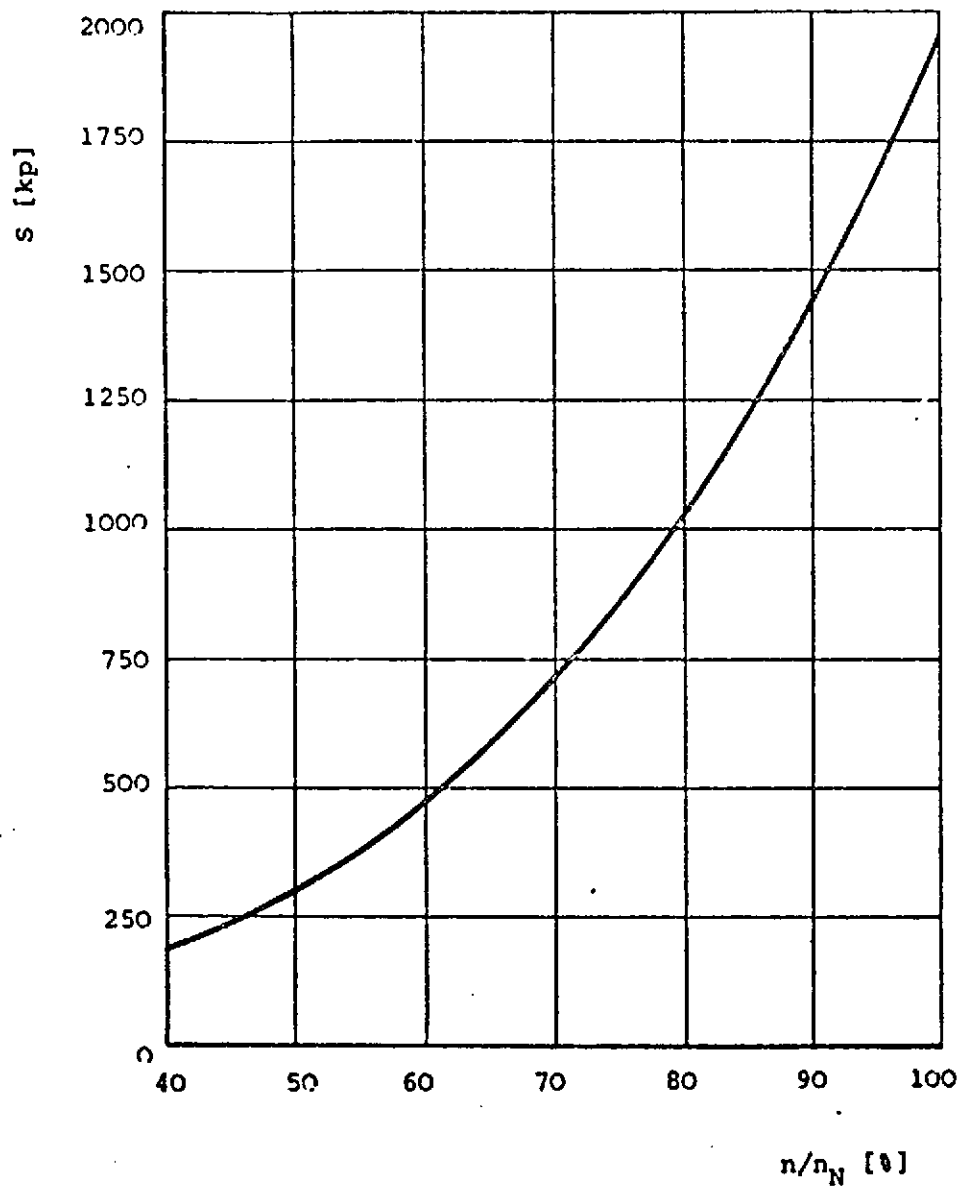


Fig. 1.2-5. Power plant thrust as a function of rpm (RB 162-4D).

ISA, $H = 0$ m, $v = 0$ m/s

$n_N = 12\,500$ rpm

/72

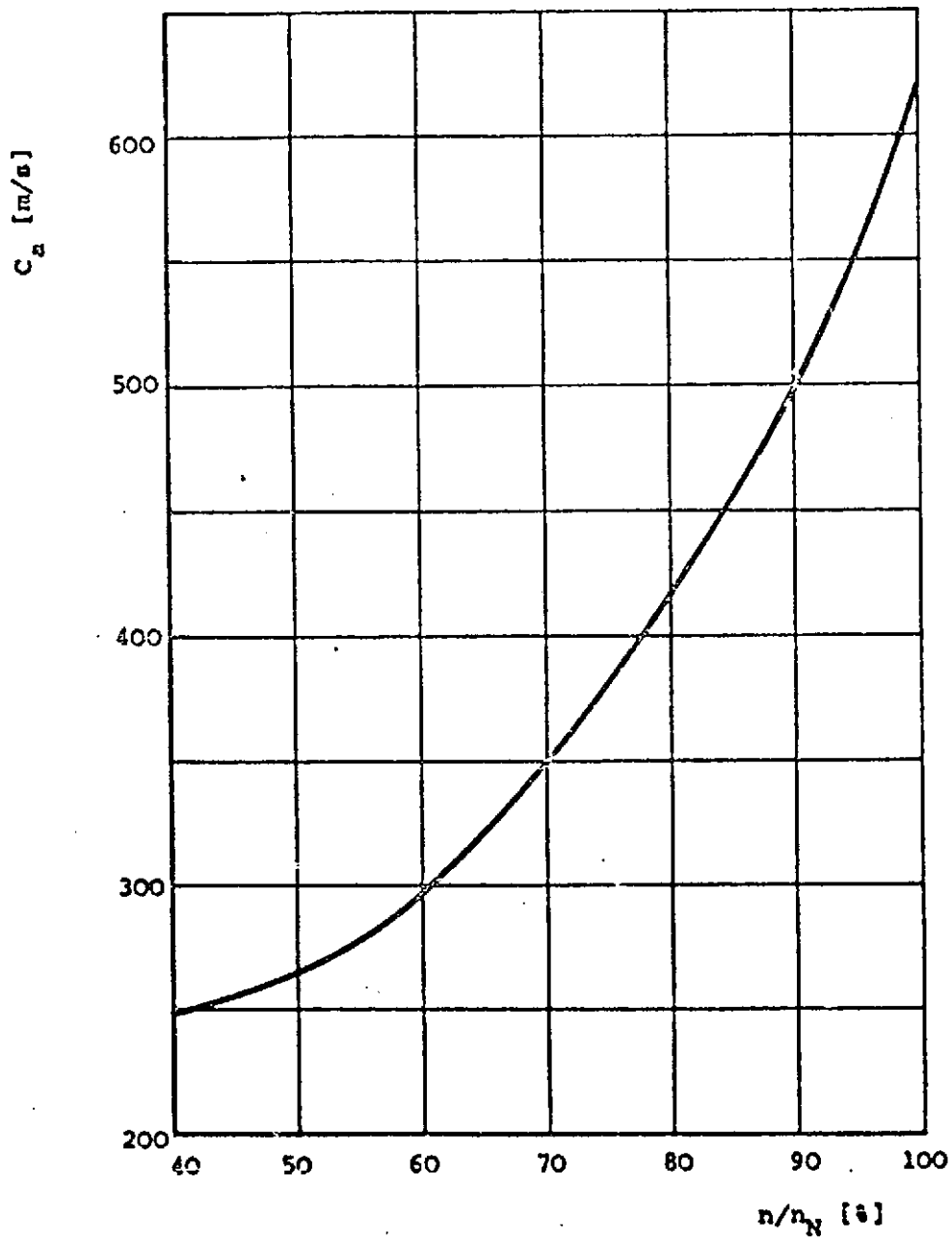


Fig. 1.2-6. Jet discharge velocity as a function of rpm (RB 162-4D).

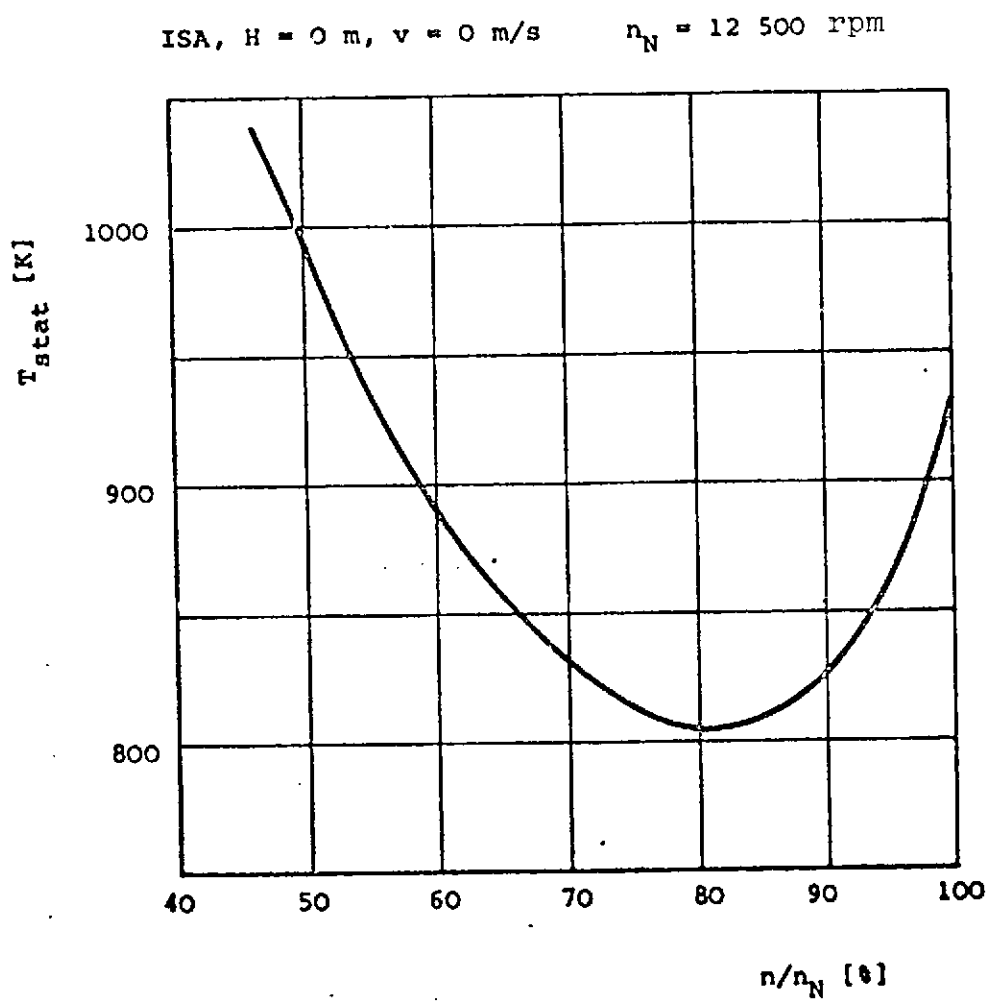


Fig. 1.2-7. Static jet discharge temperature as a function of rpm (RB 162-4D).

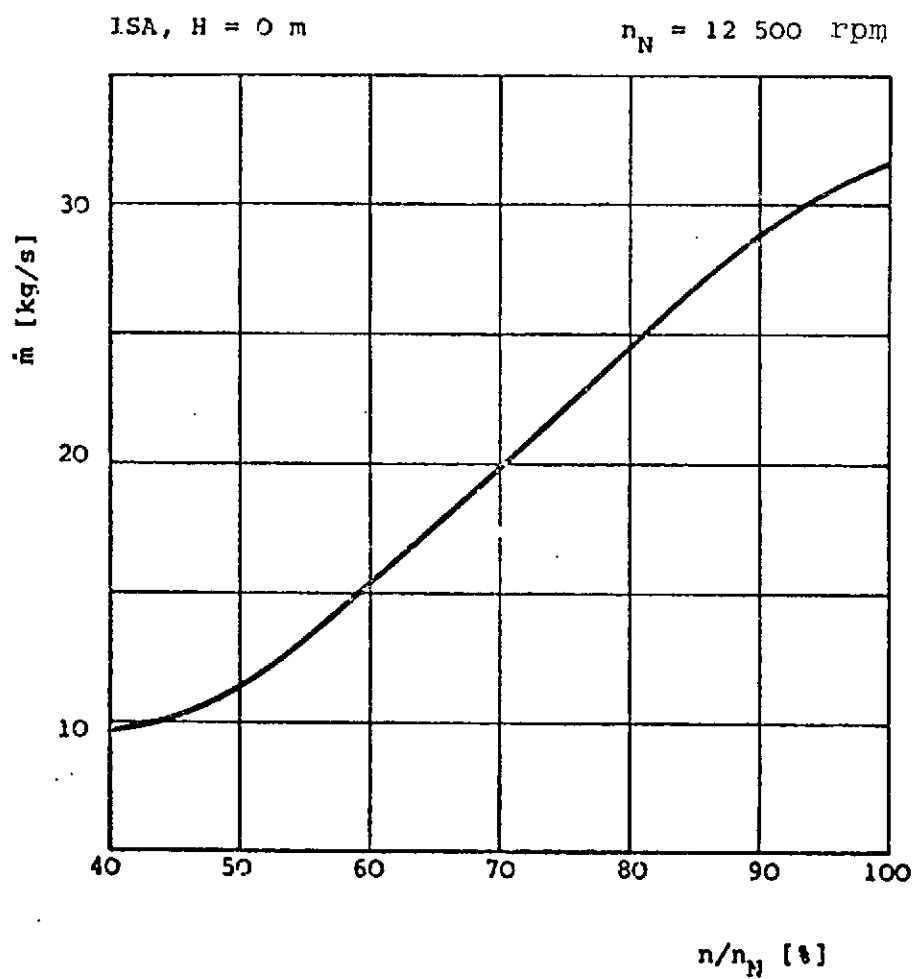


Fig. 1.2-8. Mass flow as a function of rpm (RB 162-4D).

$n_F/n_{FN} = 90\%$, $\theta = 100^\circ$ rel. to inlet axis, $R = 30.5$ m

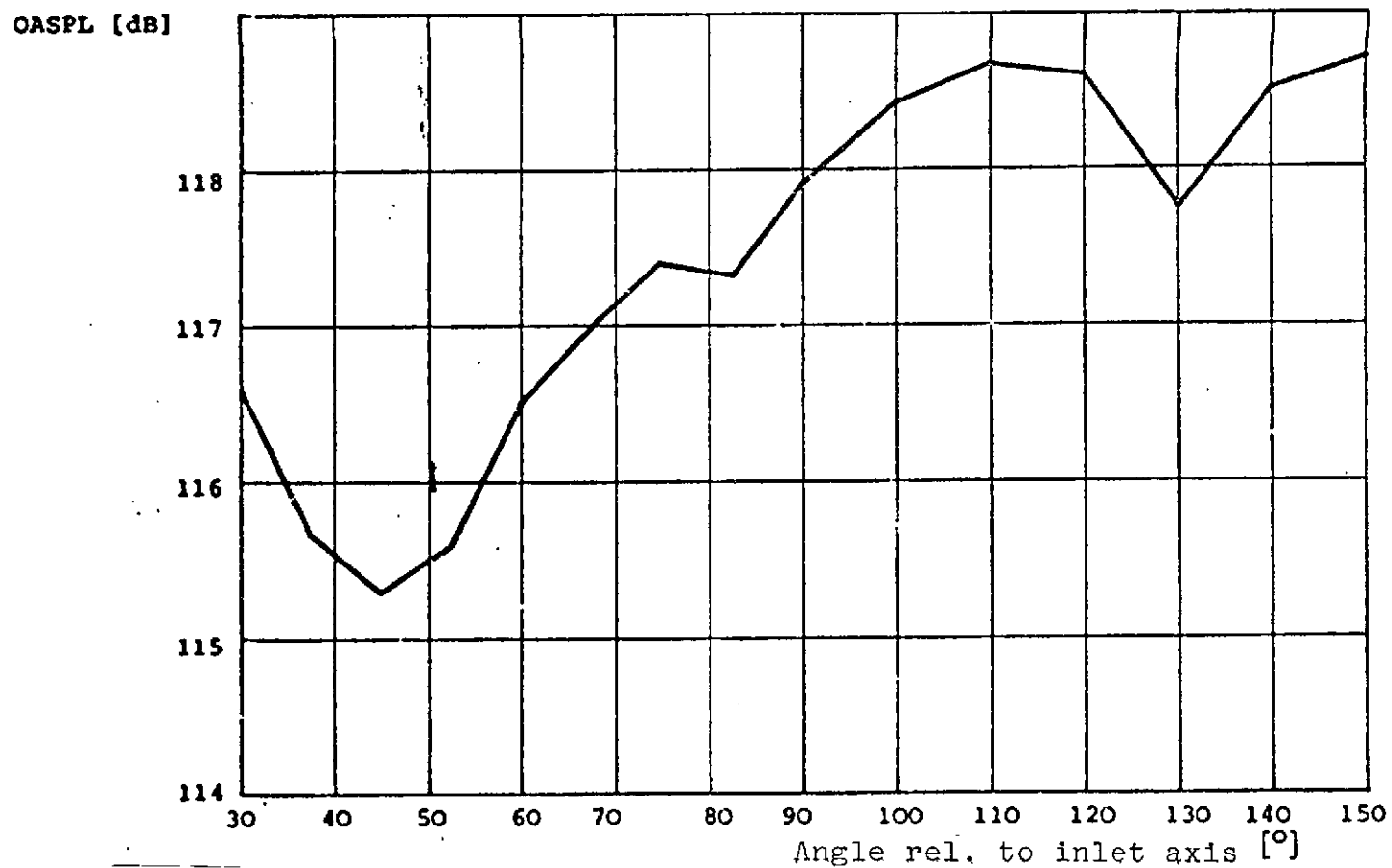


Fig. 1.3-1. BS Pg 5-2 peripheral noise level.

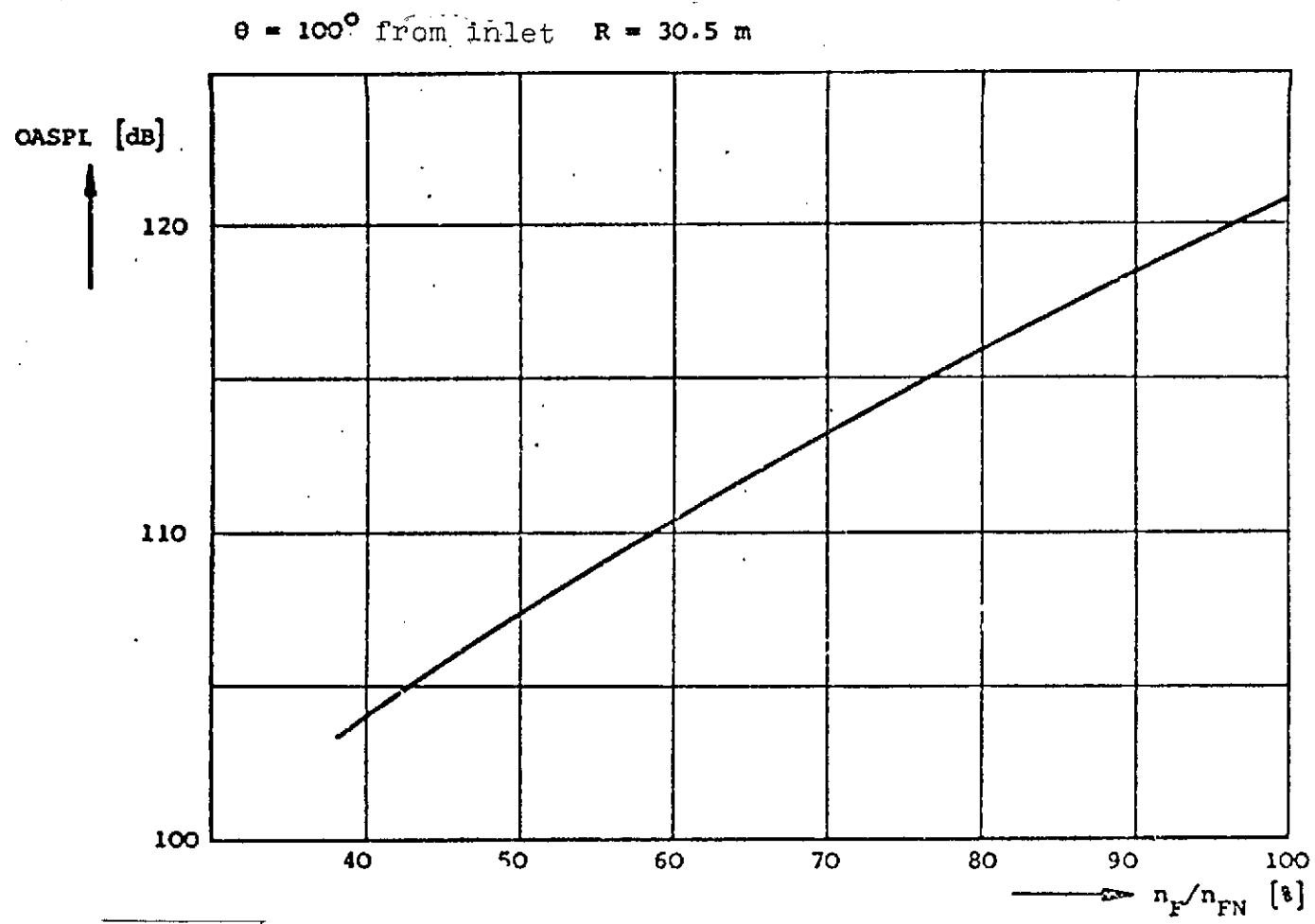


Fig. 1.3-2. BS Pg 5-2 overall sound level as a function of rpm.

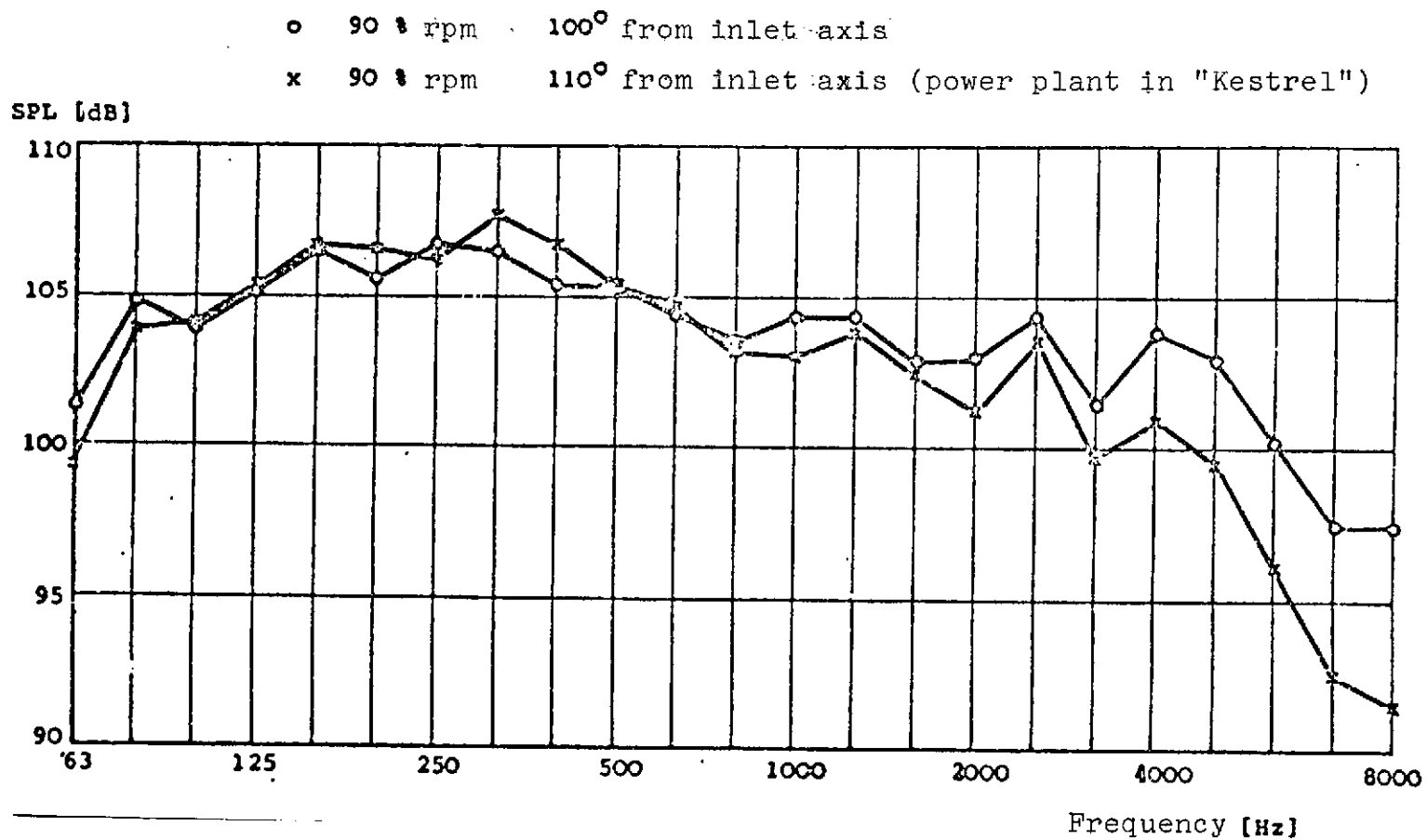


Fig. 1.3-3. 1/3-octave spectra for the BS Pg 5-12 at radius of 30.5 m.

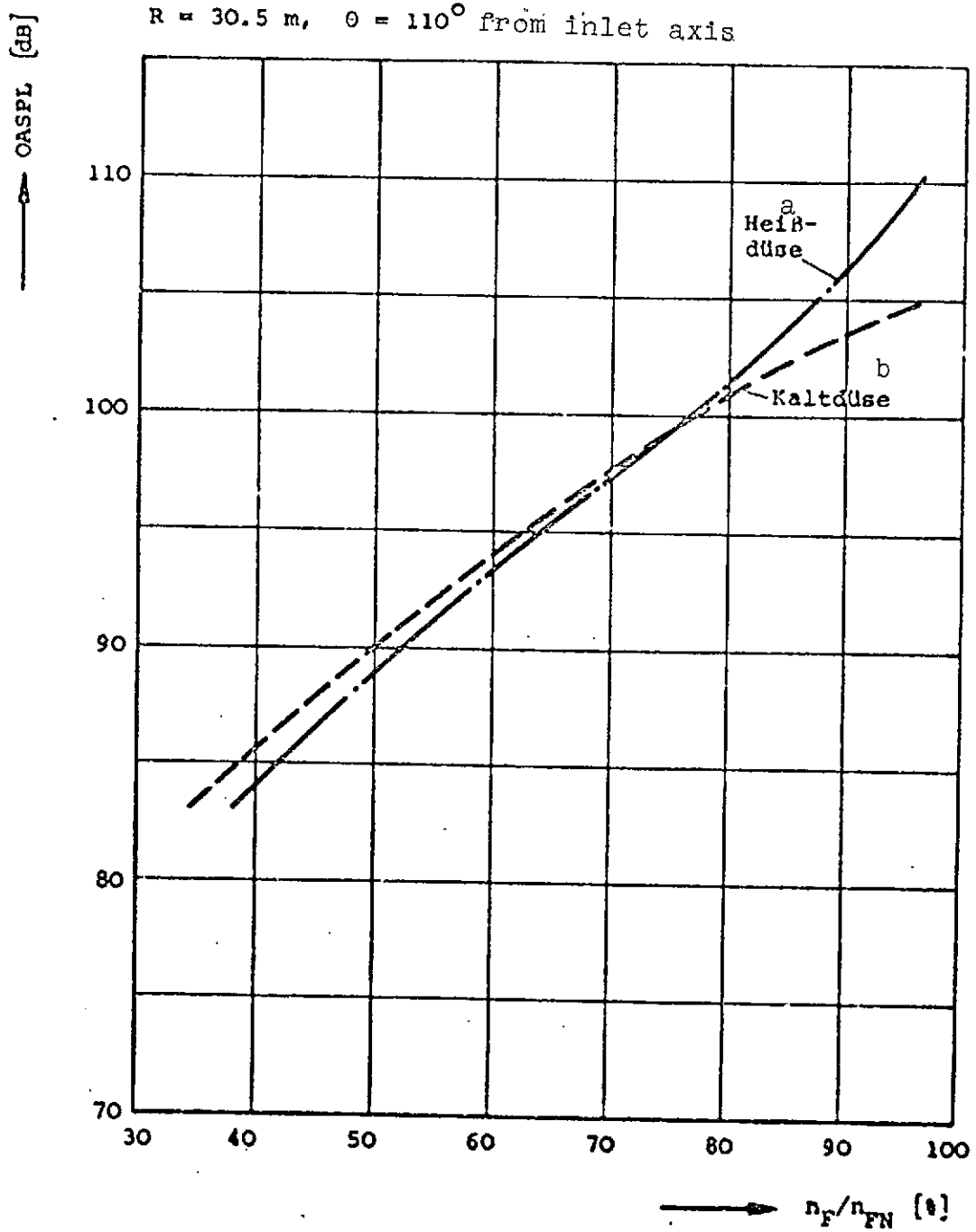


Fig. 1.3-4. BS Pg 5-2 sound components from hot and cold jets as a function of rpm.

Key: a. Hot nozzle
b. Cold nozzle

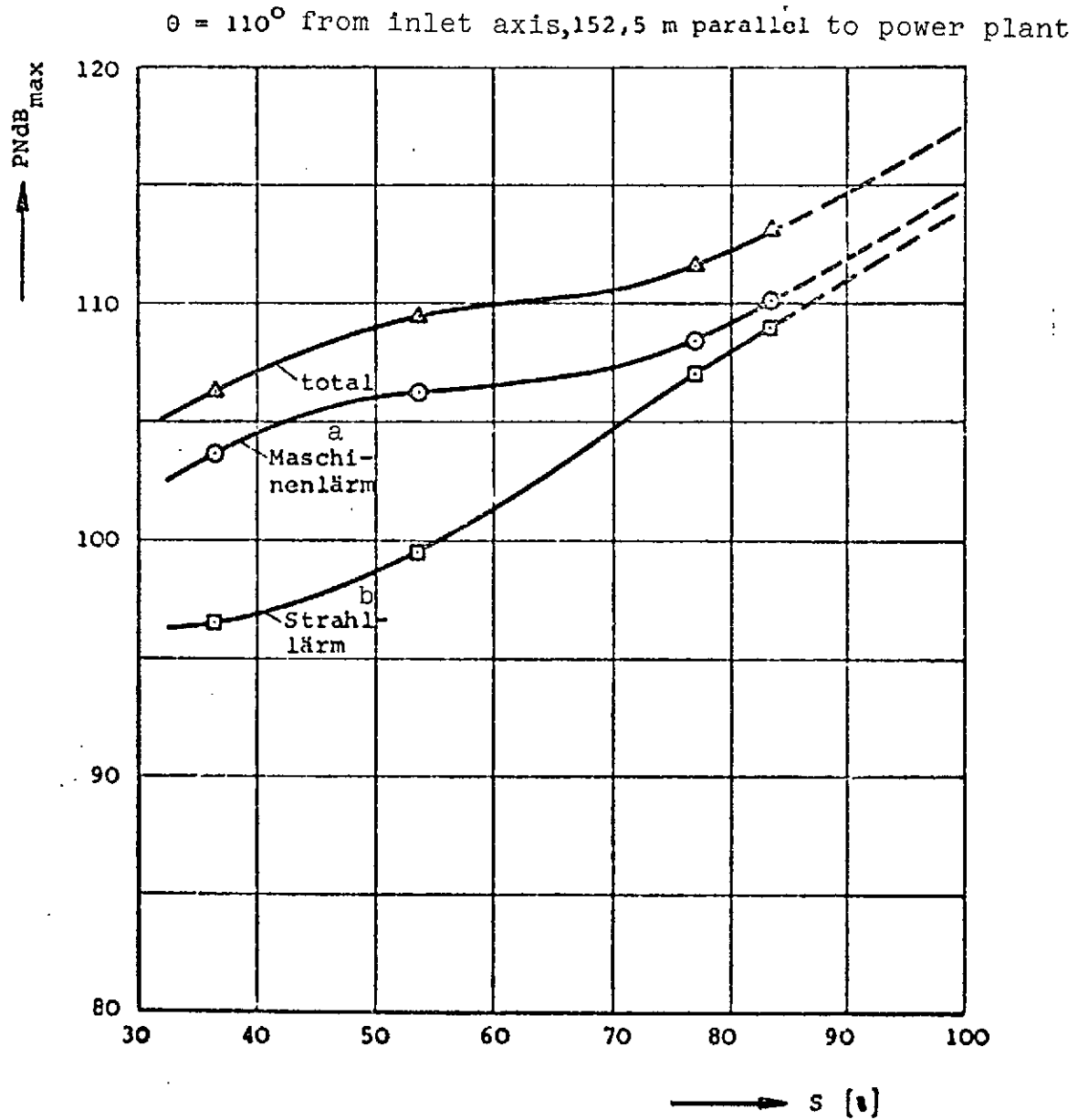


Fig. 1.3-5. BS Pg 5-2 jet and machinery noise as functions of thrust.

Key: a. Machinery noise
b. Jet noise

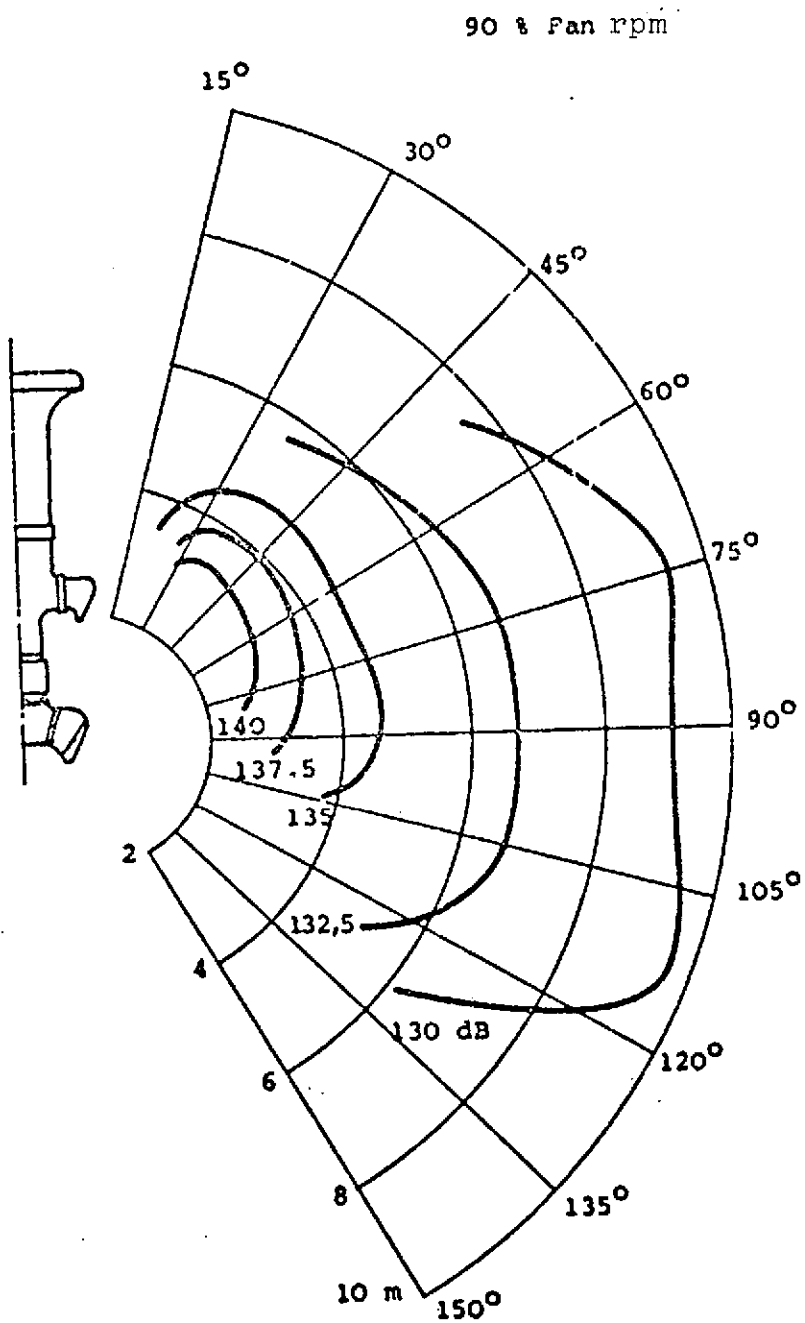


Fig. 1.3-6. BS Pg 3 overall near field sound level (cold nozzle).

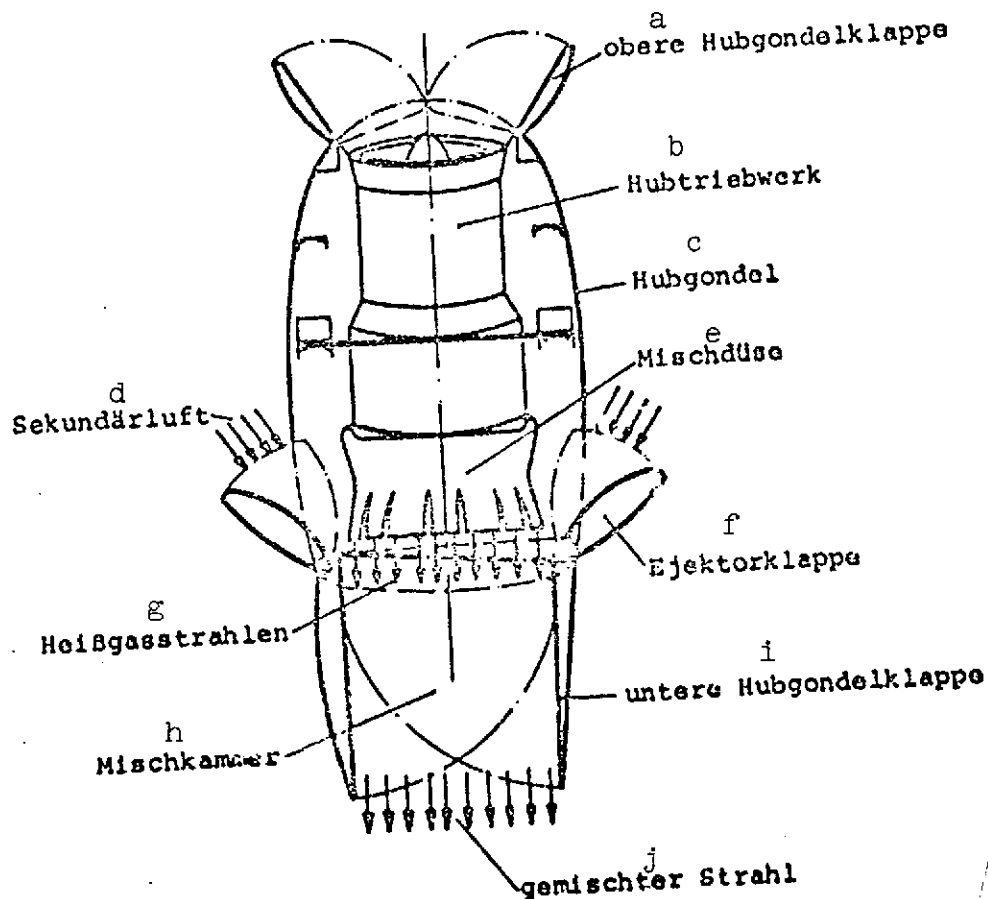


Fig. 1.4-1. Ejector thrust pod.

- Key:
- a. Upper thrust pod flap
 - b. Thrust power plant
 - c. Thrust pod
 - d. Secondary air
 - e. Mixing nozzle
 - f. Ejector flap
 - g. Hot gas jets
 - h. Mixing chamber
 - i. Lower thrust pod flap
 - j. Mixed jet

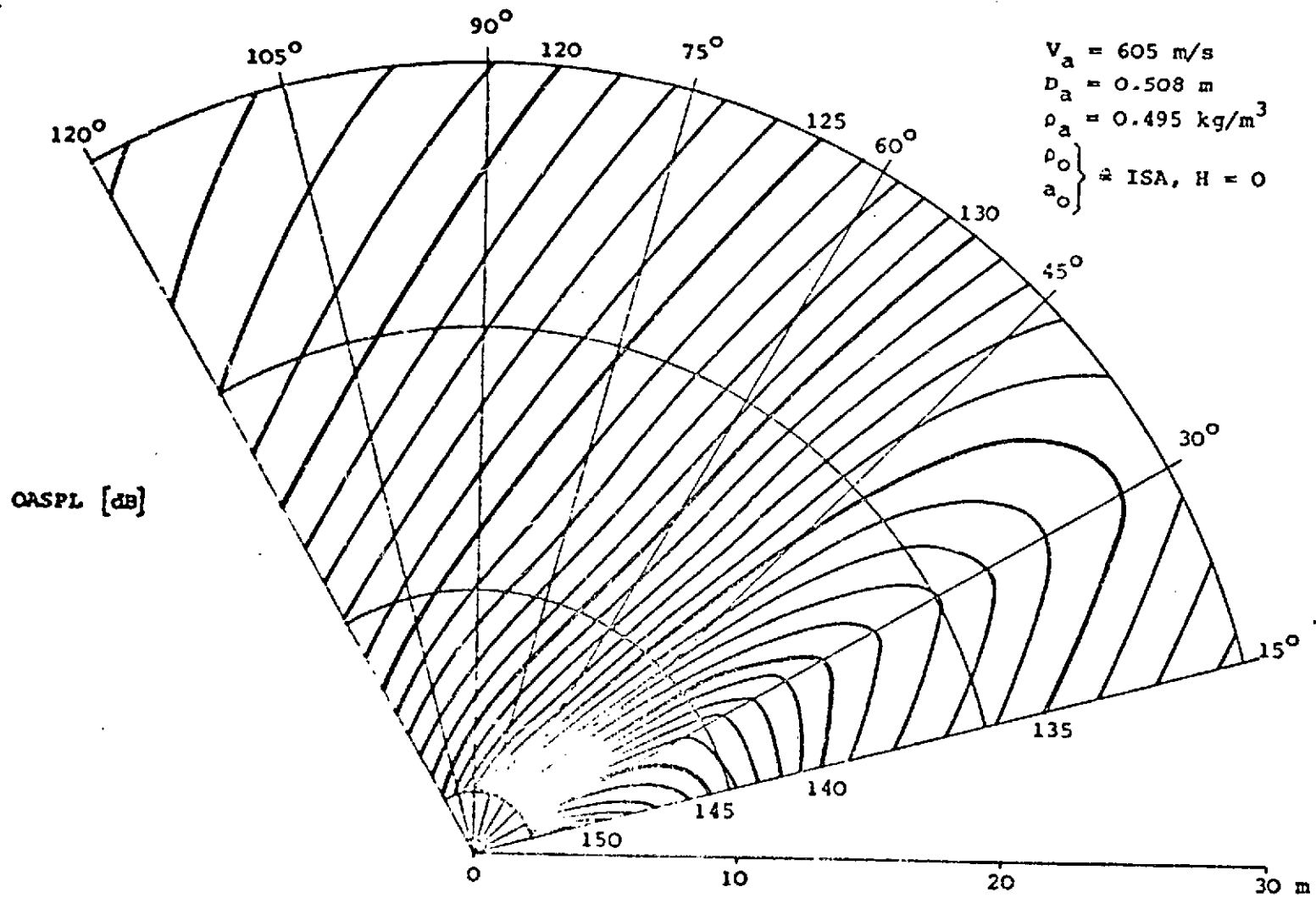


Fig. 2.1.1-1. AVON reference sound "carpet."

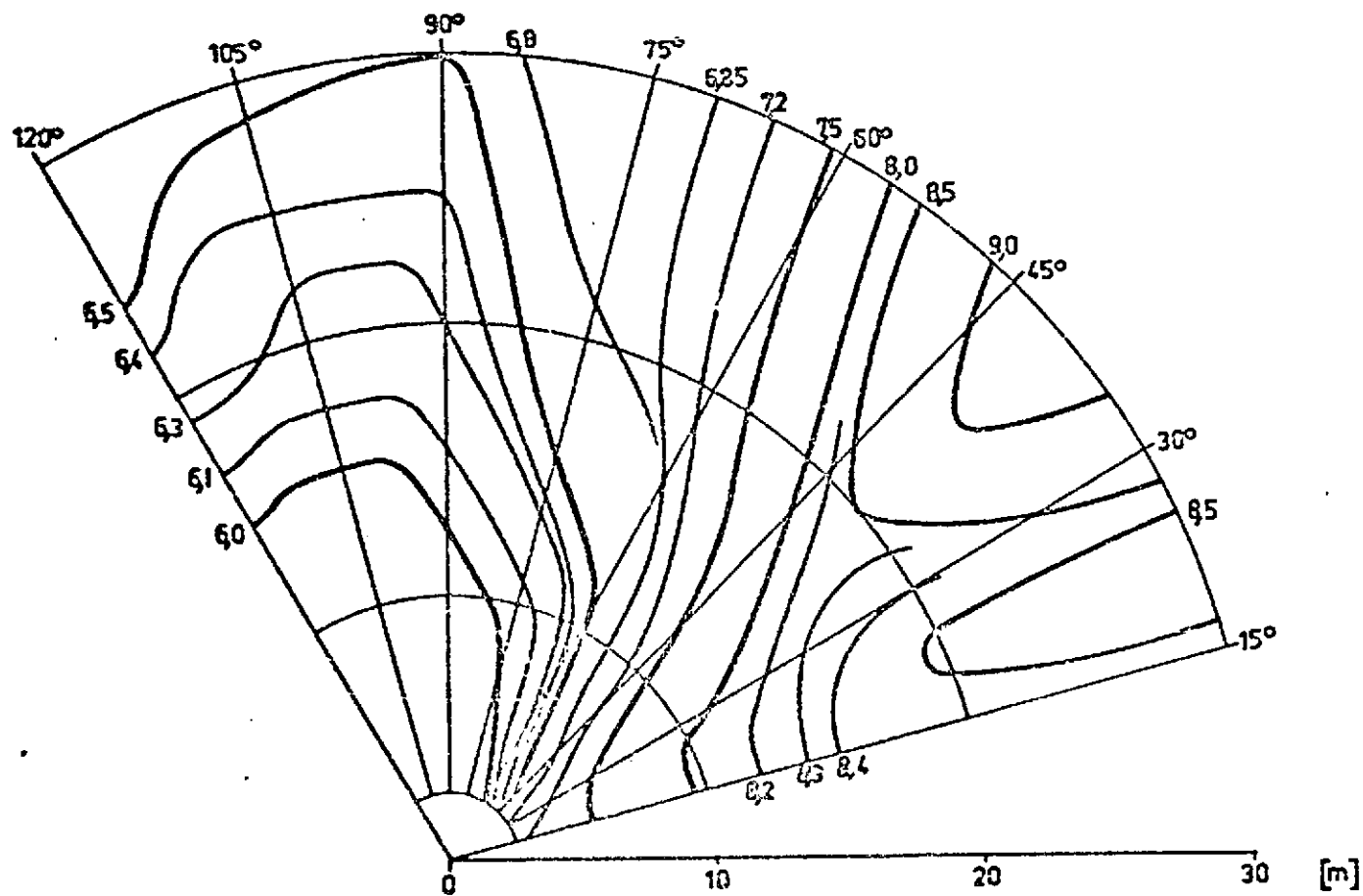


Fig. 2.1.1-2. AVON velocity exponent reference
"carpet!"

[Note: Commas in numerals are equivalent to decimal points.]

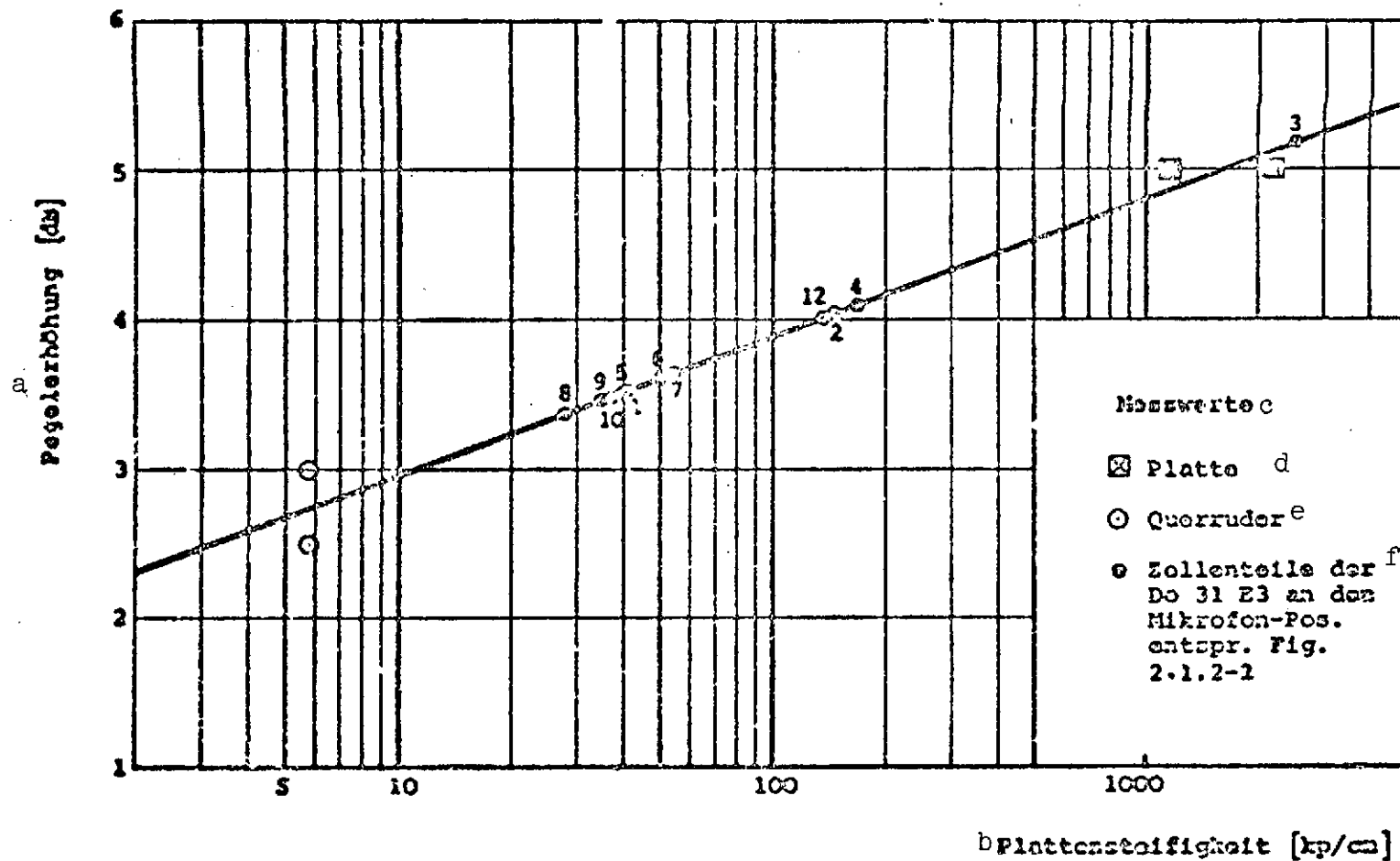


Fig. 2.1.2-1. Increases in noise level due to airframe reflection.

- Key:
- a. Increase in noise level
 - b. Panel rigidity
 - c. Measured values
 - d. Panel
 - e. Aileron
 - f. Do 31 E3 airframe components at the microphone positions shown in Fig. 2.1.2-2

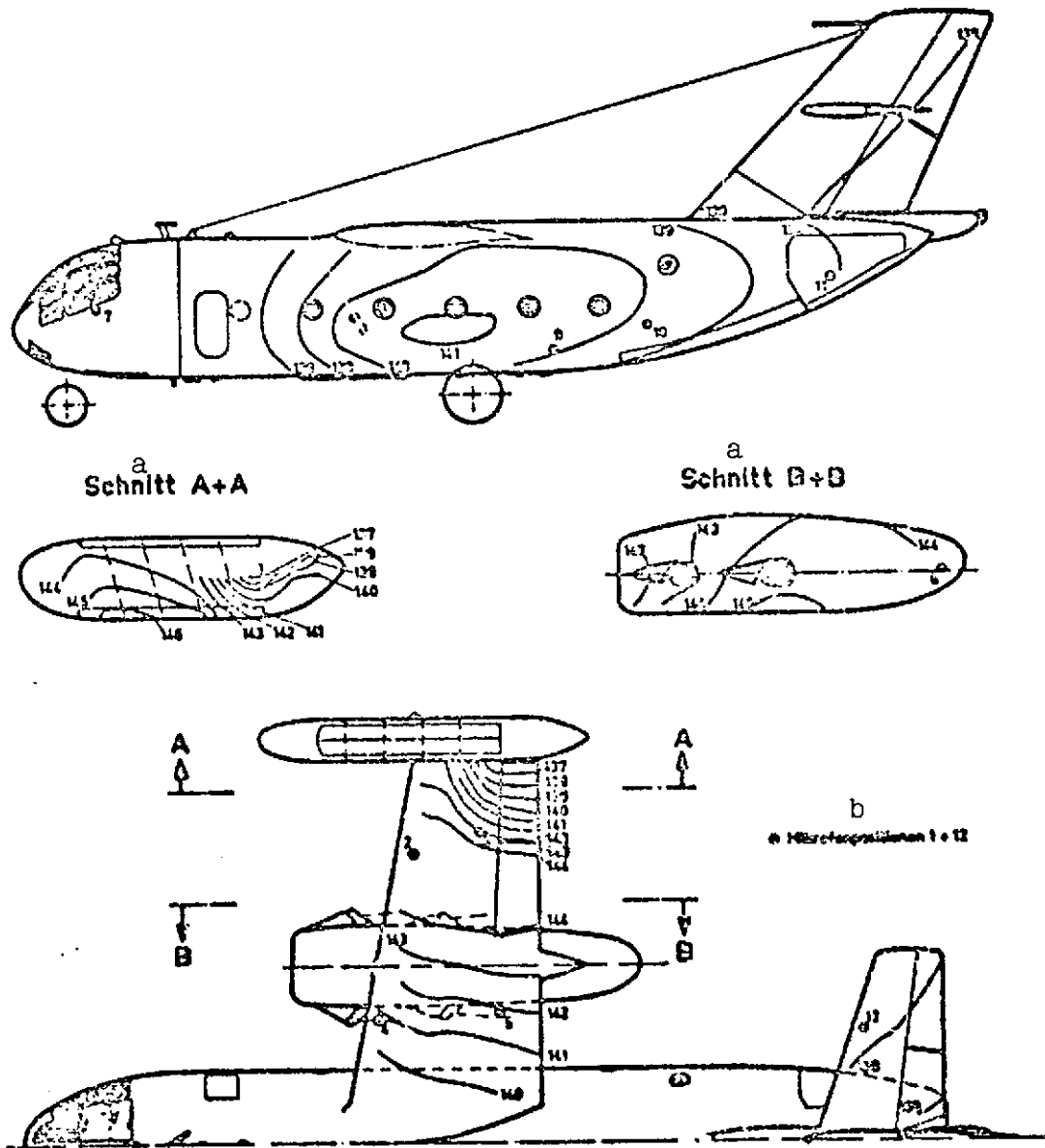


Fig. 2.1.2-2. Overall sound-level contours in the airframe of the Do 31 E3 during vertical takeoff (calculated at $H = 0$ m, jet noise with ground reflection only).

Key: a. Section
b. Microphone positions 1 + 12

TABLE 2.1.2-1. COMPARISON OF MEASURED AND CALCULATED VALUES OF TOTAL
SOUND LEVEL IN AIRFRAME OF Do 31 E3 (VTO, H = 0 m)

/86

Microphone number	1	2	3	4	5	6	7	8	9	10	11	12
Measured AOSPL [dB]	147	148	148	-	148	146	144	151	147	144	143	140
Calculated, with ground reflection OASPL [dB]	144	145	145	141	142	144	134	141	140	140	138	139
Calculated, with ground reflection and fan noise OASPL [dB]	144	145	145	141	142	144	137	144	141	140	138	139
Calculated, with ground reflection, fan and cascade noise OASPL [dB]	144	145	145	142	143	144	137	145	142	141	138	139
Increase in level due to airframe reflection [dB]	4	4	5	4	4	4	4	3	3	3	4	4
Calculated OASPL [dB]	148	149	150	146	147	148	141	148	145	144	142	143

* Without inlet noise

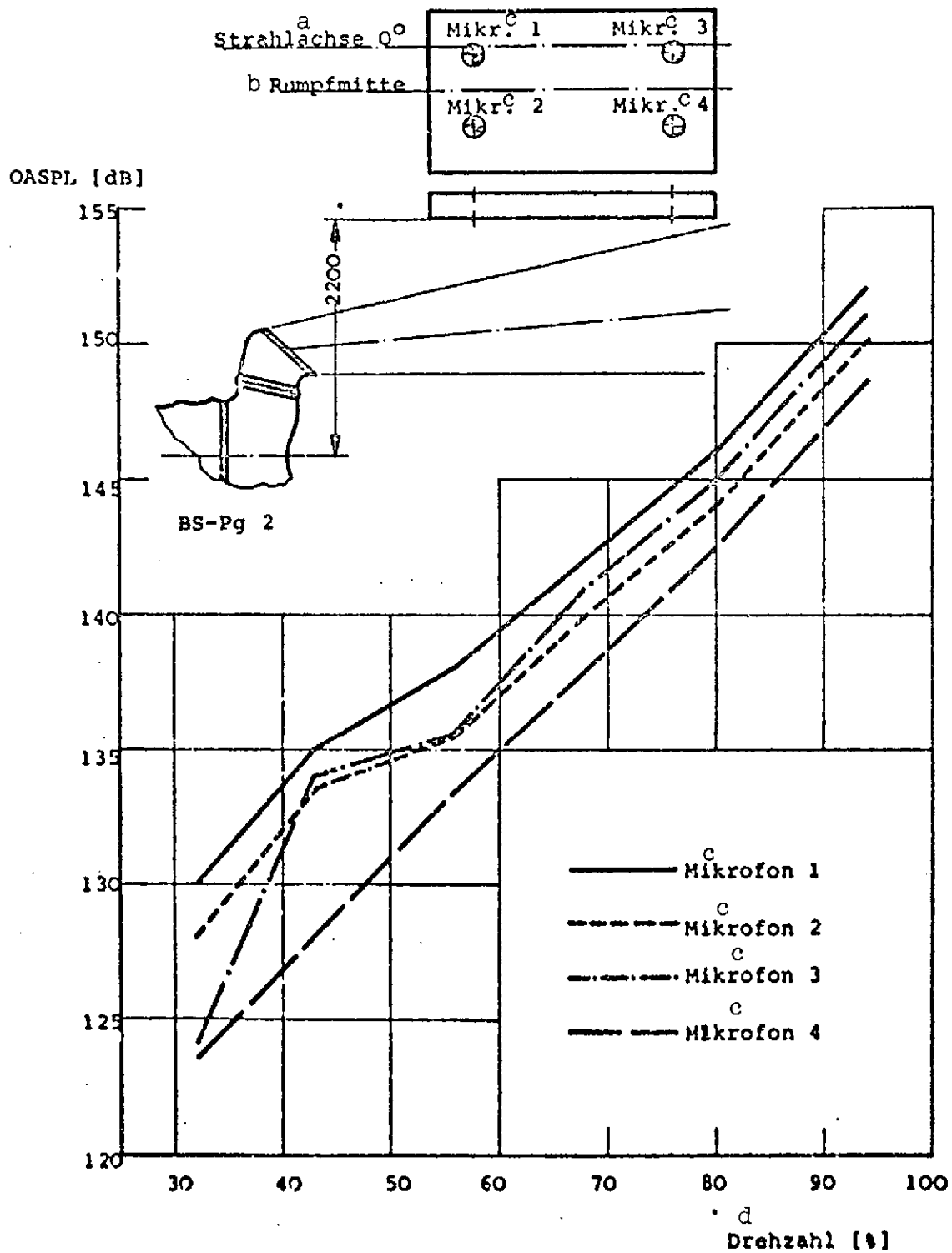


Fig. 2.2.1-1. Sound level in a fuselage segment as a function of power plant rpm.

Key: a. Jet axis
 b. Center of fuselage
 c. Microphone
 d. rpm

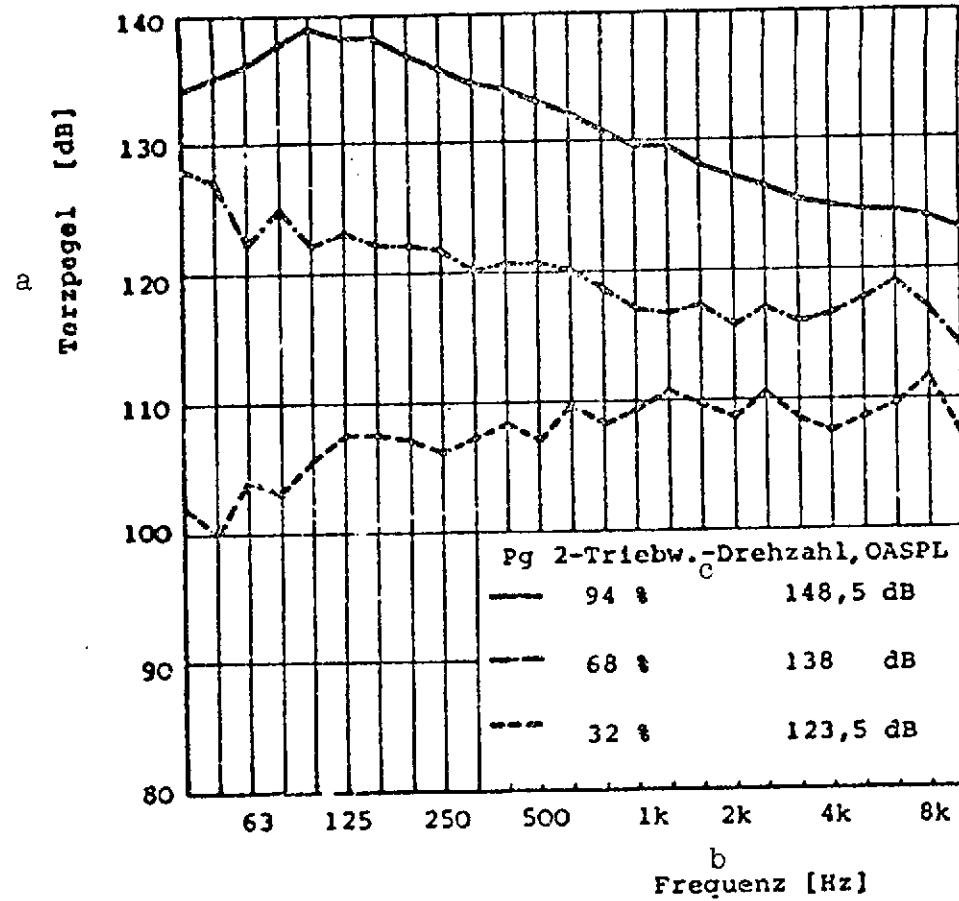


Fig. 2.2.1-2. Frequency spectra at microphone position 4.

Key: a. 1/3-octave level
 b. Frequency
 c. Pg 2 power plant rpm

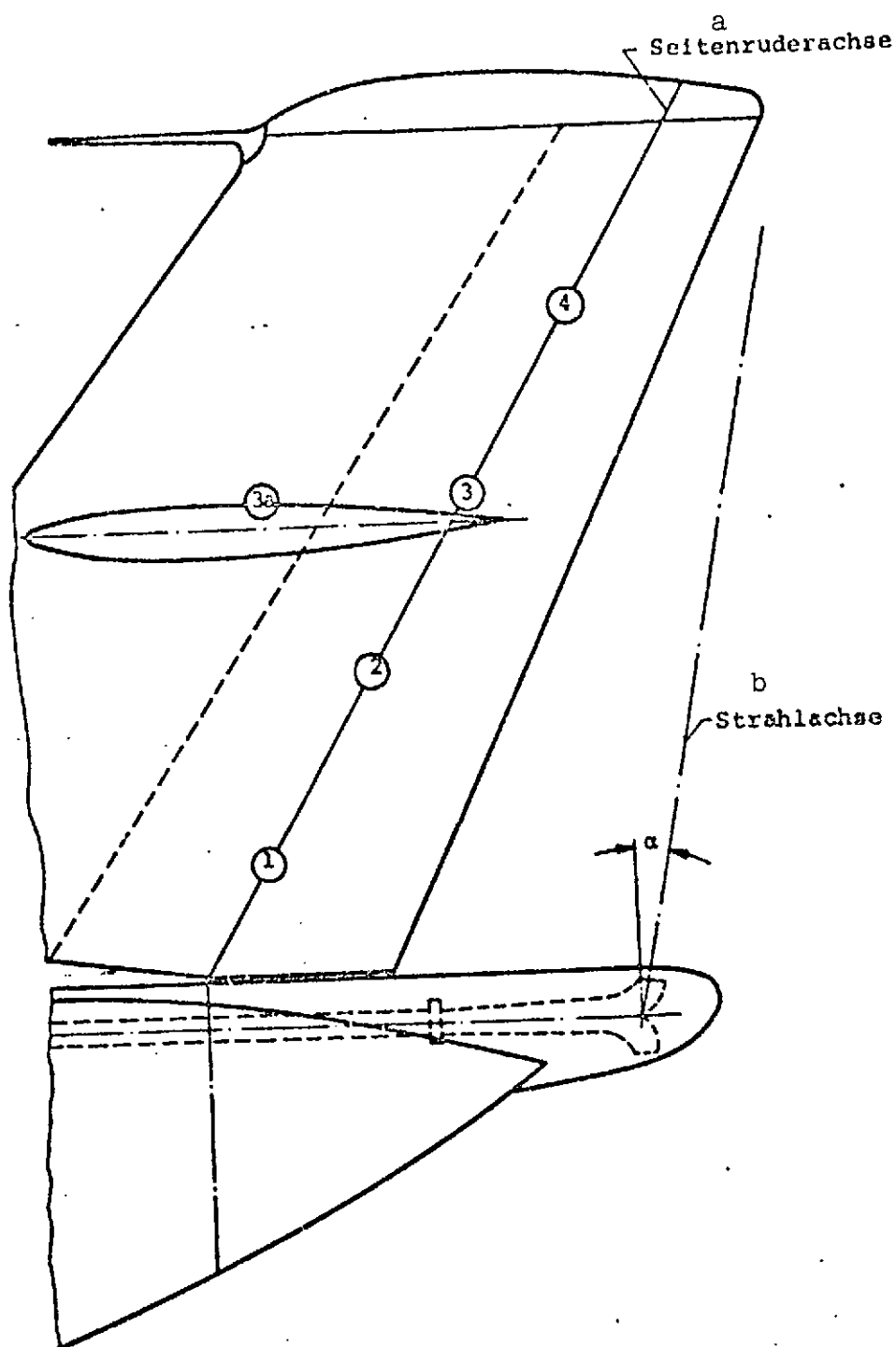


Fig. 2.2.1-3. Arrangement of measurement points.

Key: a. Rudder axis
b. Jet axis

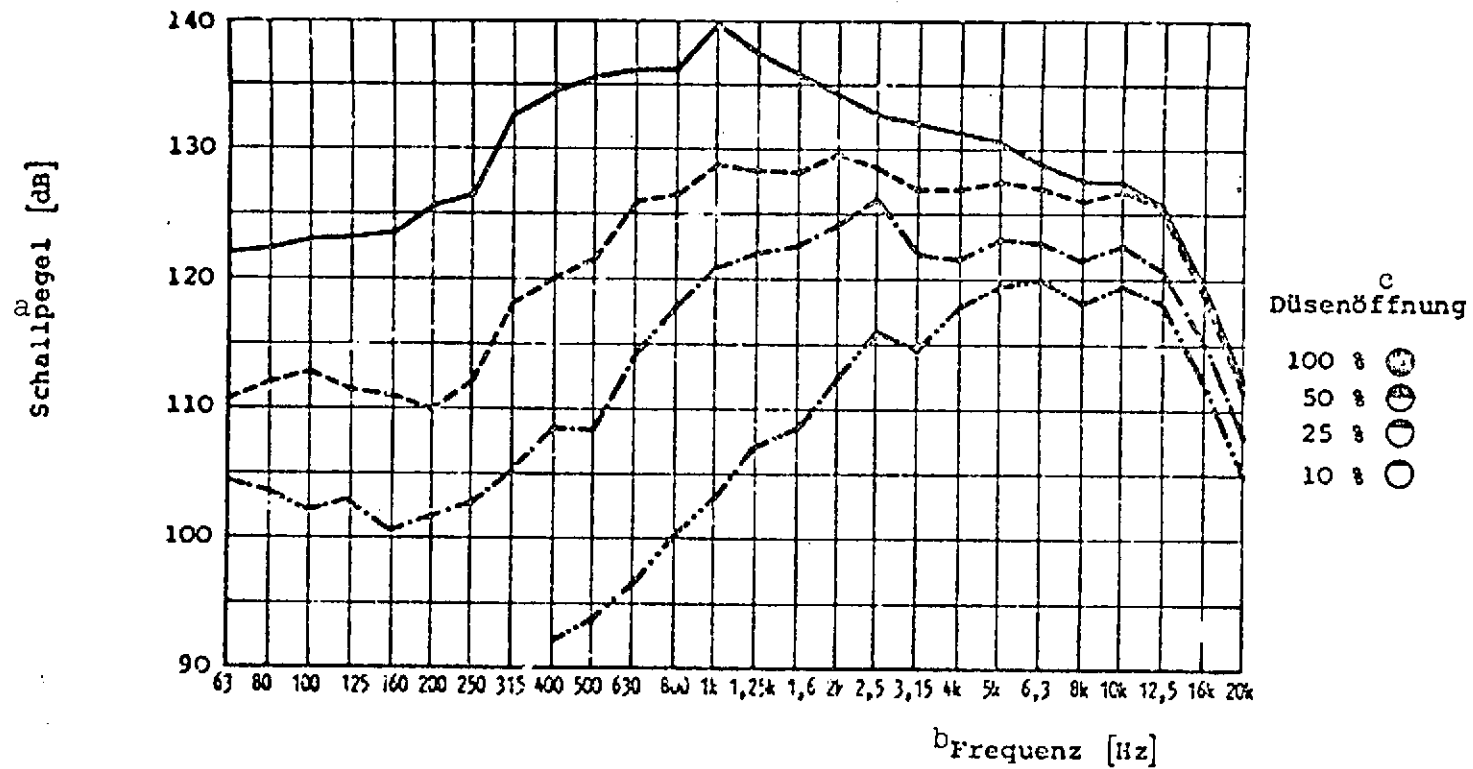


Fig. 2.2.1-4. 1/3-octave spectra of jet noise for various nozzle openings (measurement point 3; $p = 11.1$ technical atmospheres [= 1 kg force/cm²] absolute).

Key: a. Sound level
b. Frequency
c. Nozzle opening

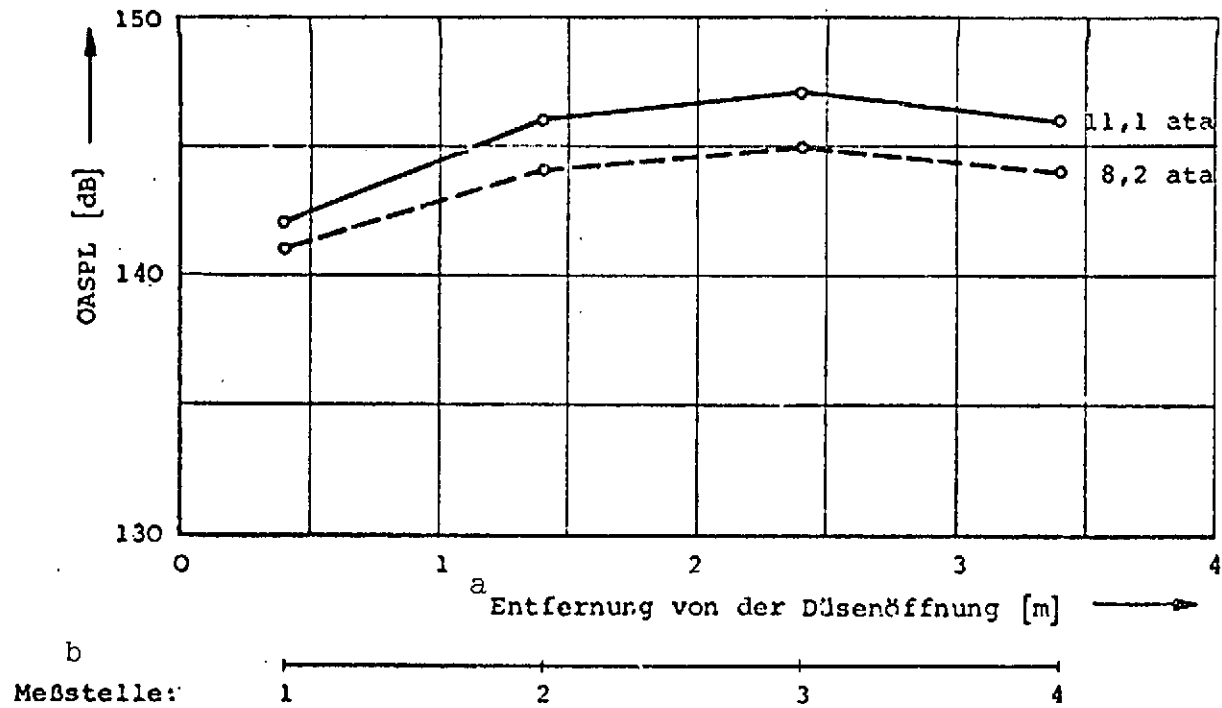


Fig. 2.2.1-5. Overall sound level as a function of distance (nozzle opening 100%).

Key: a. Distance from nozzle opening
 b. Measurement point
 ata = technical atmospheres absolute

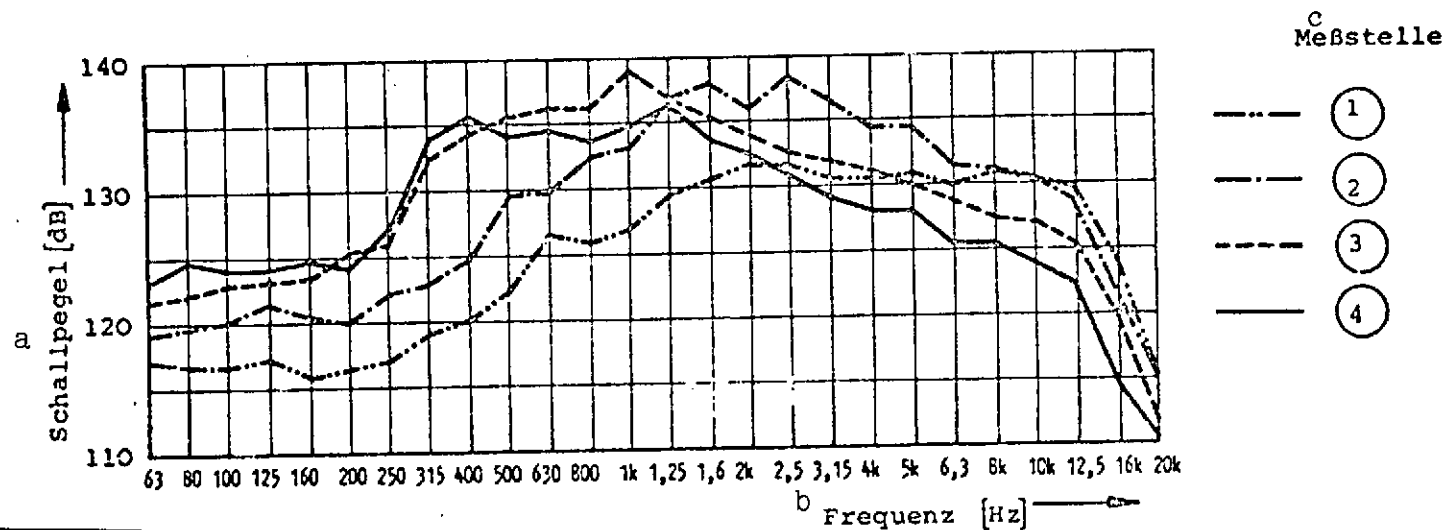
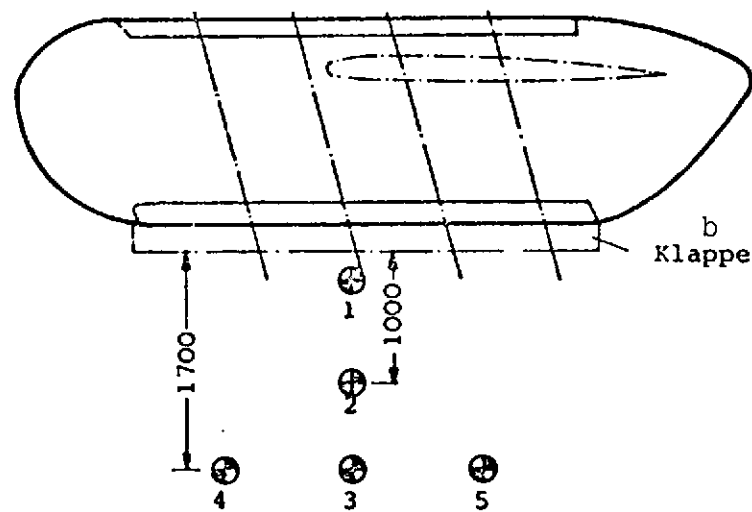
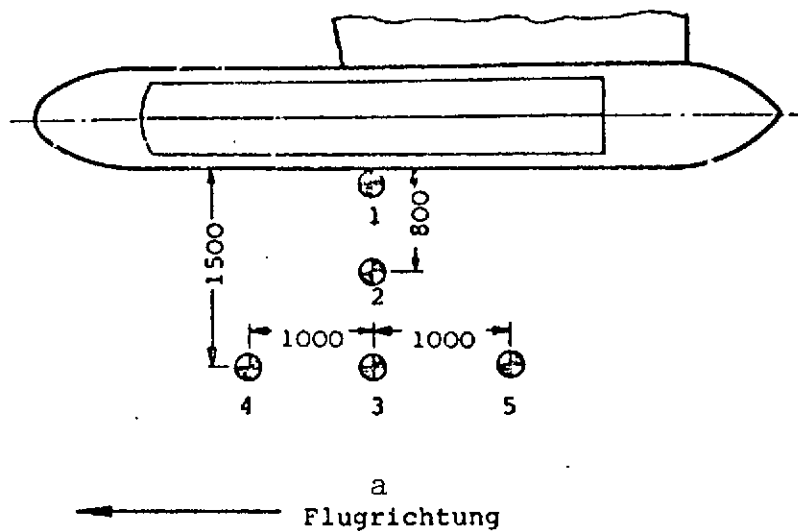


Fig. 2.2.1-6. 1/3-octave spectra of jet noise at different distances from the nozzle opening ($p = 11.1$ technical atmospheres absolute; nozzle opening 100%).

Key: a. Sound level
b. Frequency
c. Measurement point



c
Schallpegel [dB]

d Meßstelle	1	2	3	4	5
e Leerlauf	144	145	146	145	-
60 %	151	152	154	152	151
80 %	156	157	-	-	-

Fig. 2.2.1-7. Sound level of thrust power plants.

Key: a. Direction of flight
b. flaps
c. Sound level
d. Measurement point
e. Idle

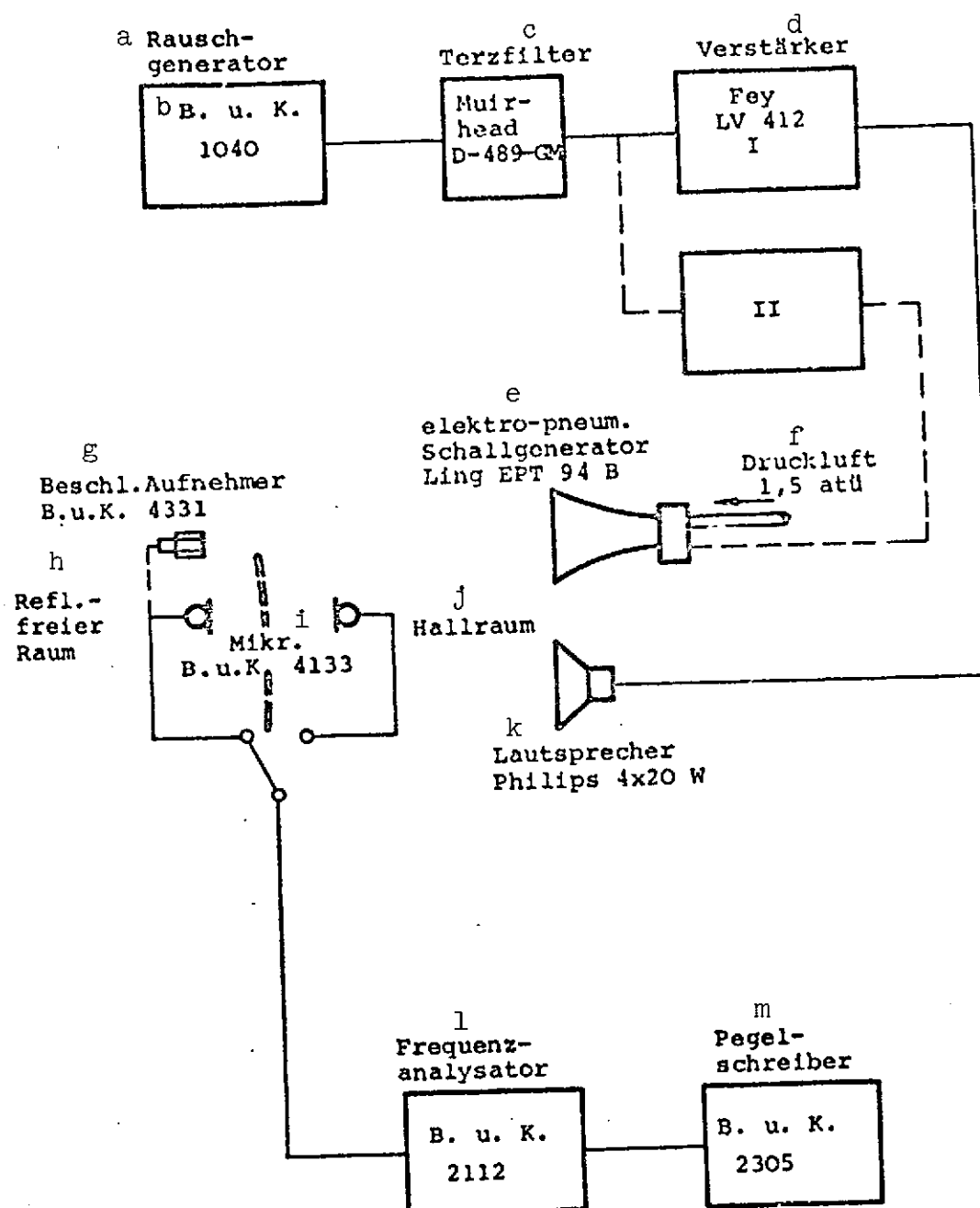
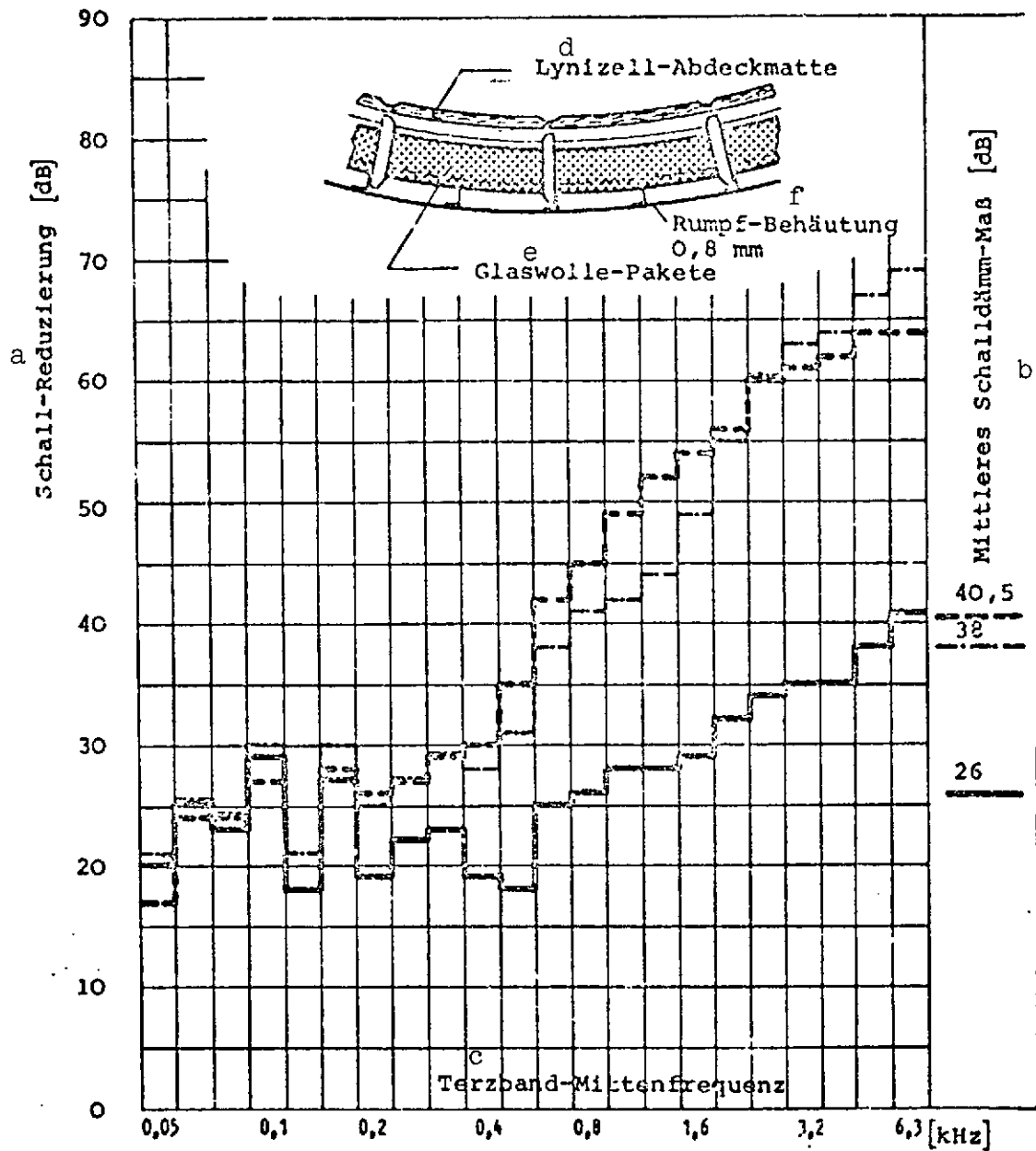


Fig. 2.2.2-1. Block diagram of measurement instruments.

- Key:
- | | |
|--|-------------------------|
| a. Noise generator | h. Reflection-less room |
| b. Manufacturer | i. Microphone |
| c. 1/3-octave filter | j. Live room |
| d. Amplifier | k. Loudspeaker |
| e. Electropneumatic sound source | l. Frequency analyzer |
| f. Compressed air at 1.5 technical atmospheres gauge | m. Level recorder |
| g. Acceleration pickup | |



e Glaswolle-Paket	g Flächengewicht insgesamt	h unverkleidet
80 mm dick j	1,24 kp/m ²	i Auskleidung I
120 mm dick	1,83 kp/m ²	j Auskleidung II

Fig. 2.2.2-2. Do 31 E3 acoustic damping (linings I and II).

Key:

- a. Reduction in sound
- b. Mean acoustic damping
- c. Center frequency of 1/3-octave band
- d. Lynizell covering pad
- e. Glass wool packet

- f. Fuselage skin
- g. Total weight per unit area
- h. Unlined
- i. Lining
- j. Thick

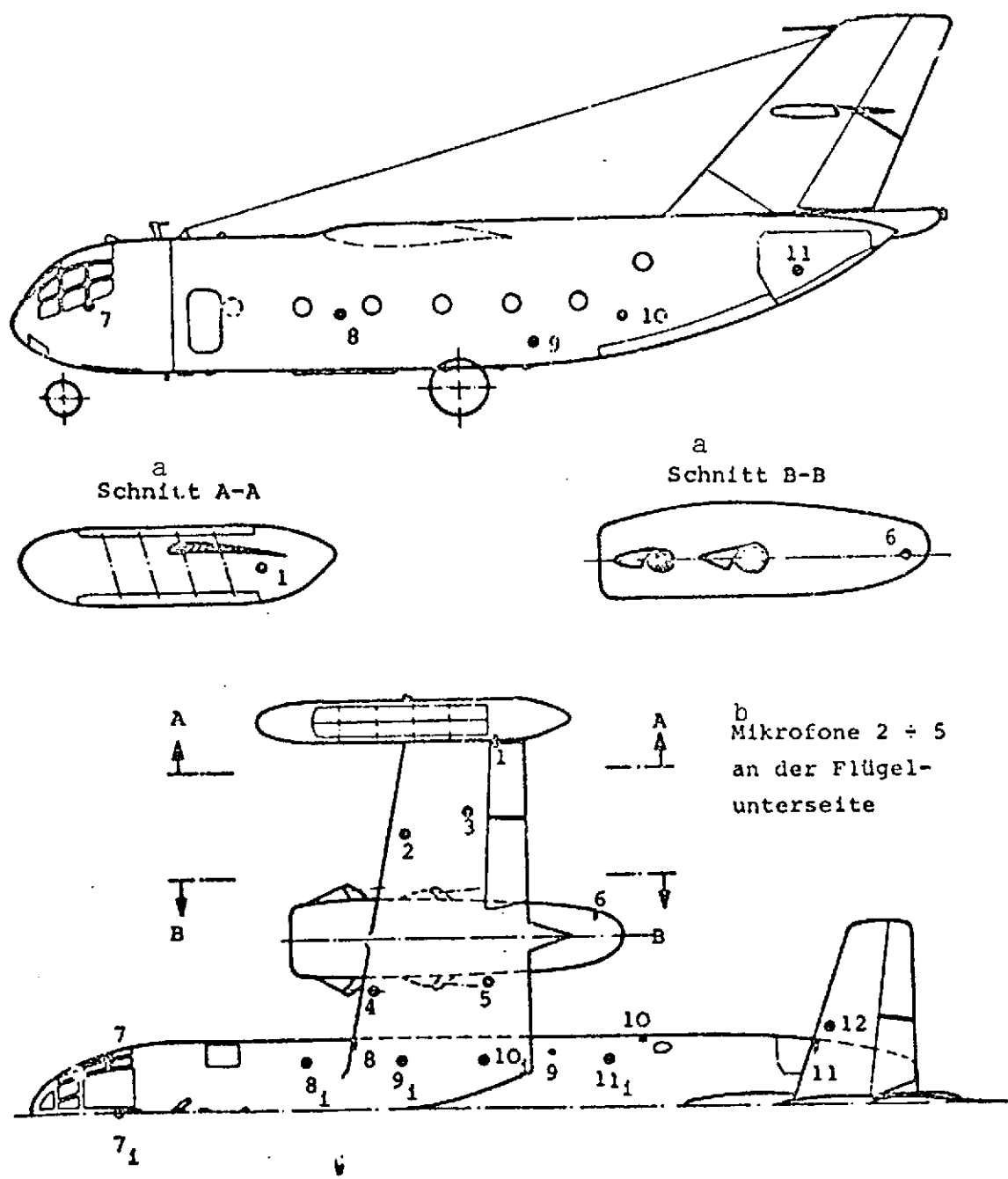


Fig. 2.2.3-1. Do 31 E3 microphone positions on airframe.

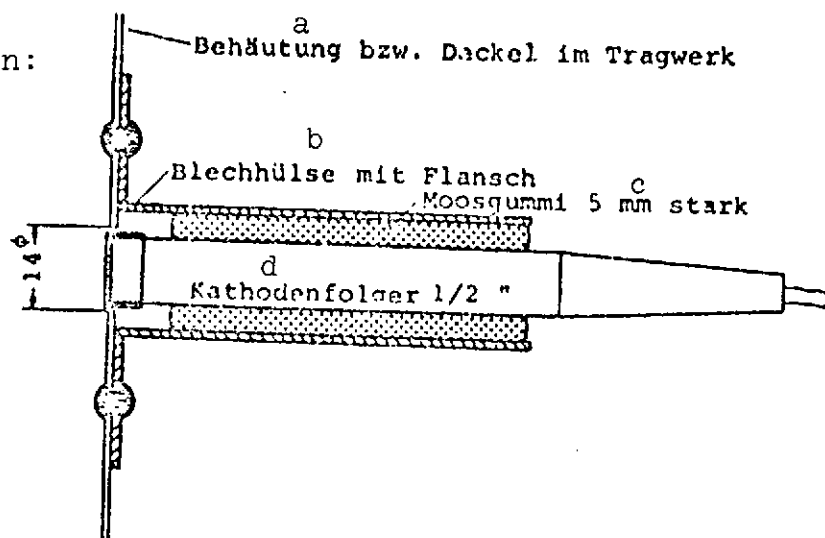
Key: a. Section
b. Microphones 2-5 on underside of wing

TABLE 2.2.3-1. Do 31 E3 CABIN NOISE LEVELS

Flight phase	BS F ₅ -2 rpm [8]	RB 162-40 rpm	Weighting	Sound levels at microphones				
				7 ₁	8 ₁	9 ₁	10 ₁	11 ₁
Conventional takeoff	83		dB (11n)	116-119	127-129	128-130	128-130	129-131
			dB (A)	113-115	125-127	125-127	126-127	126-128
Cruising I	72		dB (11n)	110-112	123-126	121-122	120-122	120-122
			dB (A)	107-108	119-121	119-121	118-119	118-119
Vertical landing	82	11.300	dB (11n)	120-122	126-128	127-129	127-128	126-128
			dB (A)	114-117	124-126	124-126	124-126	124-126

The values listed apply to the Do 31 E3 without lining

Microphone installation:



Remark: The sheet metal jacket was longitudinally slotted.
A tension ring puts light pressure on the foam rubber.

Fig. 2.2.4-1. Microphone installation and measurement setup.

Key: a. Skin or cover in wing assembly
b. Sheet metal jacket with flange
c. Foam rubber, 5 mm thick
d. Cathode follower

[Fig. 2.2.4-1 continued on following page]

Measurement setup: Microphone positions

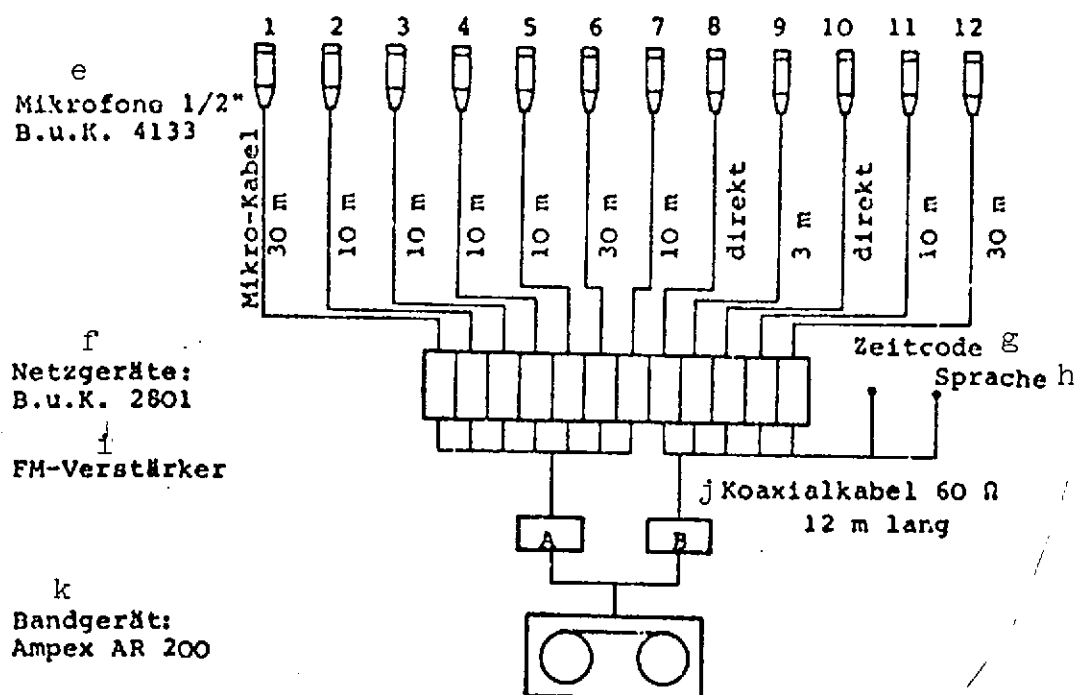


Fig. 2.2.4-1

Key: e. Microphones
 f. Power supply units
 g. Time code
 h. Speech
 i. FM amplifier
 j. Coaxial cable, 12 m long
 k. Tape recorder

[cont.]

TABLE 2.2.4-1. Do 31 E3 SOUND LEVELS IN AIRFRAME (OVERVIEW)

/99

Flight phase	Trial No.	85 Pg 5-2		RB 162-40 [rpm]	Sound levels [dB] at microphones											
		rpm	nozzle [x] setting		1	2	3	4	5	6	7	8	9	10	11	12
Vertical takeoff, on ground	61	64	70°	11200-11600	143-146	146-149	145-147	-	159-161	140-142	140-142	145-149	144-149	138-142	135-139	130-142
	61	60	70°	11200-11600	143-145	147-150	145-147	-	158-162	144-146	137-141	146-149	144-148	130-141	138-141	142-145
	61	52	70°	10400	140-142	144-146	142-144	-	154-155	140-142	137-139	142-144	141-146	135-138	136-140	139-142
Vertical takeoff, with liftoff	58	39	76°	10500-10000	145-148	-	146-149	-	147-151	150-153	142-144	151-152	148-150	-	142-146	-
	50	81	80°	11500-11800	145-147	146-148	146-148	-	140-150	145-146	143-145	151-152	147-150	142-144	138-143	157-160
Hover I, alt. 14.5 + 16 m	60	81	90°	11400-11700	141-143	143-144	142-144	-	141-142	140-143	137-138	145-147	141-143	136-138	136-137	134-136
Hover II, alt. 21 + 23 m	60	81	90°	11400-11700	140-142	143-144	143-144	-	142-143	142-143	136-139	148-149	142-143	136-138	135-137	134-136
Vertical landing	59	81	99°	11000	145-147	-	146-148	-	144-146	144-145	140-144	140-150	145-147	-	141-144	-
	60	81	99°	11400-11700	144-145	146-148	145-147	-	144-145	145-148	140-142	148-150	146-150	143-147	141-144	143-145
Conventional takeoff	59	86	34-36°		147-148	-	147-148	-	153-157	147-152	142-149	150-151	147-149	-	142-145	-
	62	83	10°		-	147-148	145-146	-	150-151	-	-	-	-	-	-	-
Cruising I	58	72	35°		139-141	-	139-141	-	145-146	142-145	132-133	144-146	135-137	-	136-142	-
	59	72	34-35°		141-142	-	141-142	-	146-148	147-152	130-132	146-147	136-138	-	135-141	-
	62	72	10°		-	143-144	141-142	-	145-146	-	-	-	-	-	-	-
Cruising II	58	88	36°		144-145	-	145-146	-	148-149	151-154	135-137	149-150	143-144	-	137-140	-
Conventional landing	58	74	10/76°		140-141	-	-	-	144-146	147-151	149-151	145-146	137-138	-	136-142	-

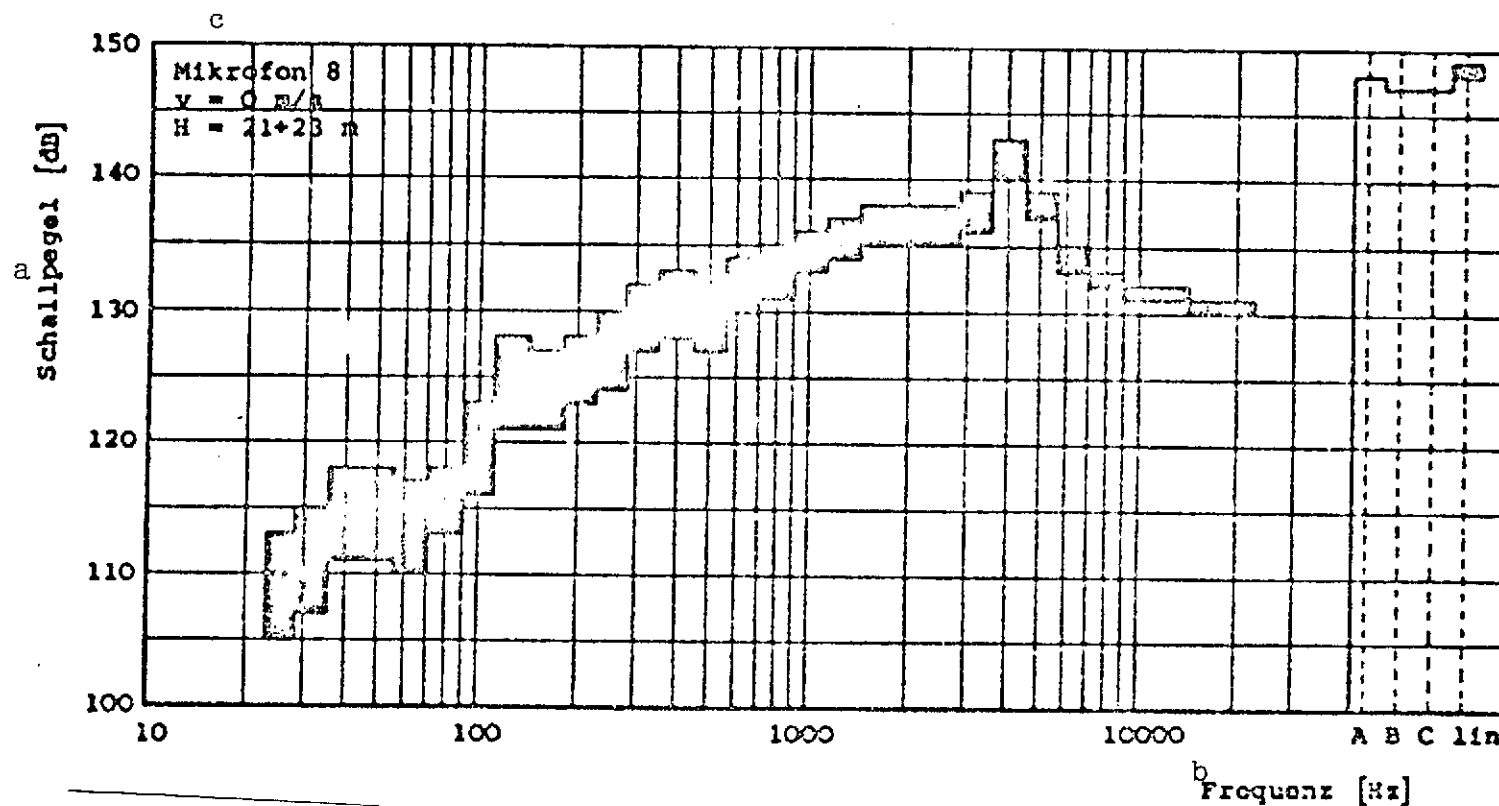


Fig. 2.2.4-2. Measured frequency spectrum in Do 31 E3 airframe. Phase of flight: vertical climb ($H = 21 - 23 \text{ m}$) (two cruising power plants at 81% n_F , nozzle setting 98° , eight lift power plants at 11,400-11,700 rpm).

Key: a. Sound levels
 b. Frequency
 c. Microphone

TABLE 2.2.4-3. Do 31 E3 SOUND LEVELS IN AIRFRAME
 PHASE OF FLIGHT: CRUISING II
 (2 CRUISING POWER PLANTS AT 88% n_F , NOZZLE SETTING 36°,
 $v = 77 - 90$ m/s)

/102

Reproduced from
 best available copy.



1/3- octave band	Microphones											
	1	2	3	4	5	6	7	8	9	10	11	12
25	106-116		101-111		110-120	127-134	126-133	113-116	113-120		116-123	
31.5	106-115		102-111		111-119	124-134	125-135	112-120	113-120		117-124	
40	107-118		104-113		113-120	124-135	126-137	115-123	117-124		119-128	
50	112-120		105-113		113-120	133-143	136-147	115-124	117-126		121-129	
63	115-124		106-115		115-122	133-143	136-147	115-126	120-128		124-132	
80	115-123		106-114		115-120	133-143	133-142	110-124	120-128		121-129	
100	118-124		113-122		121-128	135-145	136-143	120-128	122-130		124-136	
125	120-127		117-125		124-133	140-145	136-143	123-130	125-132		126-138	
160	122-129		118-124		122-130	140-146	136-143	123-130	123-130		129-136	
200	123-129		117-126		123-130	138-145	137-142	125-132	126-130		129-137	
250	124-130		123-129		124-131	138-145	137-143	125-133	125-130		129-139	
315	124-129		124-130		127-132	138-145	138-142	129-135	129-135		129-137	
400	125-131		127-132		130-135	137-142	137-142	131-137	126-132		129-136	
500	126-131		128-133		131-136	136-141	136-141	133-137	127-132		129-136	
630	127-131		130-134		132-137	135-140	133-138	130-137	128-133		129-136	
800	126-130		131-136		133-137	135-139	134-138	132-136	129-133		129-135	
1000	128-132		132-136		134-138	134-138	132-136	130-134	129-132		129-135	
1250	130-134		133-136		136-139	133-137	129-134	132-137	128-133		129-135	
1600	131-136		133-136		136-137	133-135	129-134	132-140	127-132		129-135	
2000	132-135		133-135		135-138	132-136	129-134	130-134	127-130		129-134	
2500	132-135		133-135		137-139	129-135	129-134	136-139	127-130		129-134	
3150	132-134		132-134		136-138	129-132	129-132	136-137	127-130		129-134	
4000	134-136		133-135		136-138	128-131	129-135	135-137	128-131		129-135	
5000	130-132		133-135		135-137	127-129	129-132	135-137	126-131		129-135	
6300	129-130		132-134		133-135	126-127	119-121	112-134	128-130		126-127	
8000	130-132		132-134		135-137	123-125	118-120	110-117	120-131		126-127	
10000	131-132		134-134		136-137	120-122	118-120	110-111	120-129		119-121	
12500	132-133		133-134		137-138	119-120	119-121	120-130	128-129		119-120	
16000	133		133-134		137-138	117-119	117-119	126-130	128-129		116-117	
20000	132		131-132		135-136	117-119	117-118	124-130	127-128		113-114	
dB(A)	143-144		144-145		148	145-149	144-145	149-149	149-149		143-144	
dB(B)	143-144		144-145		147-148	147-147	143-145	149-149	142-143		143-147	
dB(C)	144-145		145-145		148-149	143-144	143-147	149-150	143-144		147-148	

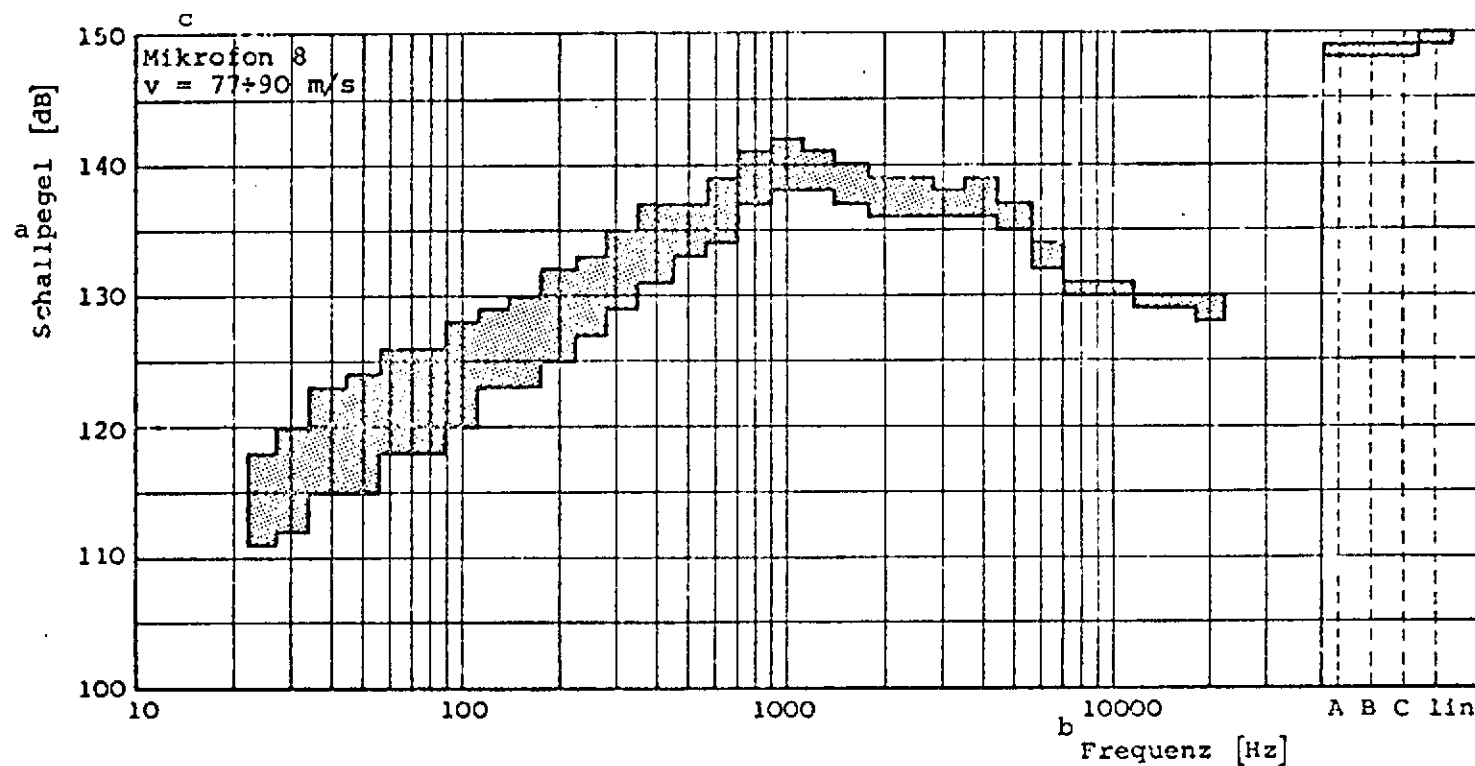


Fig. 2.2.4-3. Measured frequency spectrum in Do 31 E3 airframe.
Phase of flight: cruising II (two cruising power plants at 88% n_F ,
nozzle setting 36°).

Key: a. Sound levels
b. Frequency
c. Microphone

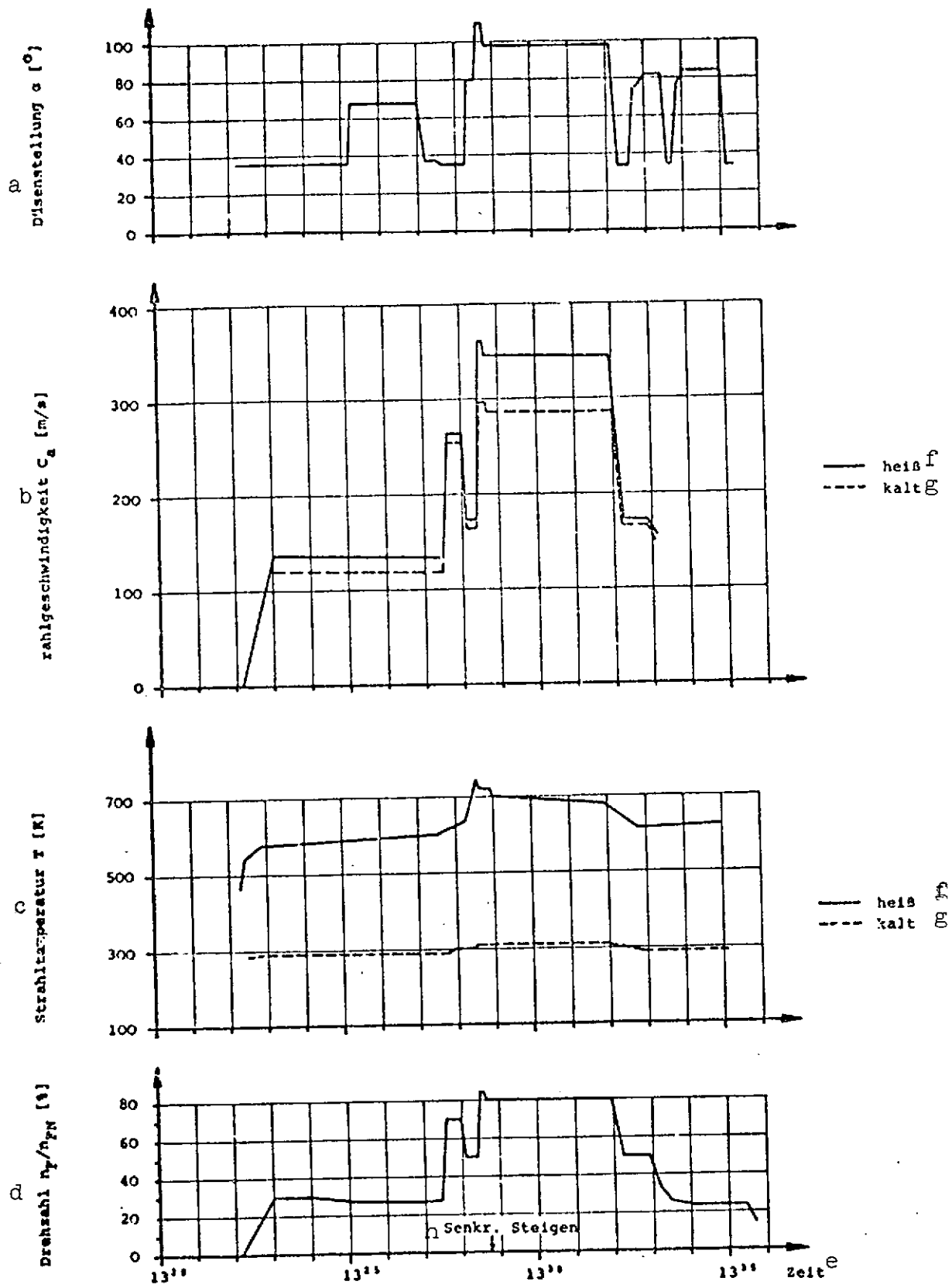


Fig. 2.2.4-4. Do 31 E3 flight and power plant parameters (time curves), BS Pg 5-2.

Key: a. Nozzle setting; b. Jet velocity; c. Jet temperature; d. Engine speed; e. Time; f. Hot; g. Cold; h. Vertical climb

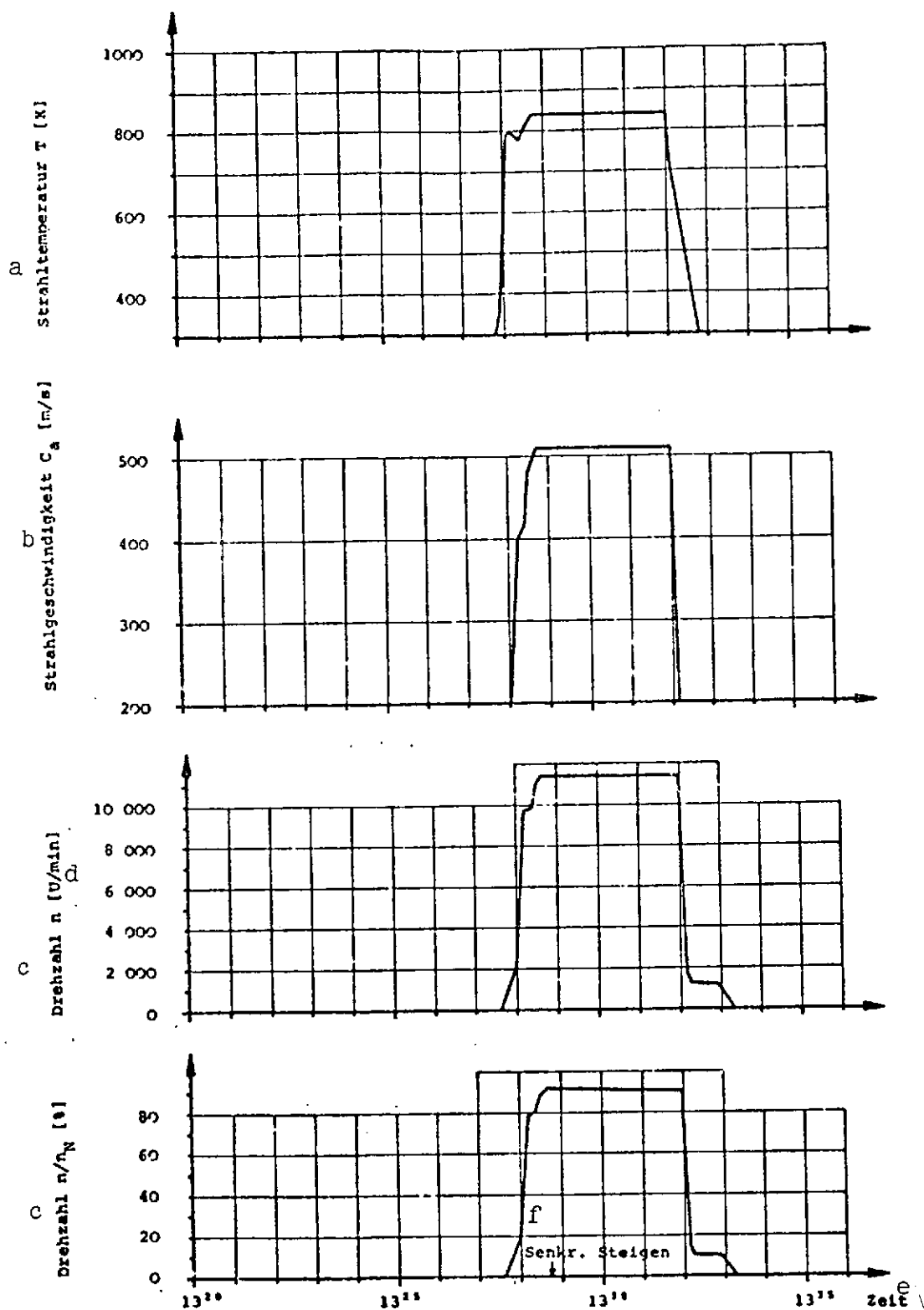


Fig. 2.2.4-5. Do 31 E3 flight and power plant parameters (time curves) RB 162-4D. Trial No. 60, Sheet II.

Key: a. Jet temperature; b. Jet velocity; c. Engine speed; d. [rpm]; e. Time; f. Vertical climb.

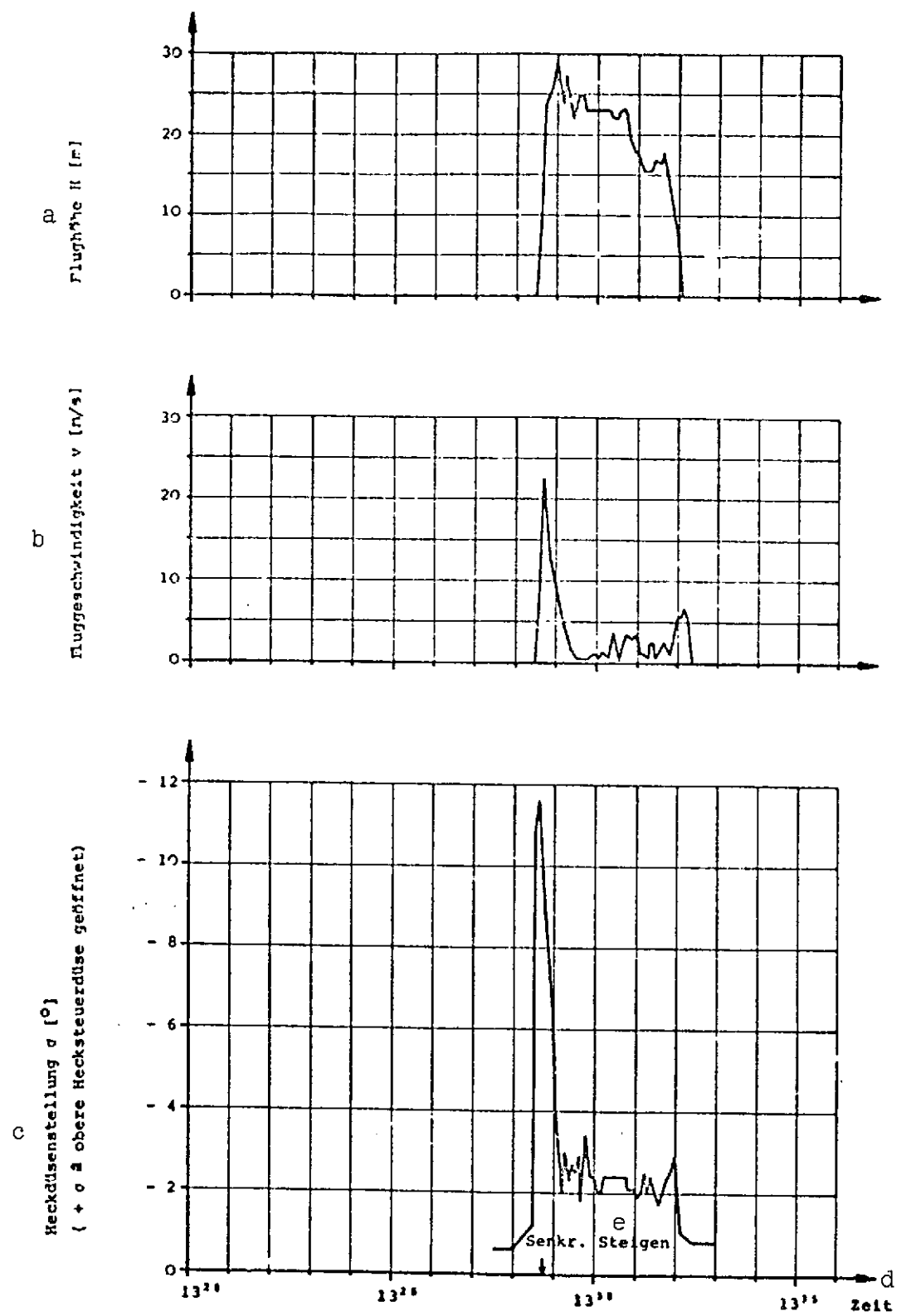


Fig. 2.2.4-6. Do 31 E3 flight and power plant parameters (time curves). Trial No. 60, Sheet III.

Key: a. Altitude; b. Aircraft speed; c. Tail nozzle setting (+ σ means upper tail control nozzle open); d. Time; e. Vertical climb

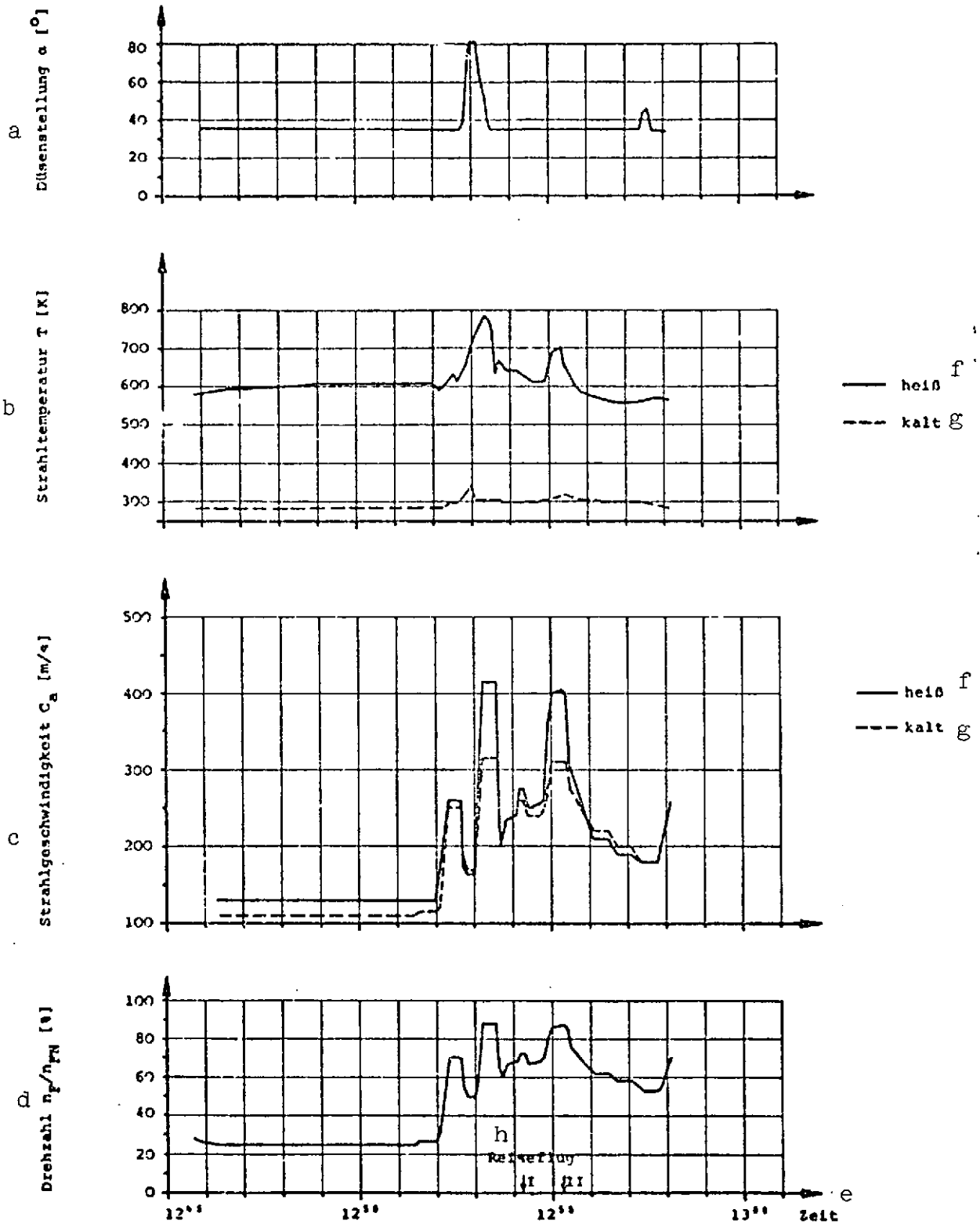


Fig. 2.2.4-7. Do 31 E3 flight and power plant parameters (time curves) BS Pg 5-2. Trial No. 58, Sheet I.

Key: a. Nozzle setting; b. Jet temperature; c. Jet velocity; d. Engine speed; e. Time; f. Hot; g. Cold; h. Cruising

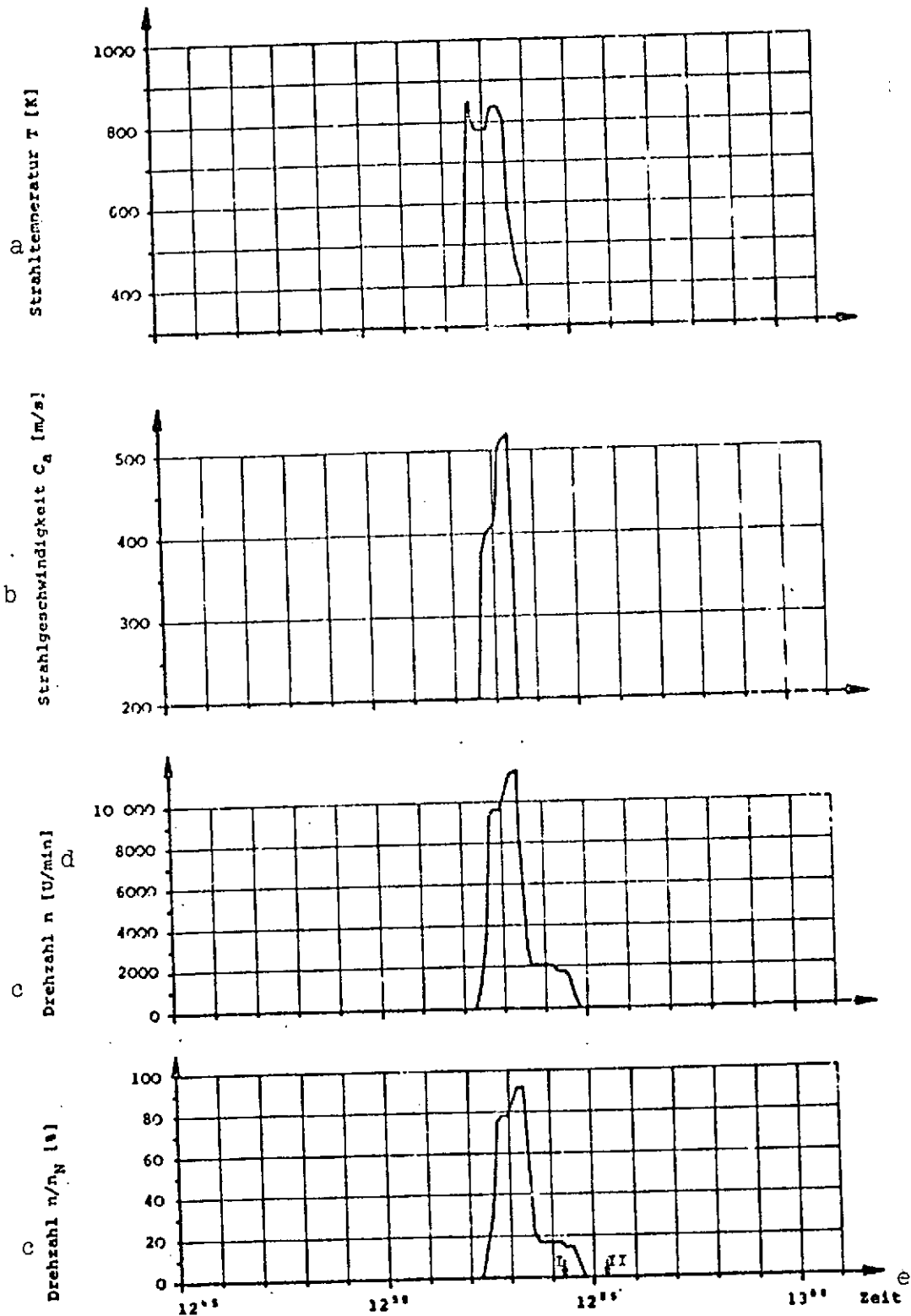


Fig. 2.2.4-8. Do 31 E3 flight and power plant parameters (time curves). RB 162-4D. Trial No. 58, Sheet II.

Key: a. Jet temperature; b. Jet velocity; c. Engine speed; d. [rpm]; e. Time

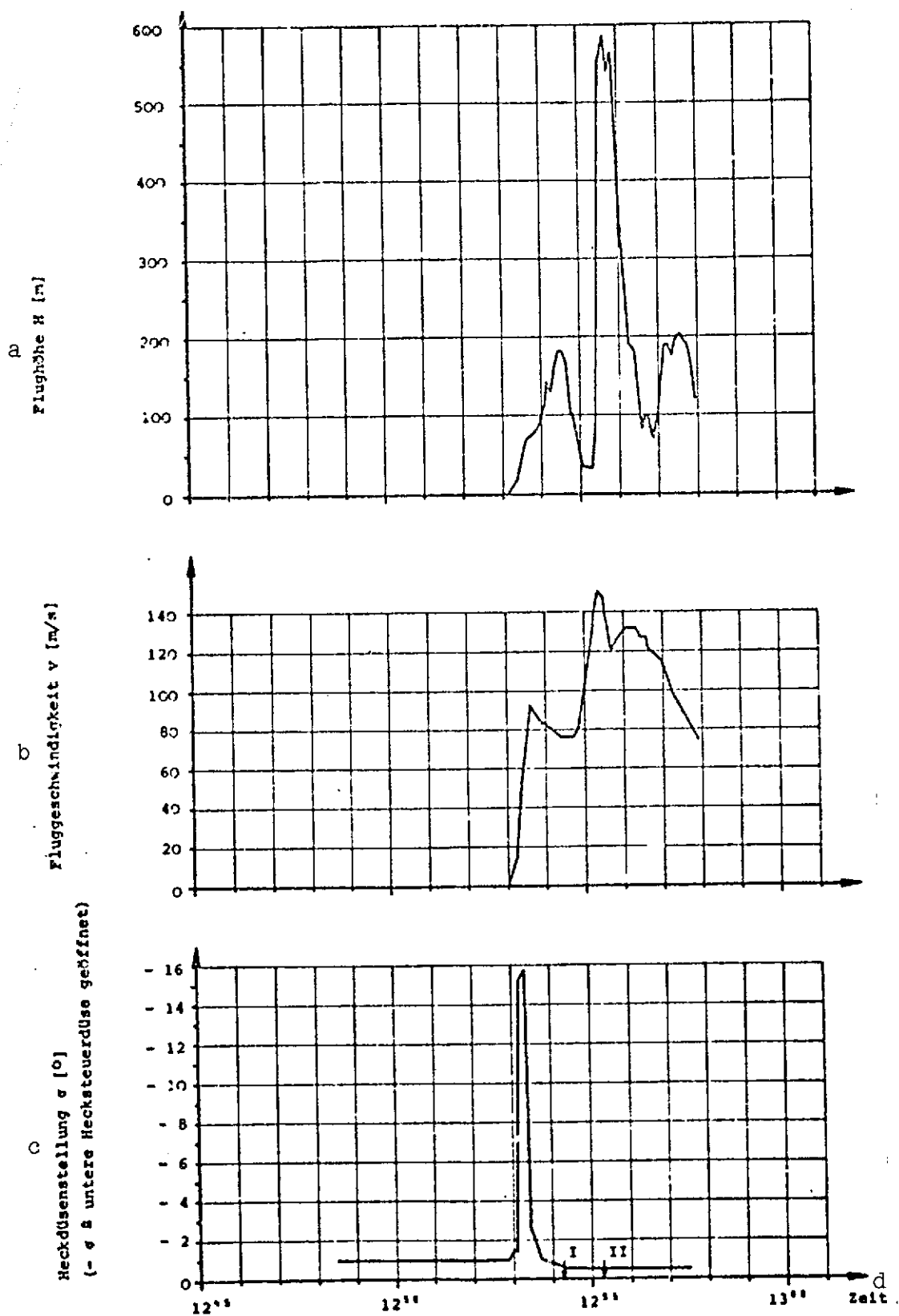


Fig. 2.2.4-9. Do 31 E3 flight and power plant parameters (time curves). Trial No. 58, Sheet III.

Key: a. Altitude; b. Aircraft speed; c. Tail nozzle setting (- σ means lower tail control nozzle open); d. Time

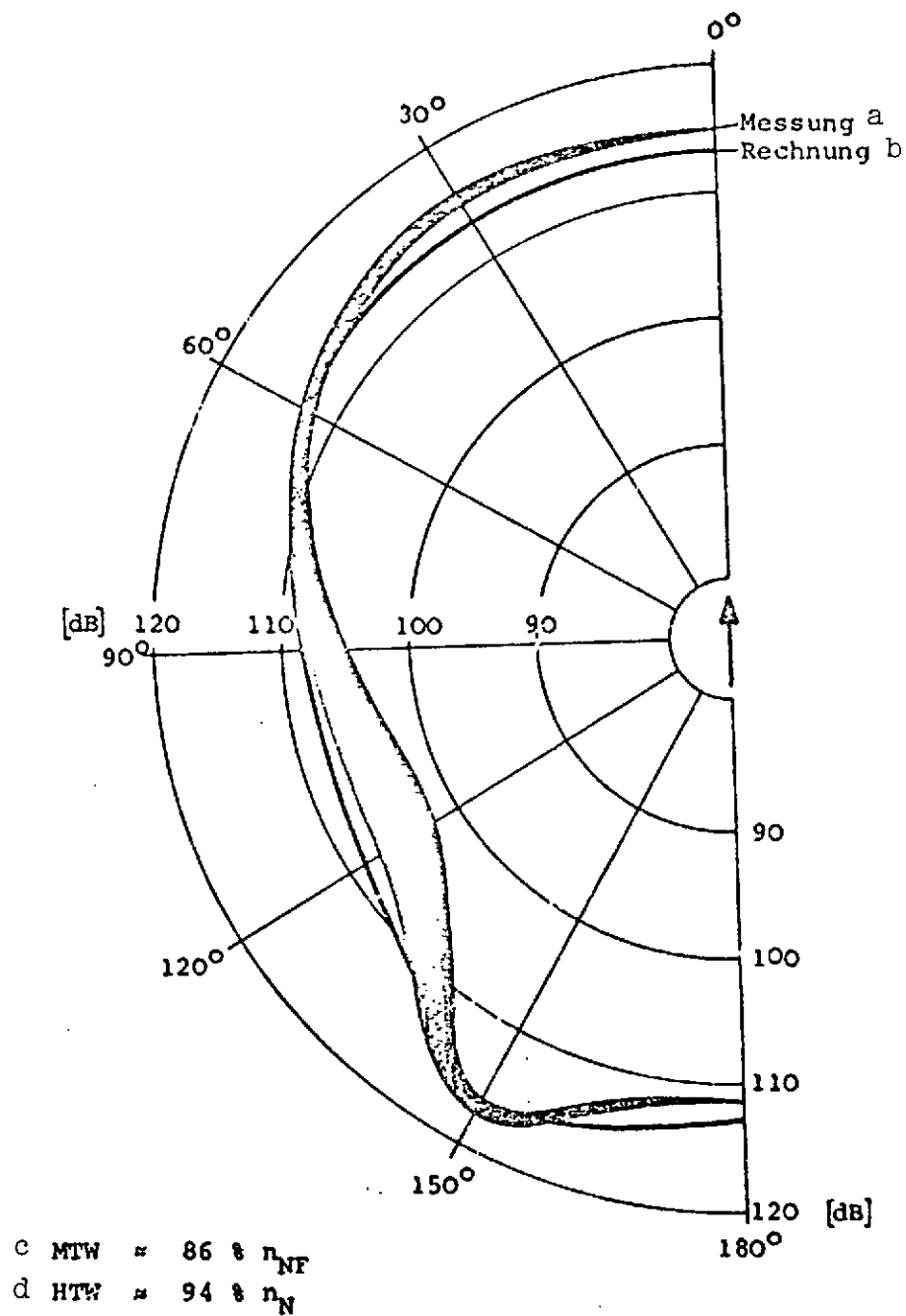


Fig. 3.1.1-1. Do 31 E3 vertical takeoff ($H = 0$).
Overall peripheral levels at radius of 100 m.

Key: a. Measured
 b. Calculated
 c. Cruising power plants
 d. Lift power plants

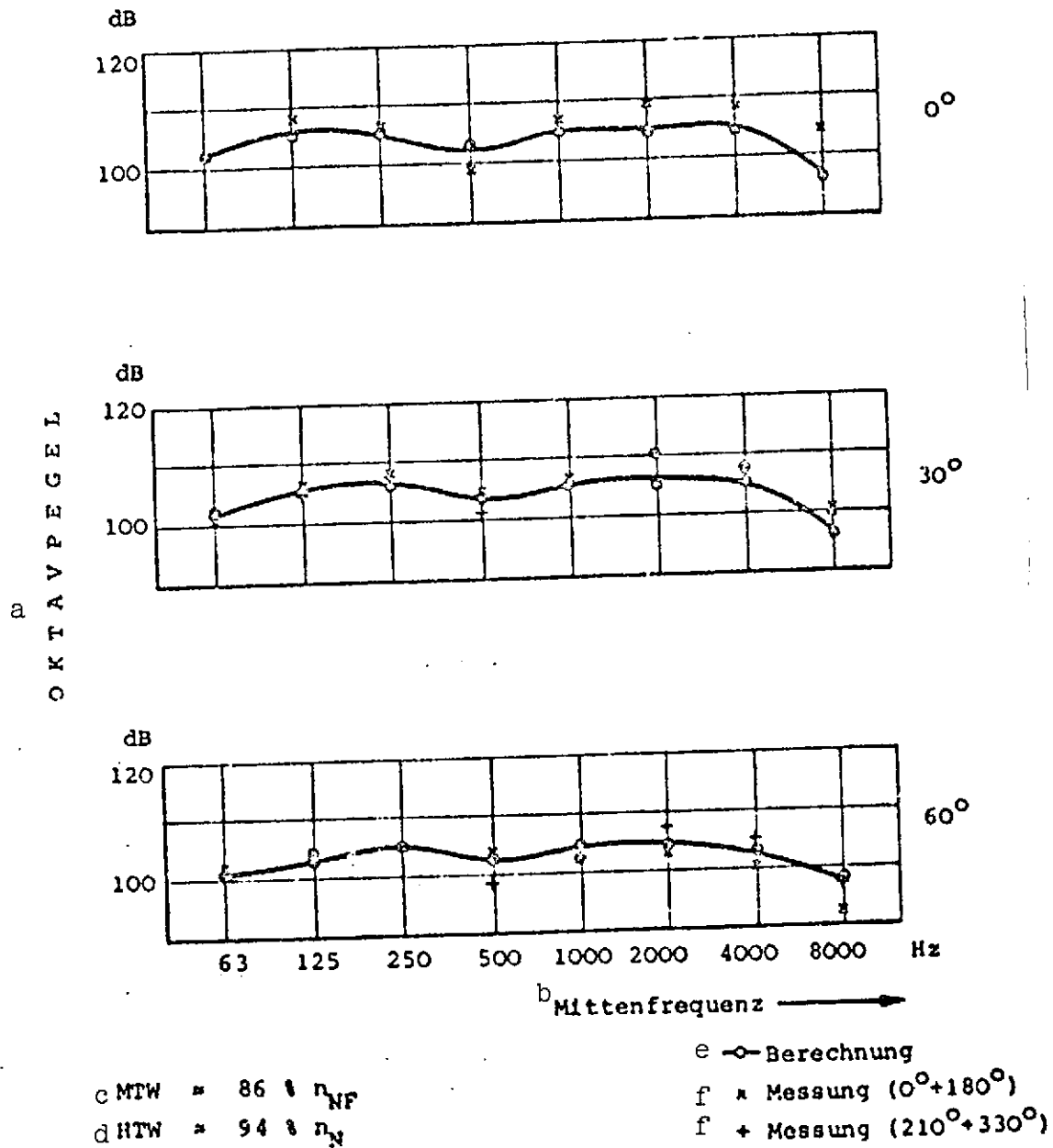


Fig. 3.1.1-2. Do 31 E3 vertical takeoff ($H = 0$ m).
Peripheral octave spectra at 100 m.

Key: a. Octave level
b. Center frequency
c. Cruising power plants
d. Lift power plants
e. Calculated
f. Measured

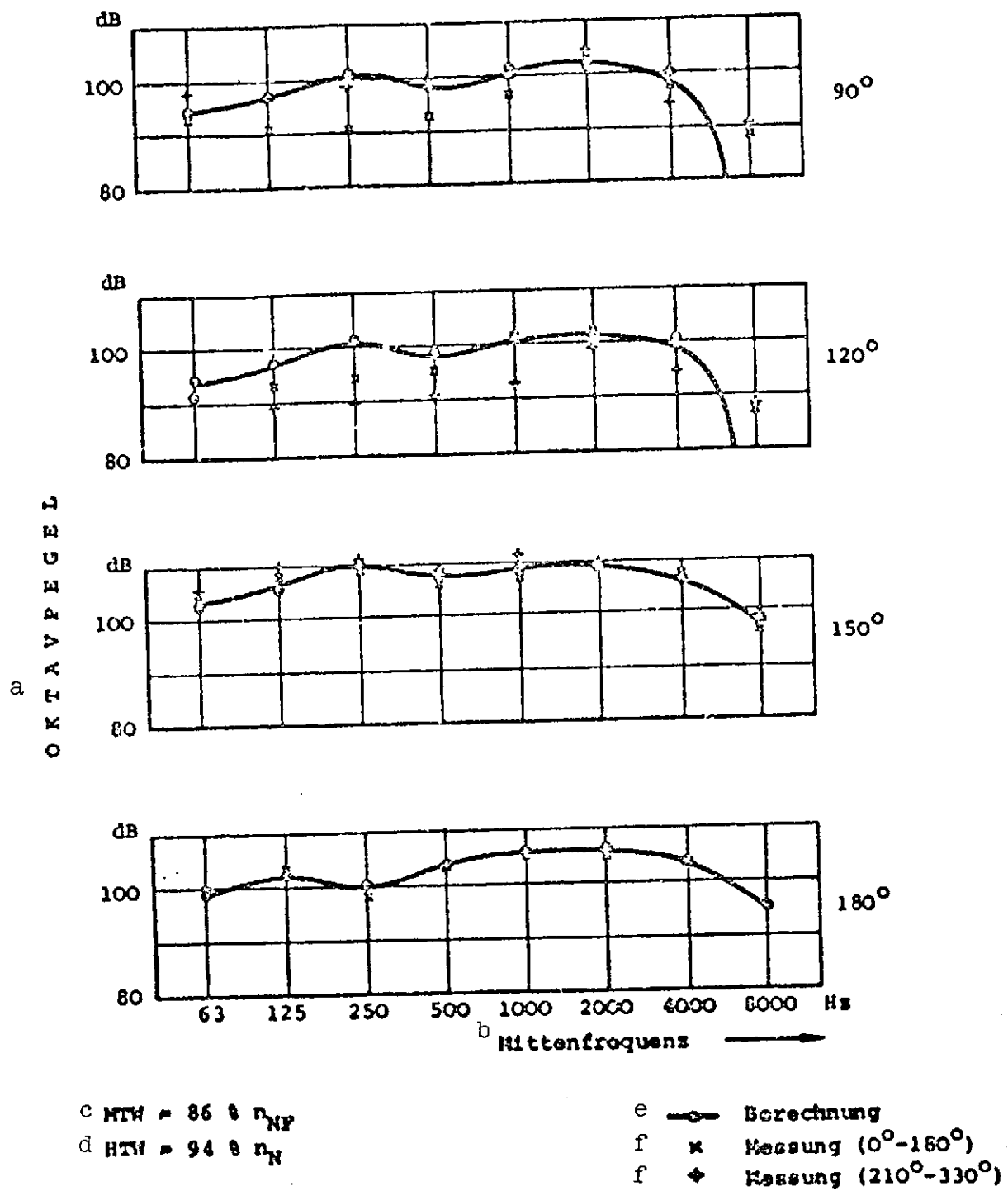


Fig. 3.1.1-3. Do 31 E3 vertical takeoff ($H = 0$ m).
Peripheral octave spectra at 100 m.

Key:

- a. Octave level
- b. Center frequency
- c. Cruising power plants
- d. Lift power plants
- e. Calculated
- f. Measured

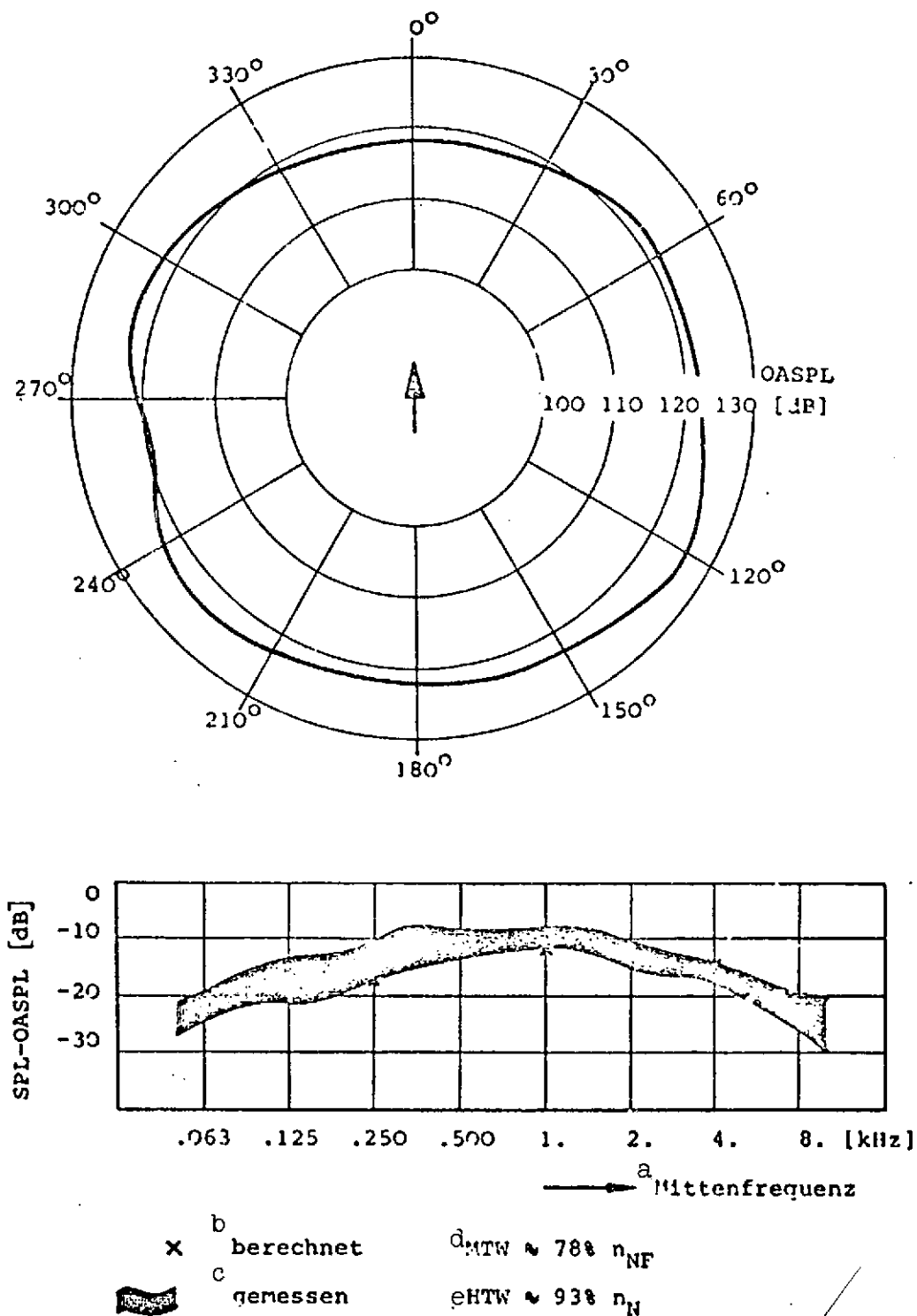


Fig. 3.1.1-4. Do 31 E3 peripheral sound level at 100 m. Hover at H = 30 m.

Key:

- a. Center frequency
- b. Calculated
- c. Measured
- d. Cruising power plants
- e. Lift power plants

a
[dB] Maximale Schallpegel 150 m parallel zur Startbahn

/114

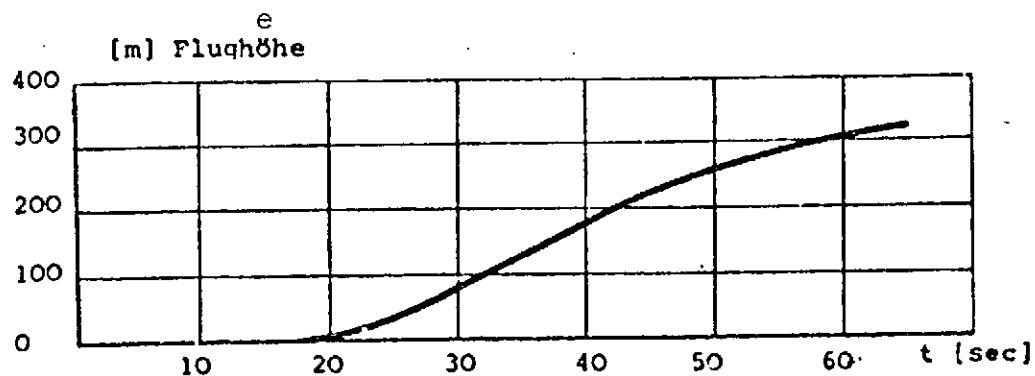
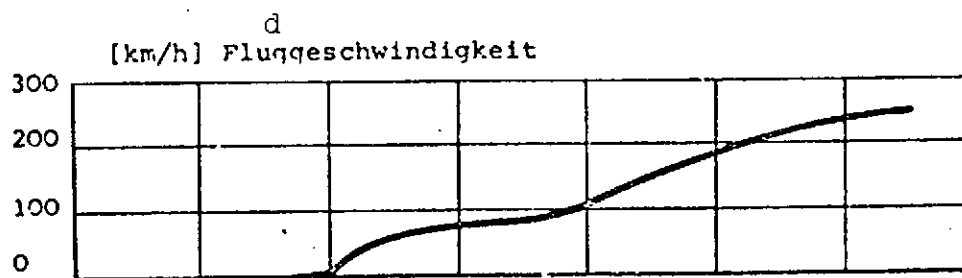
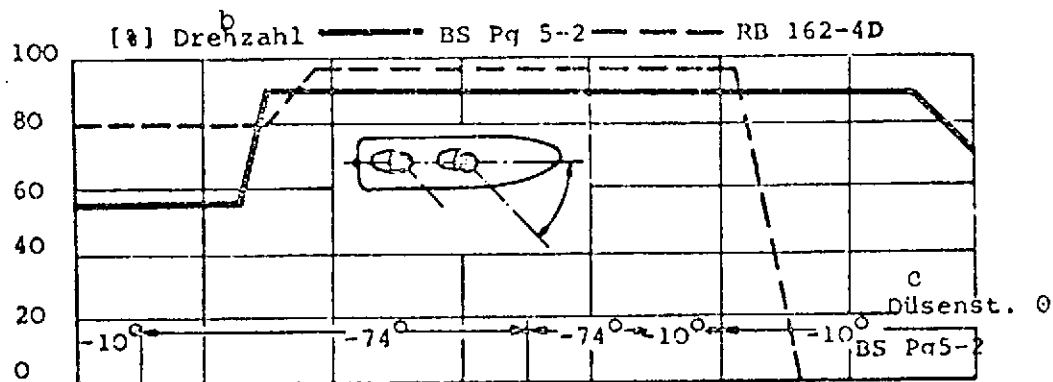
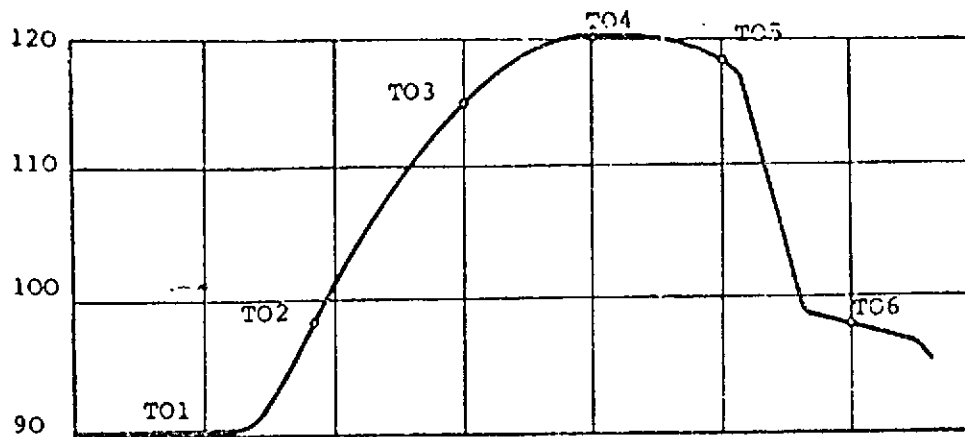


Fig. 3.1.2-1. Do 31 E3 takeoff transition.

Key: a. Maximum sound level 500 m parallel to runway; b. Engine speed; c. Nozzle setting; d. Aircraft speed; e. Altitude

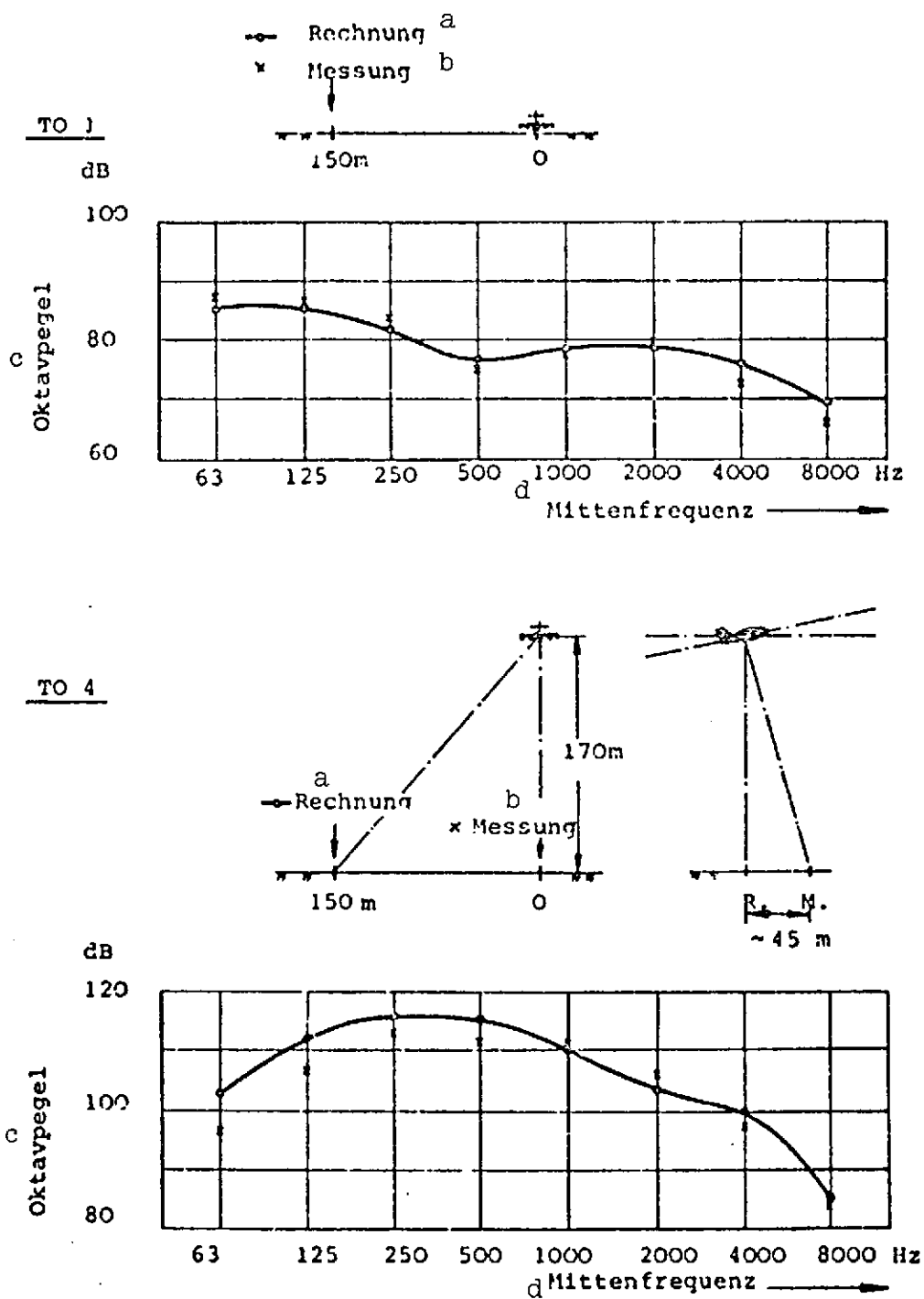


Fig. 3.1.2-2. Do 31 E3 takeoff transition. Octave spectra.

Key: a. Calculated
b. Measured
c. Octave level
d. Center frequency

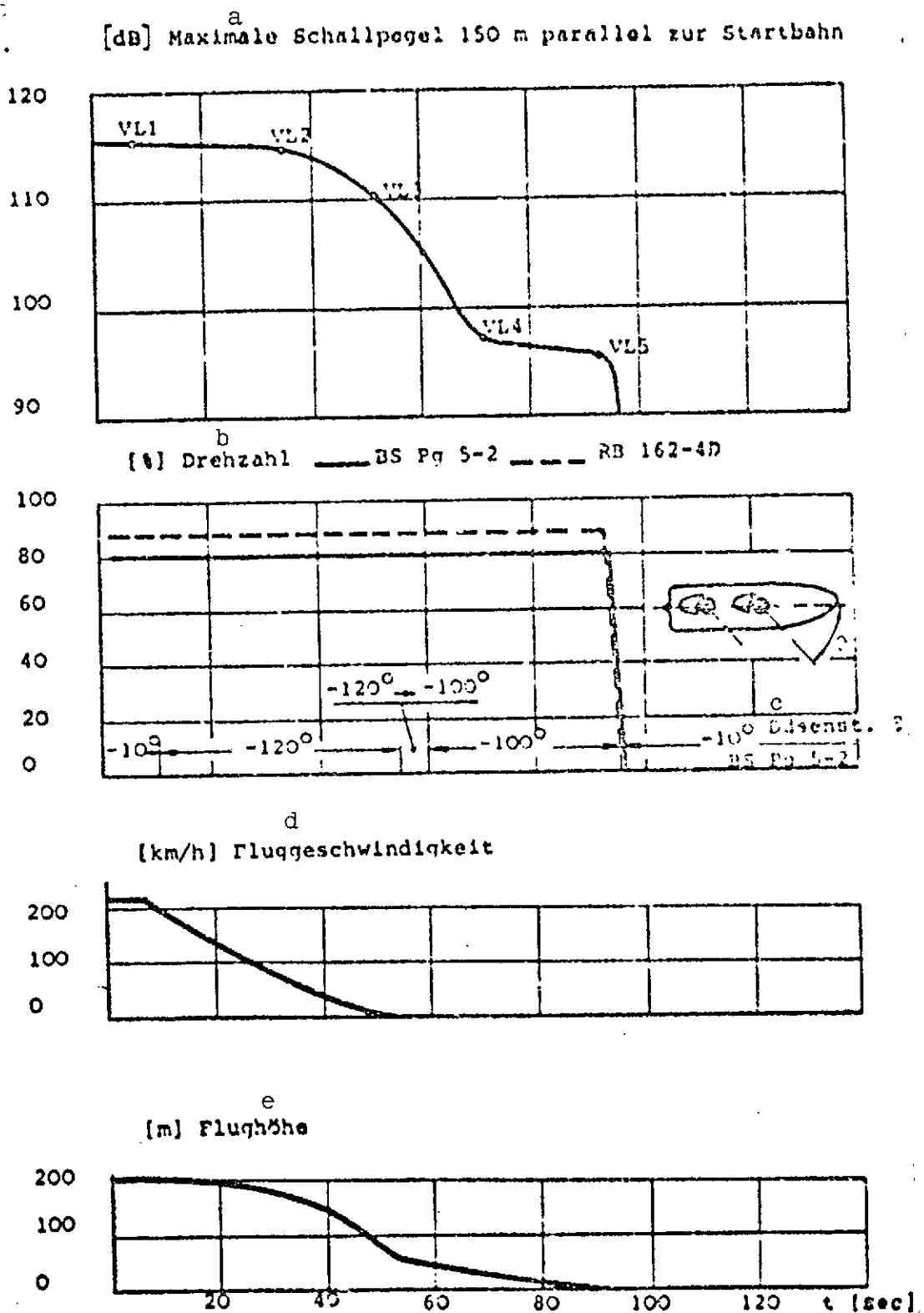
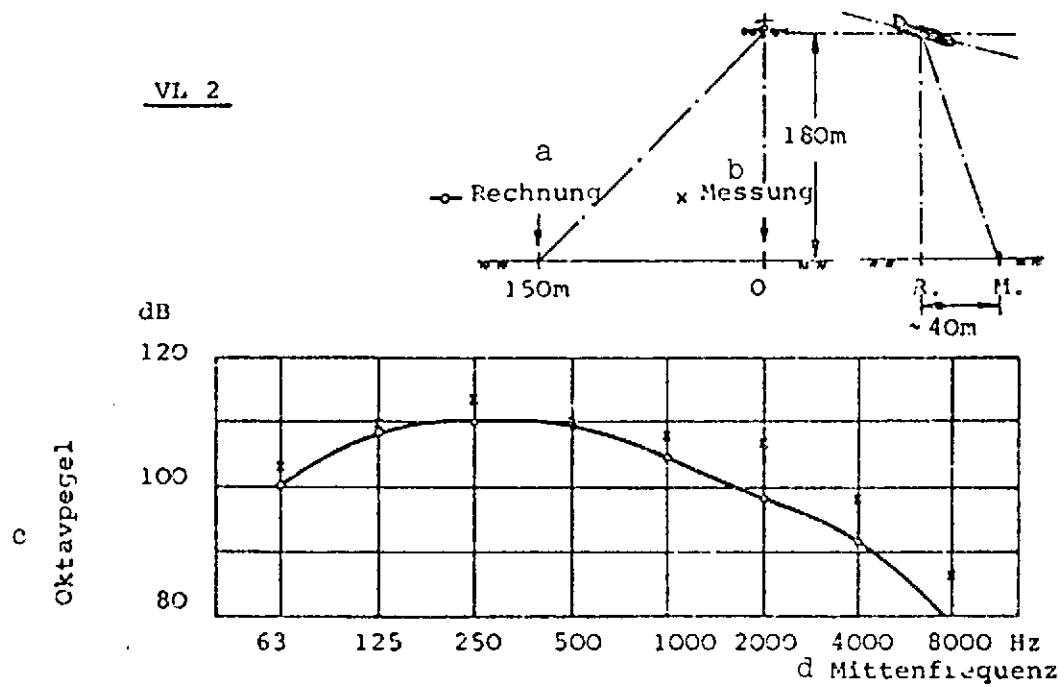


Fig. 3.1.2-3. Do 31 E3 landing transition.

Key: a. Maximum sound level 500 m parallel to runway; b. Engine speed; c. Nozzle setting; d. Aircraft speed; e. Altitude

VL 2



VL 3

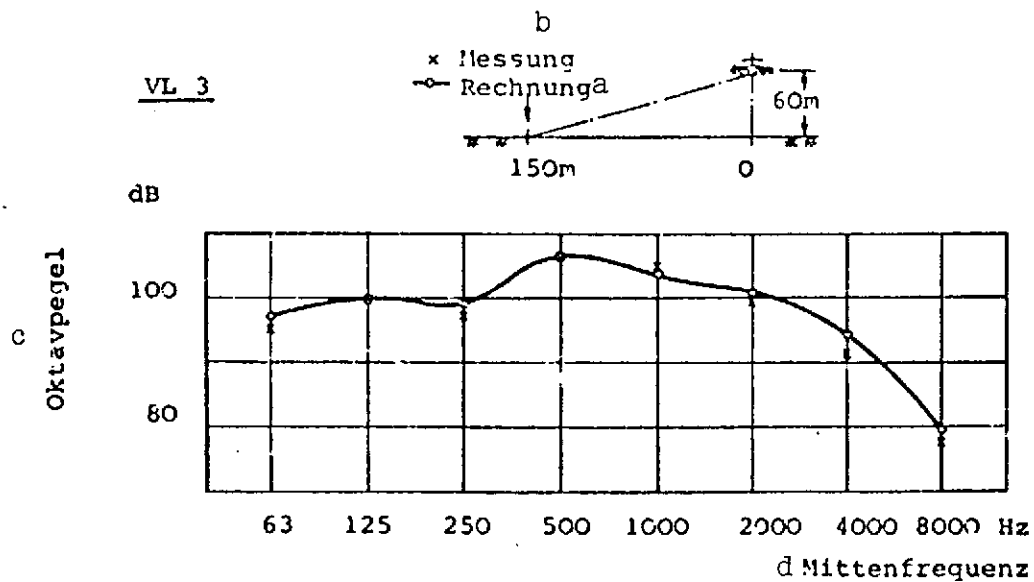
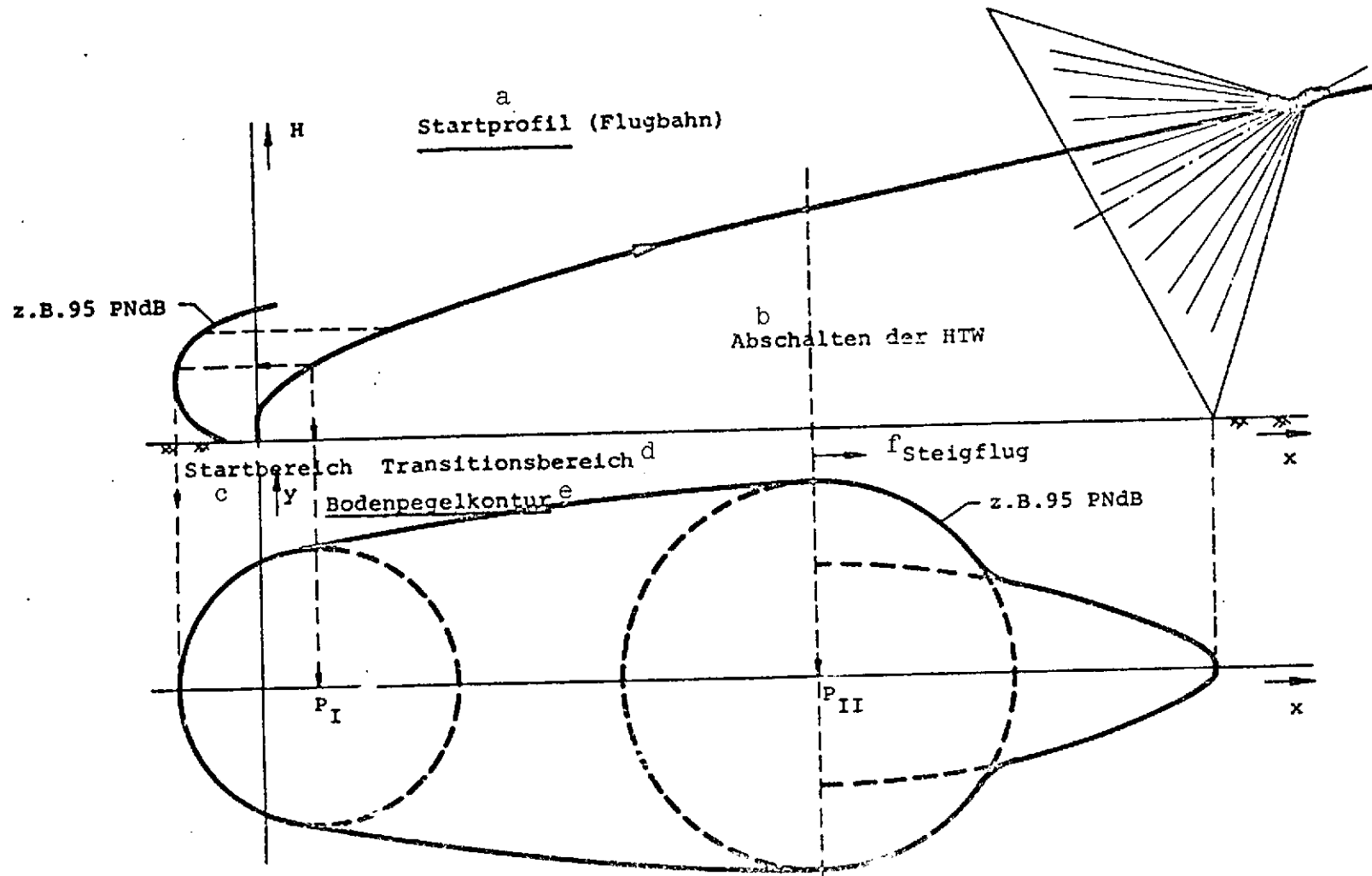


Fig. 3.1.2-4. Do 31 E3 landing transition. Octave spectra.

Key: a. Calculated
 b. Measured
 c. Octave level
 d. Center frequency



Key: a. Takeoff profile (flight path); b. Lift power plants cut out;
c. Takeoff area; d. Transition area; e. Ground noise level
contour; f. Climb; zB = for example

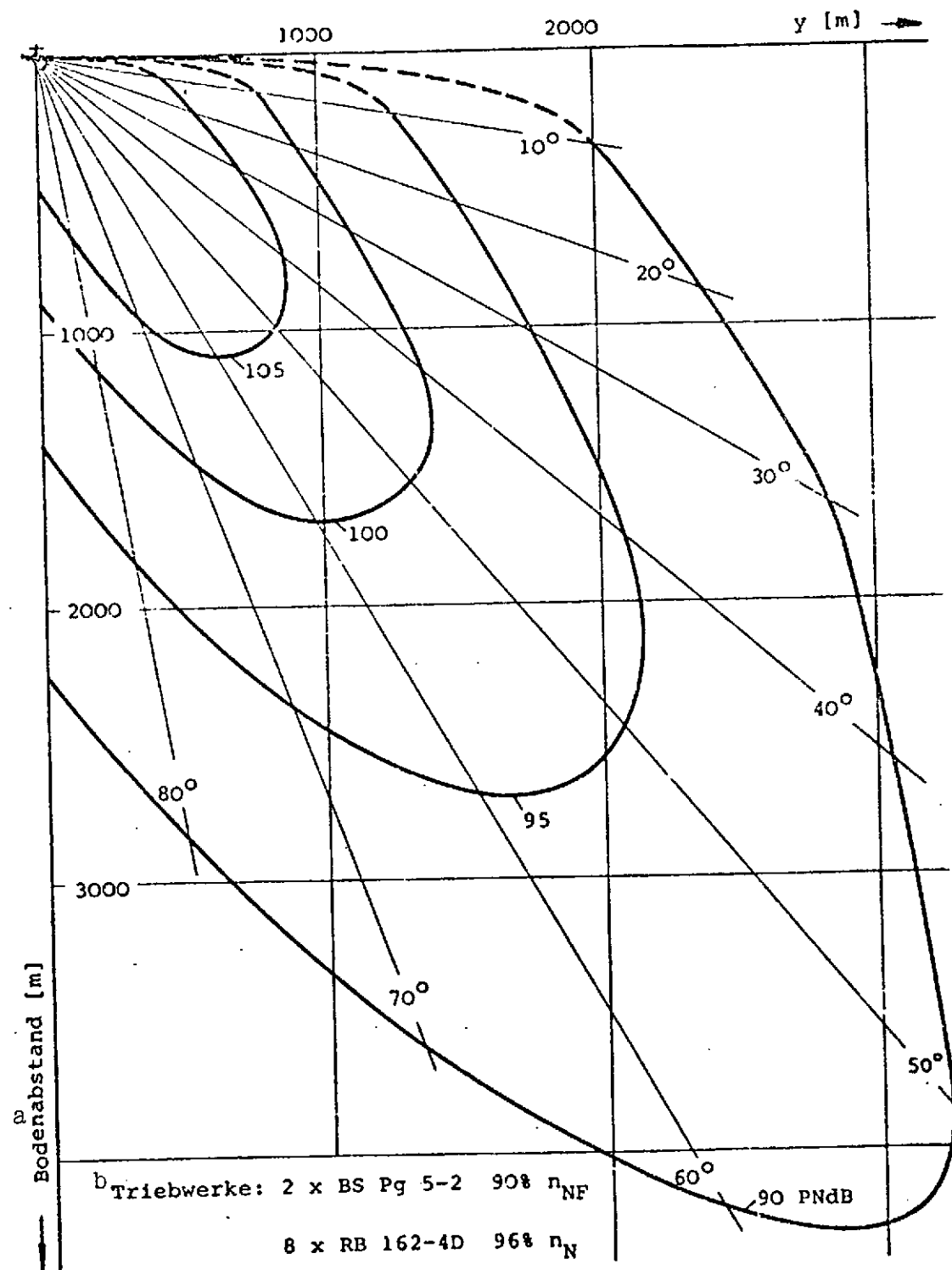


Fig. 3.1.3.1-1. Do 31 E3 ground noise level distances for vertical takeoff.

Key: a. Ground distance
b. Power plants

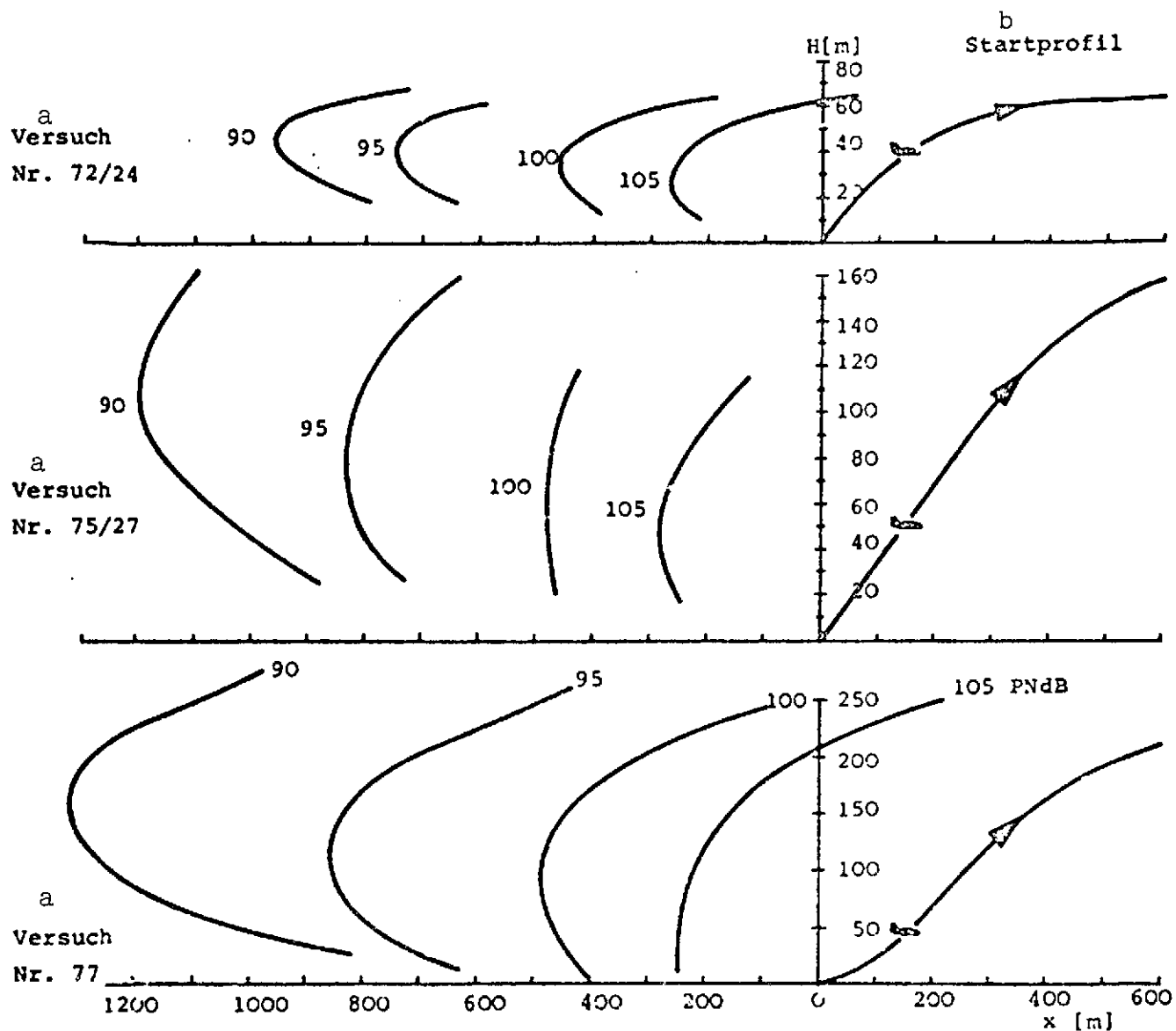


Fig. 3.1.3.1-2. Do 31 E3 ground level distances during takeoff transitions.

Key: a. Trial No.
b. Takeoff profile

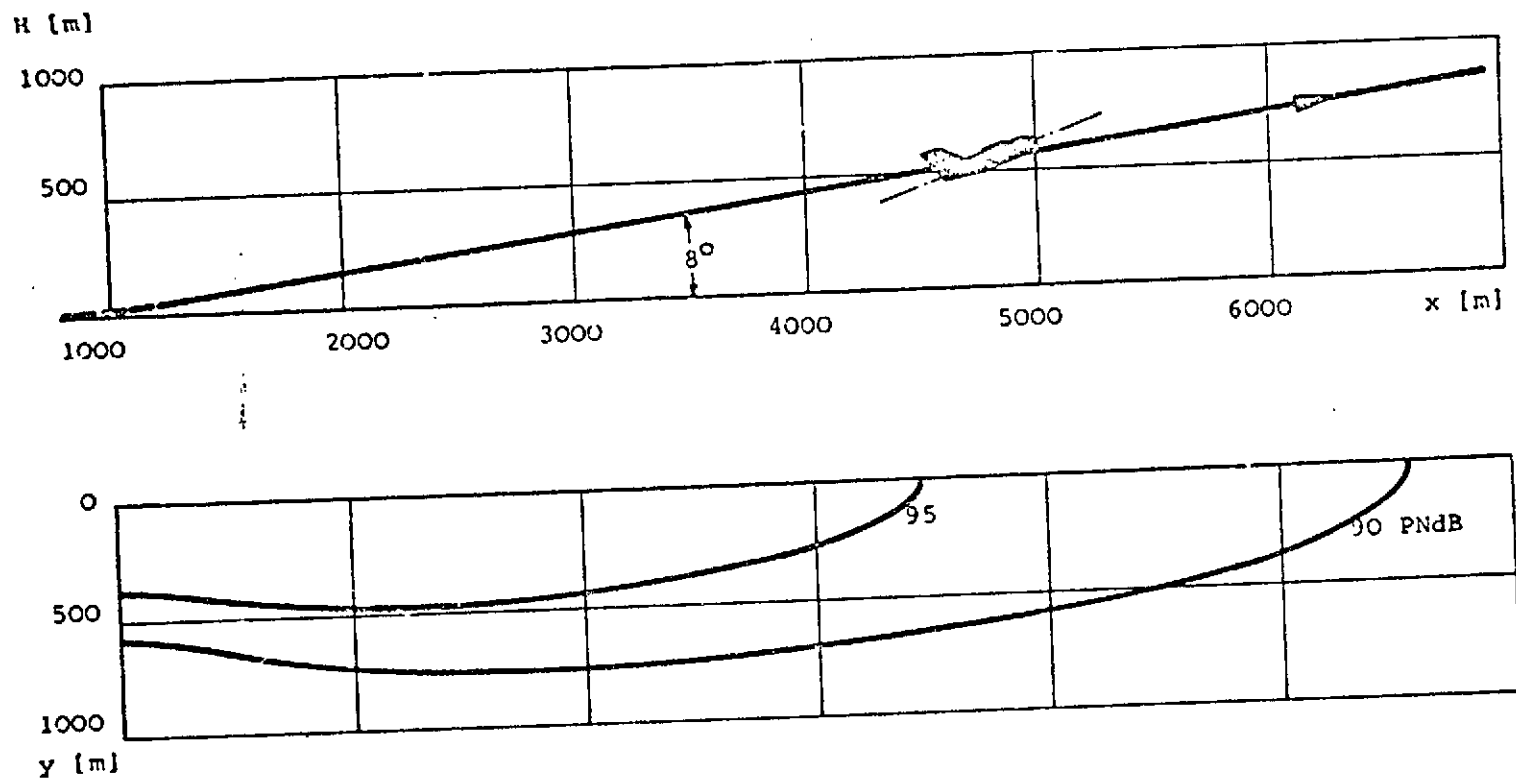
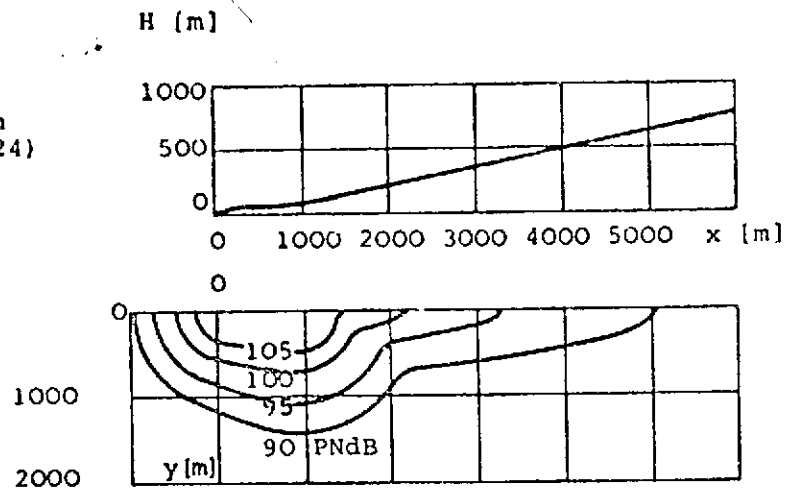
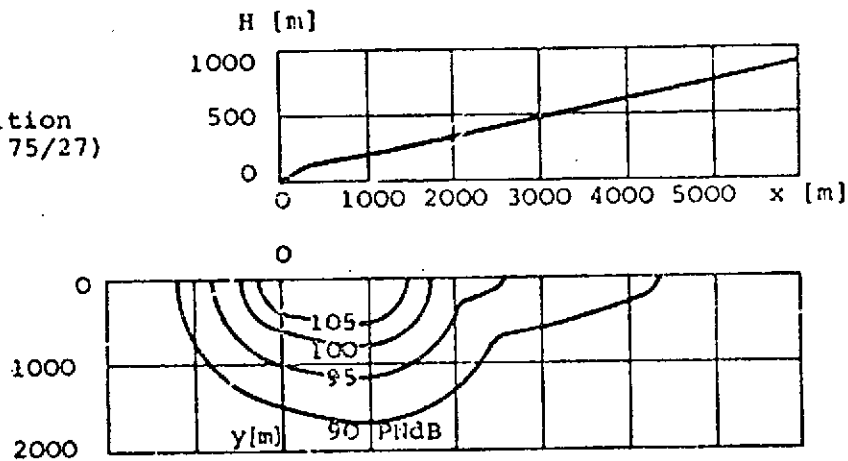


Fig. 3.1.3.1-3. Do 31 ground noise level contours during conventional takeoff.

a
Starttransition
(Vers. Nr. 72/24)



a
Starttransition
(Vers. Nr. 75/27)



a
Starttransition
(Versuch Nr. 77)

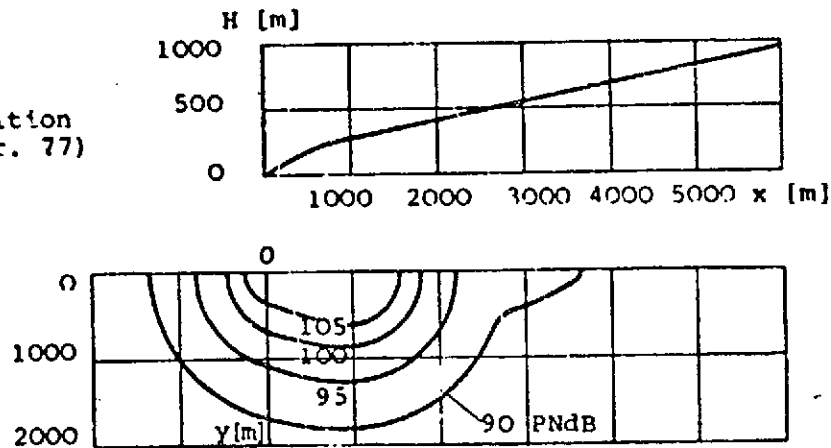


Fig. 3.1.3.1-4. Do 31 E3 ground noise level contours during various takeoff transitions.

Key: a. Takeoff transition (trial no. ...)

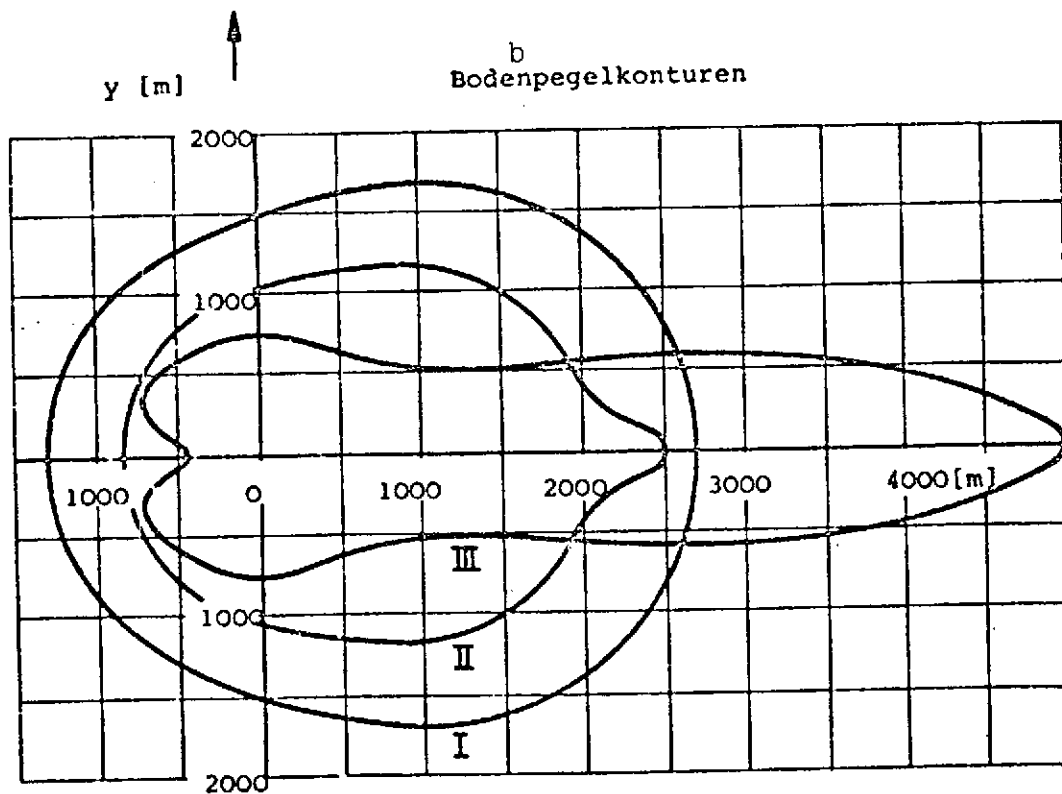
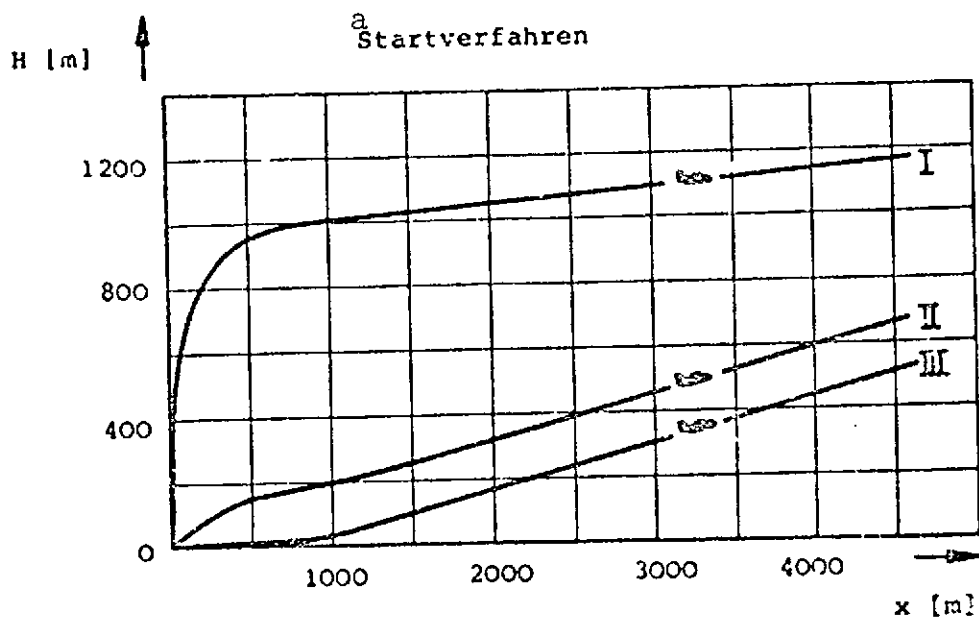


Fig. 3.1.3.1-5. 95 PNdB ground noise level contours for various Do 31 E3 takeoff procedures.

Key: a. Takeoff procedure
b. Ground noise level contours

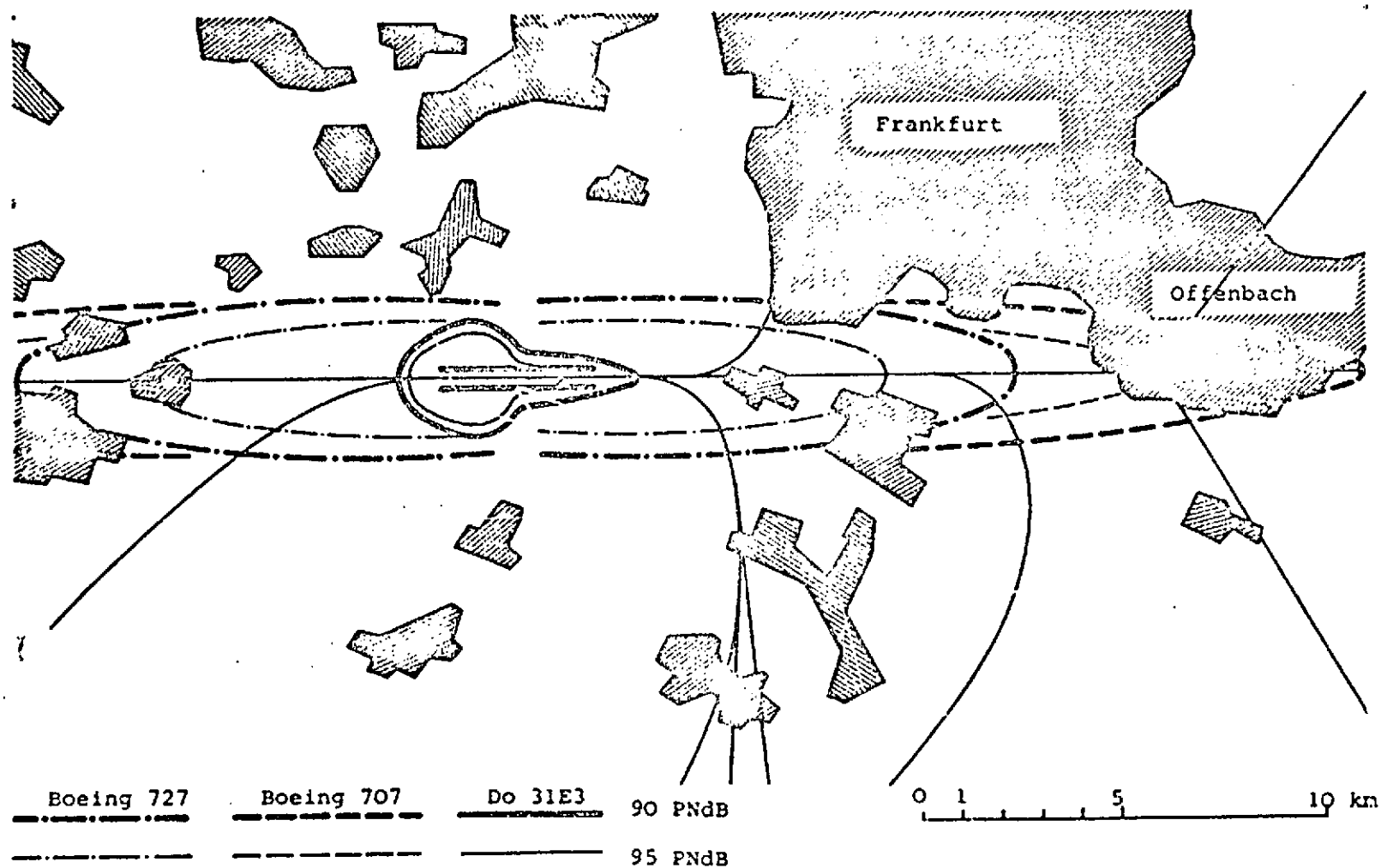


Fig. 3.1.3.2-1. Do 31 E3, Boeing 727 and Boeing 707 ground noise level contours for takeoff from the Frankfurt/Main airport.

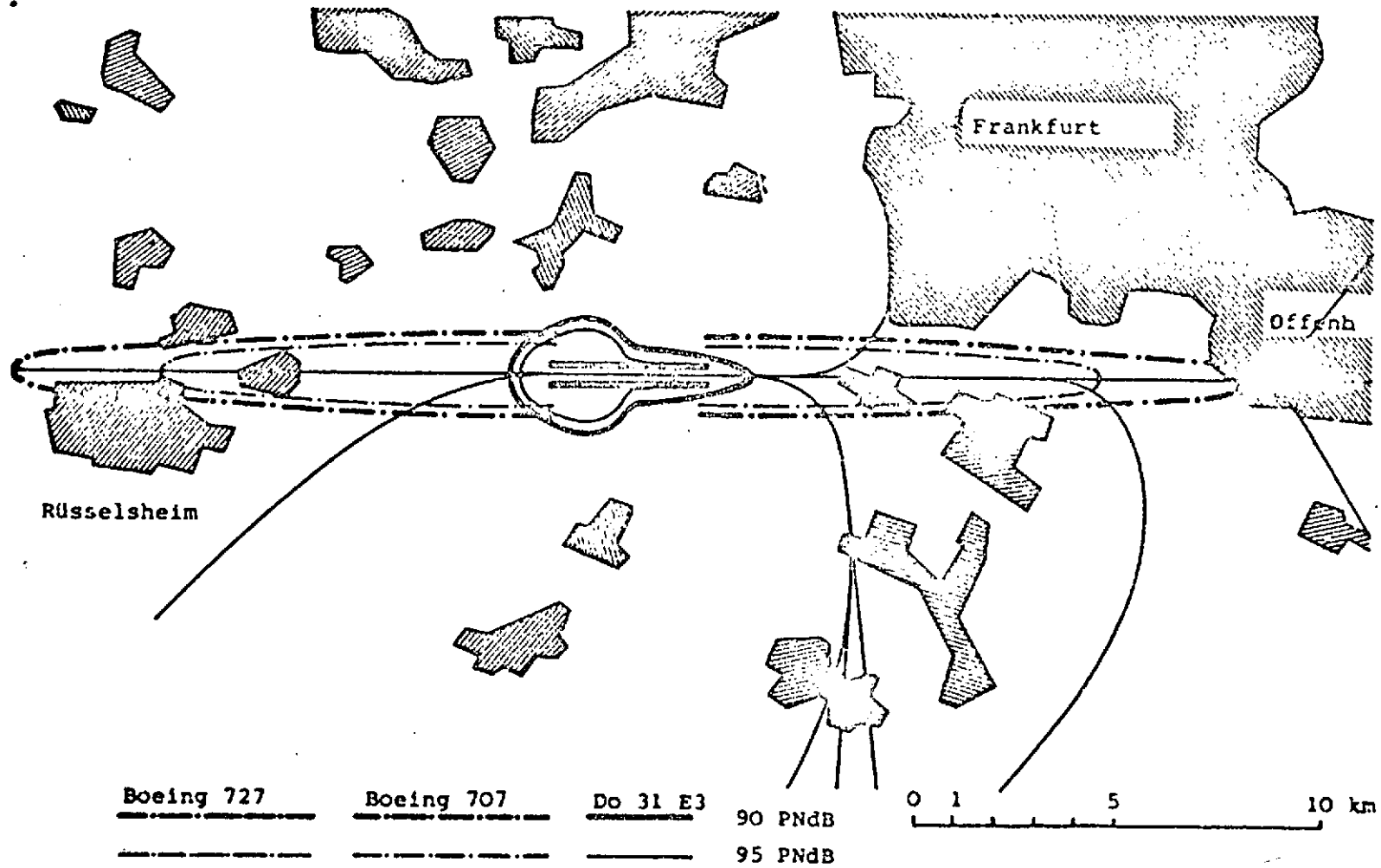


Fig. 3.1.3.2-2. Do 31 E3, Boeing 727 and Boeing 707 ground noise level contours for landing at the Frankfurt/Main airport.

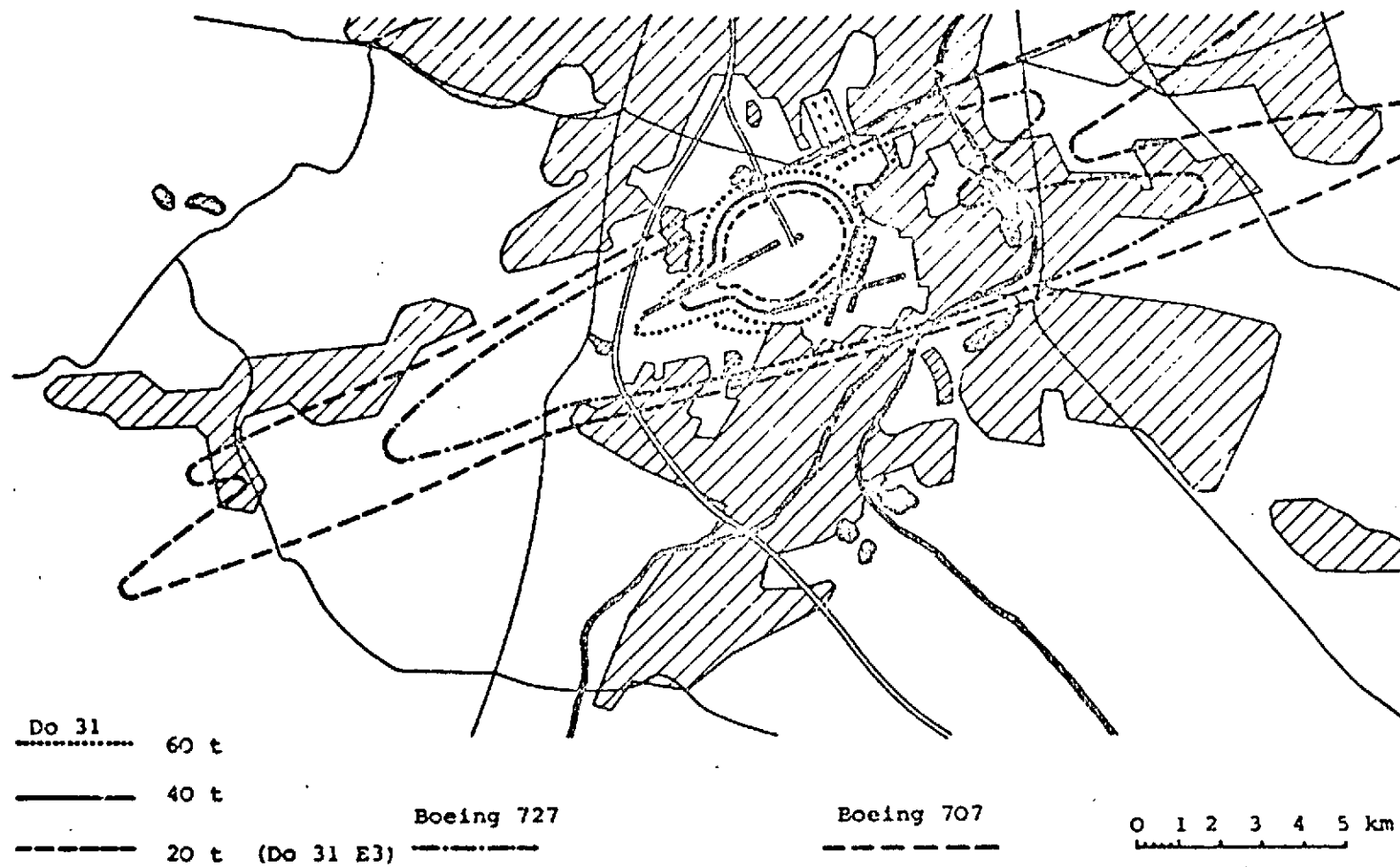


Fig. 3.1.3.2-3. Do 31, Boeing 727 and Boeing 707 95 PNdB ground noise level contours during takeoff from Paris/Orly airport.

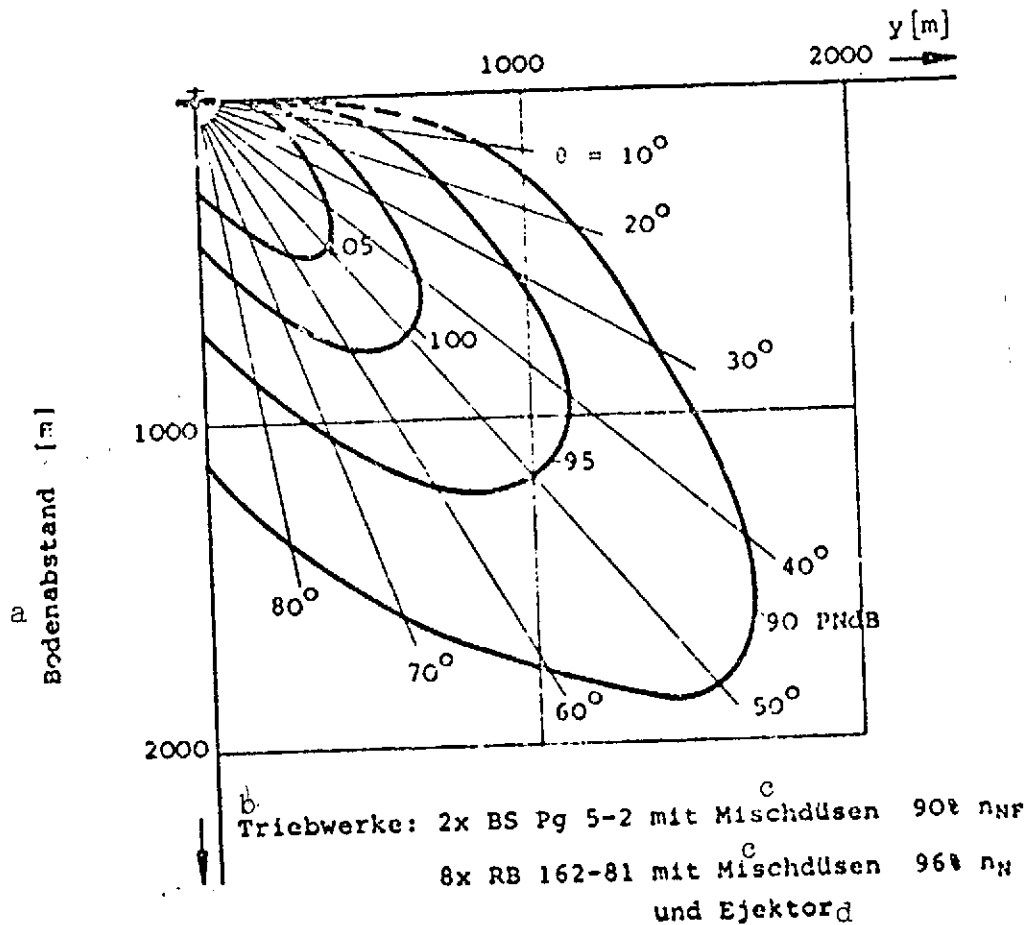


Fig. 3.1.3.3-1. Do 31 (reduced-noise version) ground noise level distances during vertical takeoff.

Key: a. Ground distance
 b. Power plants
 c. With mixing nozzles
 d. And injector

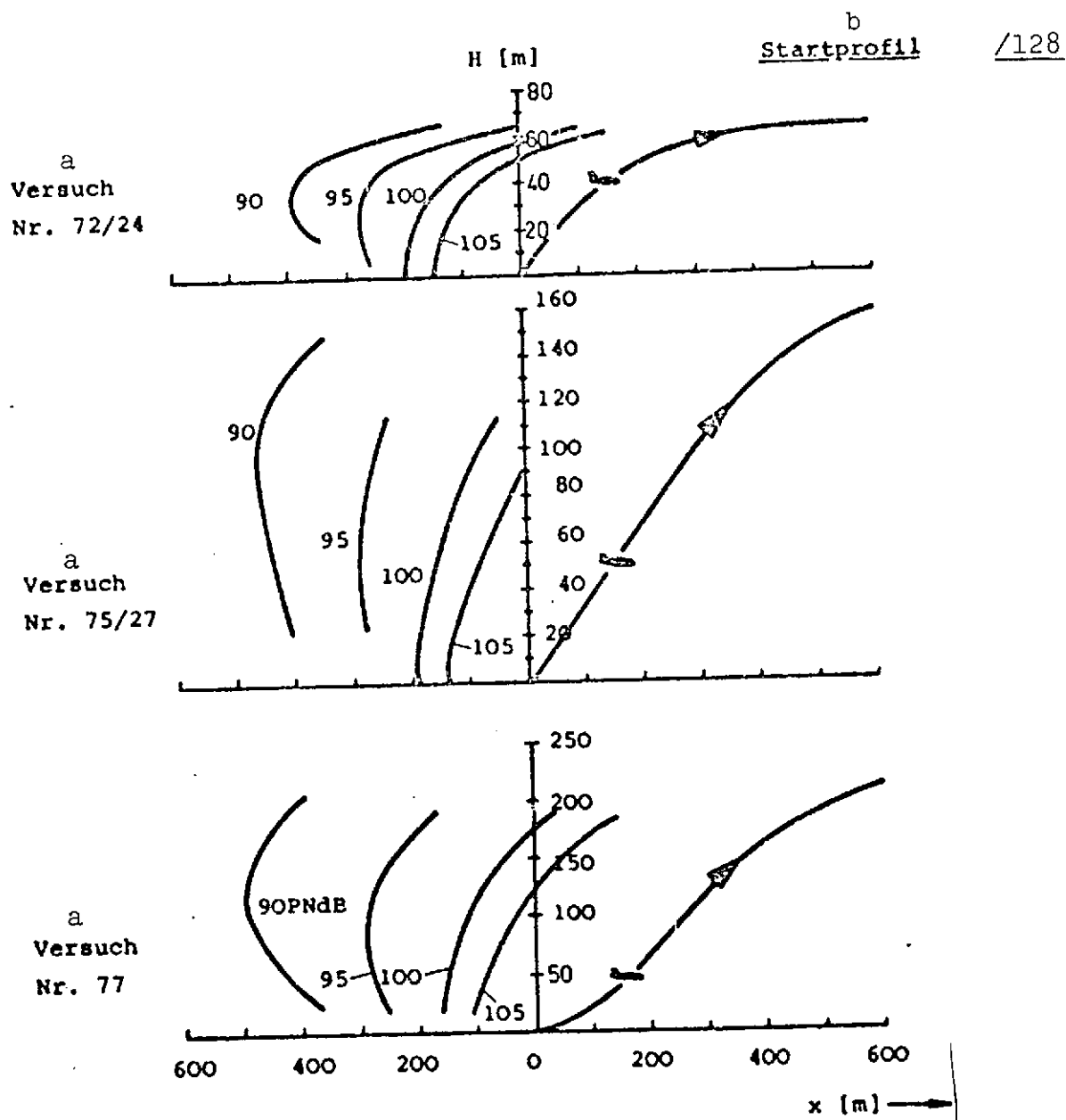


Fig. 3.1.3.3-2. Do 31 (reduced-noise version) ground noise level distances during takeoff transition.

Key: a. Trial No. ...
b. Takeoff profile

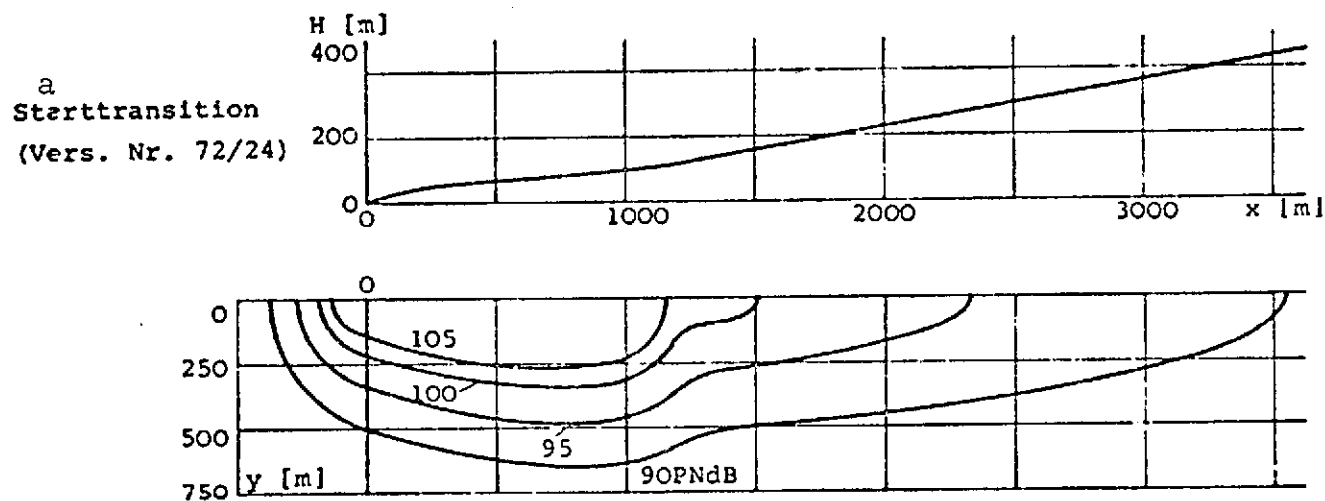


Fig. 3.1.3.3-3. Do 31 (reduced-noise version) ground noise level contours during takeoff transition.

Key: a. Takeoff transition (trial no. 72/24)

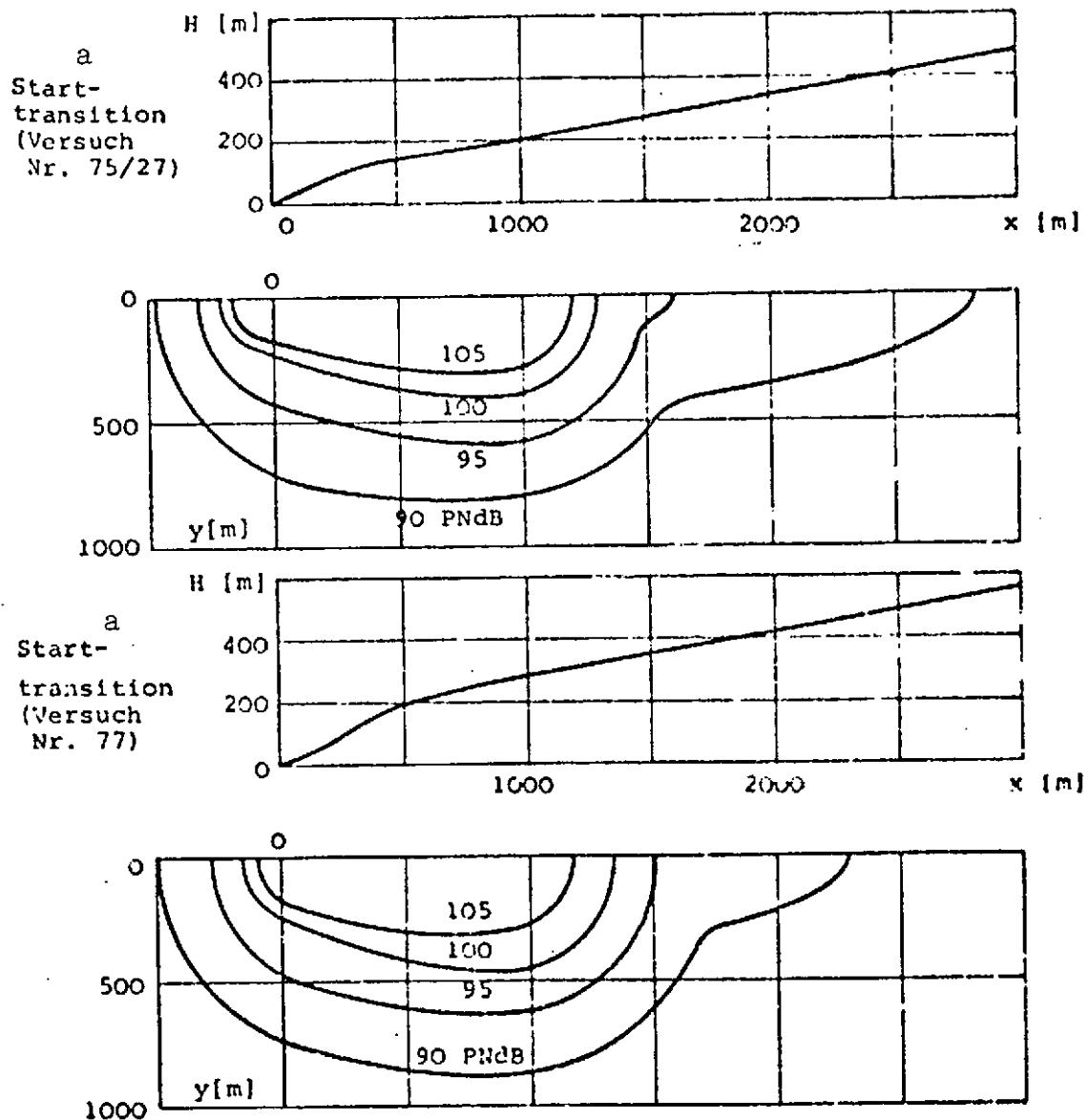


Fig. 3.1.3.3-4. Do 31 (reduced-noise version) ground noise level contours during various takeoff transitions.

Key: Takeoff transition (trial no. ...)

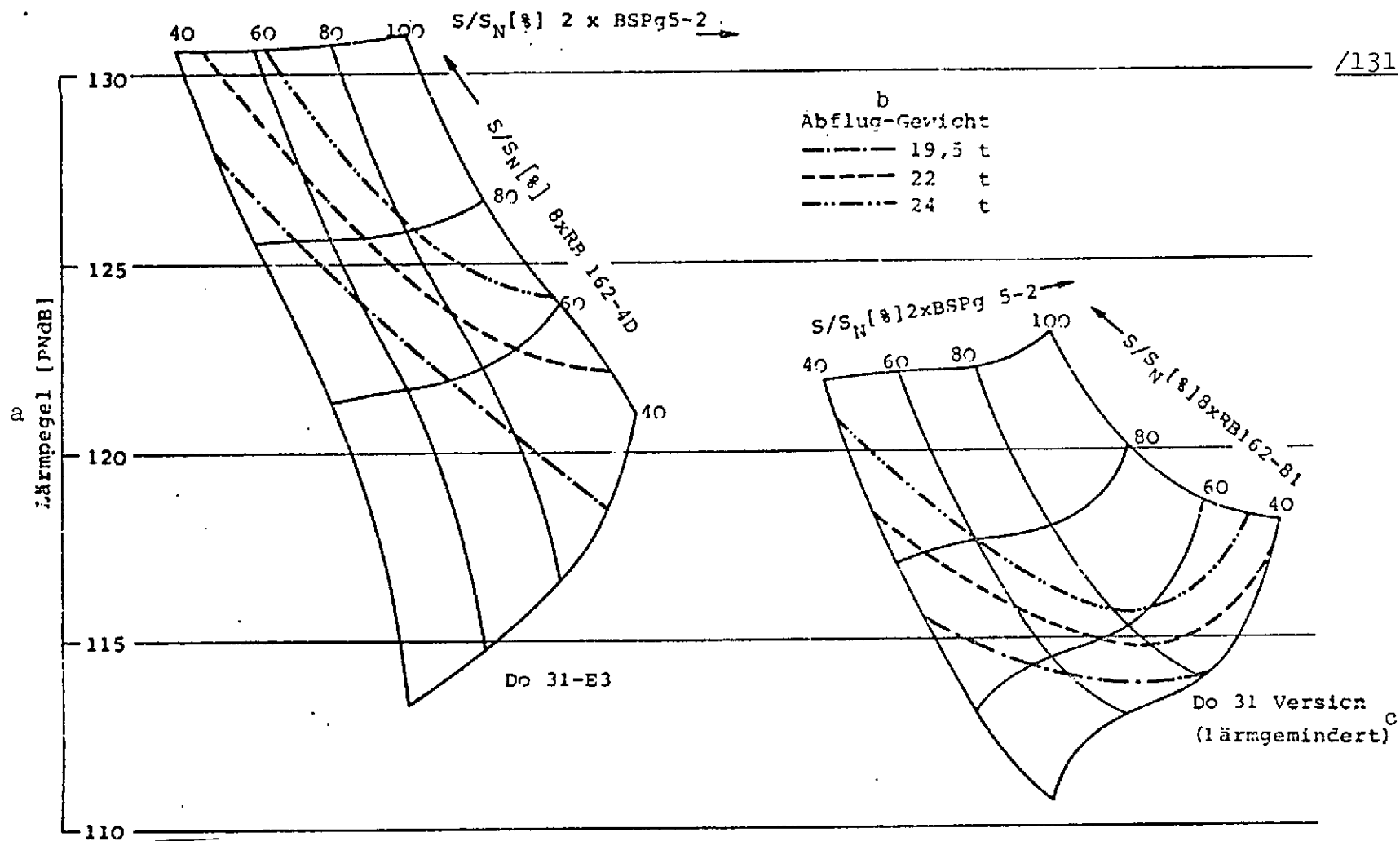


Fig. 3.1.4-1. Maximum levels on a parallel line 150 m from runway.

Key: a. Noise level
b. Takeoff weight
c. Reduced-noise version

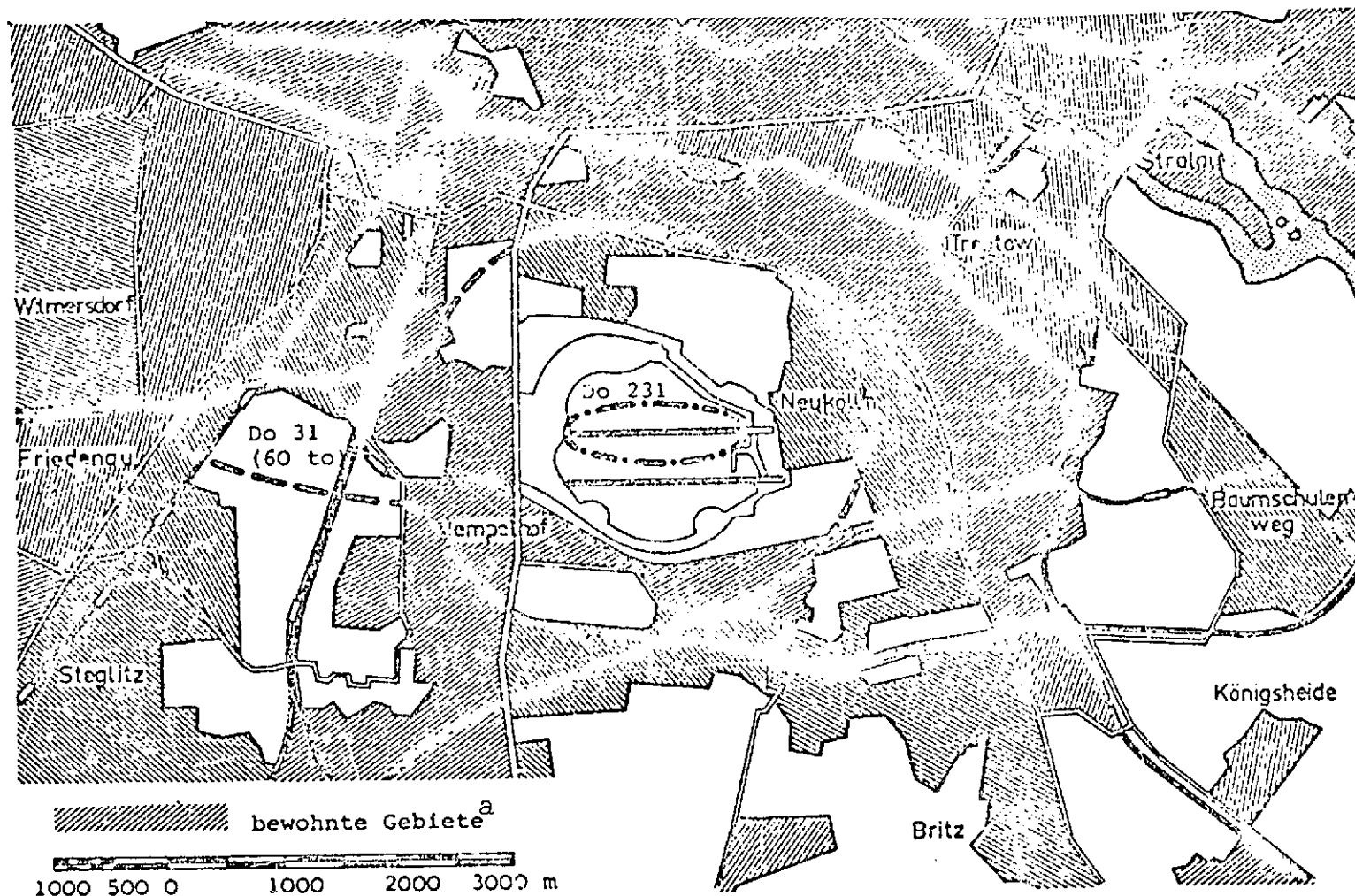


Fig. 3.1.5-1. 95 PNdB ground noise level contours for one version of Do 31 and for the Do 231 during VTO, Berlin/Tempelhof airport.

Key: a. Populated areas

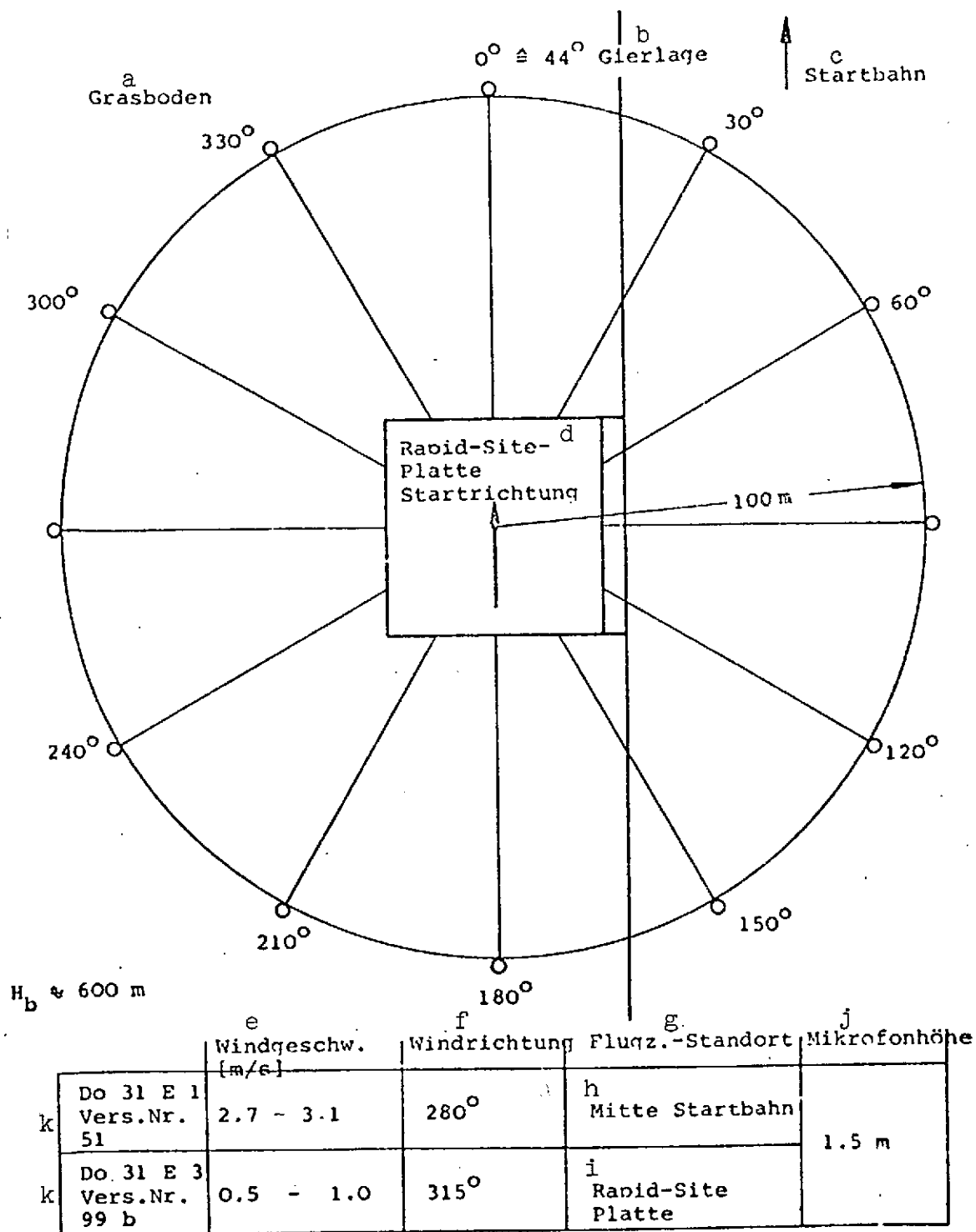


Fig. 3.2.1-1. Plan of measurement points for Do 31 far field sound tests.

Key: a. Grass-covered area
 b. Yaw
 c. Runway
 d. Rapid site platform, takeoff direction
 e. Wind speed
 f. Wind direction

g. Aircraft location
 h. Center of runway
 i. Rapid site platform
 k. Trial No.

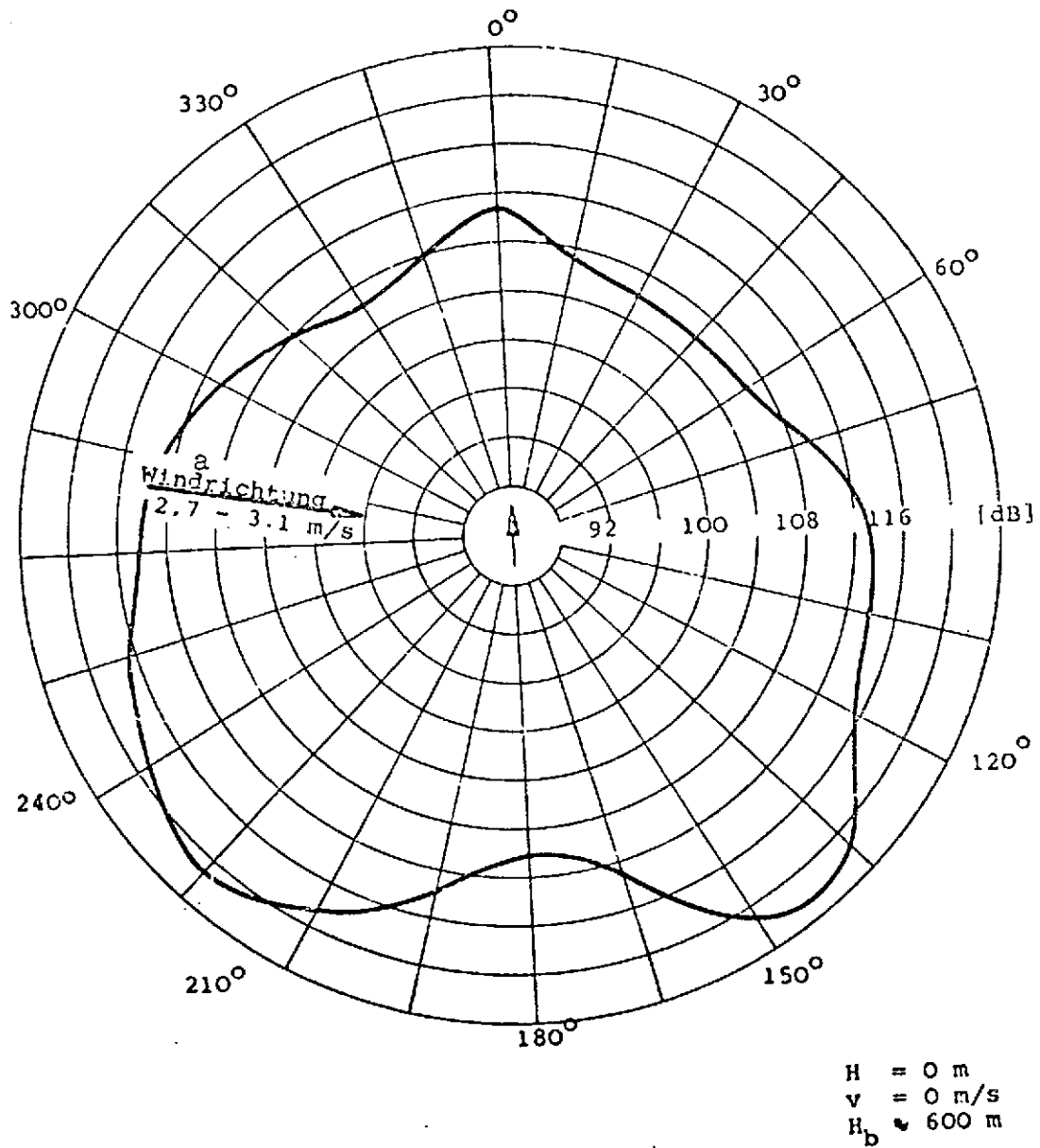
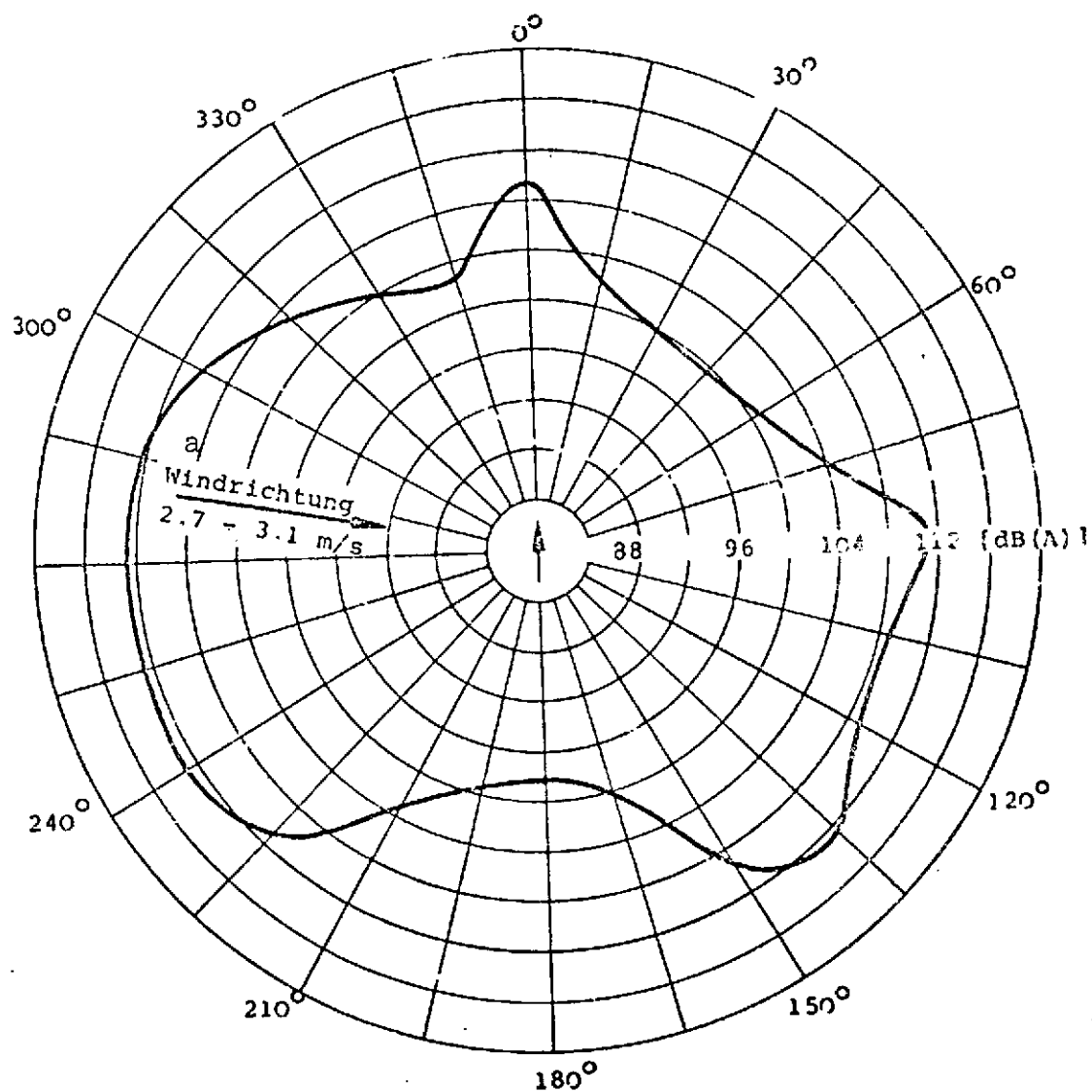


Fig. 3.2.1-2. Do 31 E1 maximum peripheral noise level [dB] at radius of 100 m (two cruising power plants at 89% n_F , nozzle setting -10°).

Key: a. Wind direction



H = 0 m
v = 0 m/s
H_b ≈ 600 m

Fig. 3.2.1-3. Do 31 E1 maximum peripheral noise level [dB (A)] at radius of 100 m (two cruising power plants at 89% n_F , nozzle setting -10°).

Key: a. Wind direction

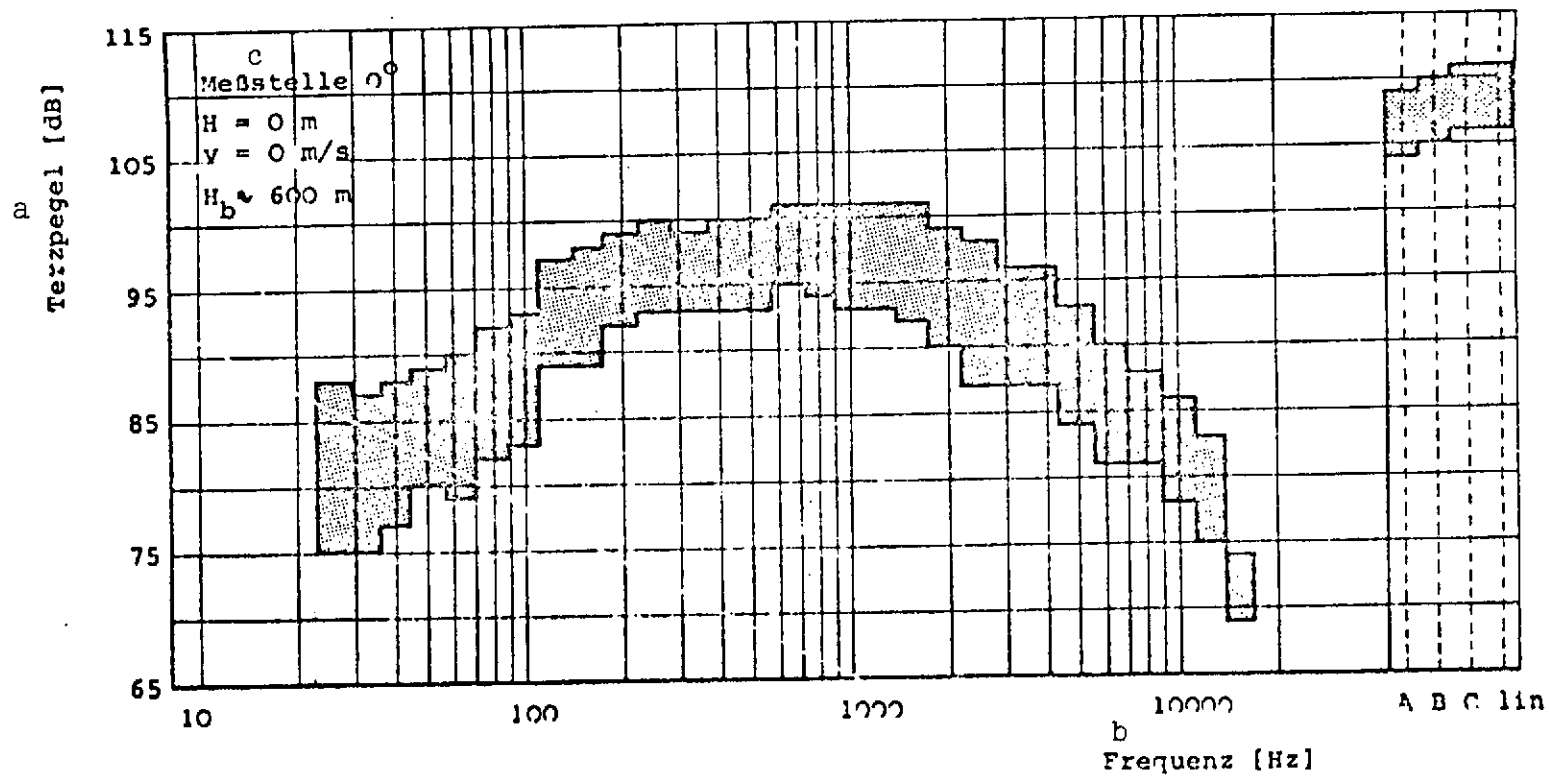


Fig. 3.2.1-4. Measured Do 31 El frequency spectrum at radius of 100 m (two cruising power plants at 89% n_F , nozzle setting -10°).

Key: a. 1/3 octave level
 b. Frequency
 c. Measurement point

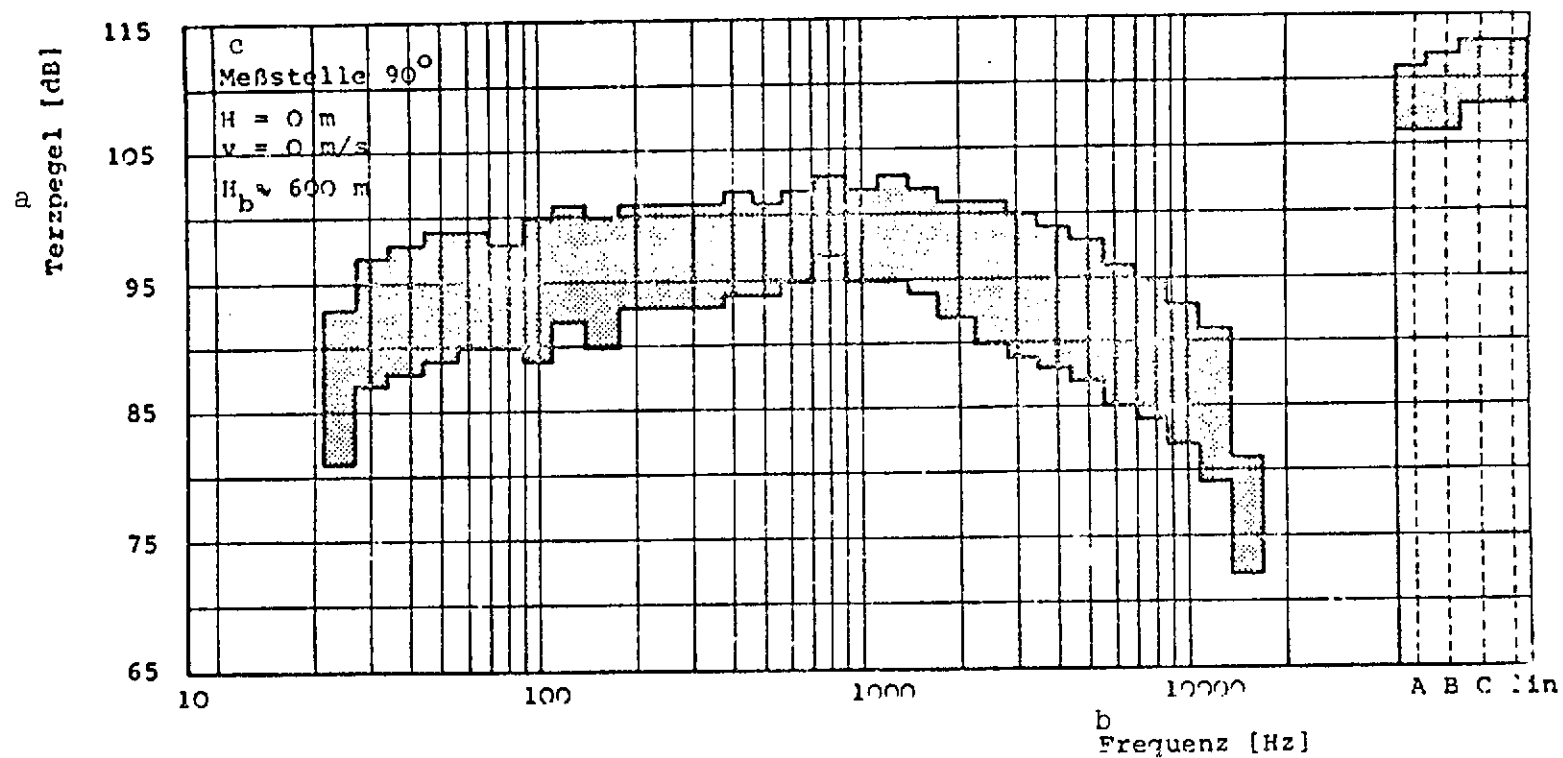


Fig. 3.2.1-5. Measured Do 31 E1 frequency spectrum at radius of 100 m (two cruising power plants at 89% n_F , nozzle setting -10°).

Key: a. 1/3 octave level
 b. Frequency
 c. Measurement point

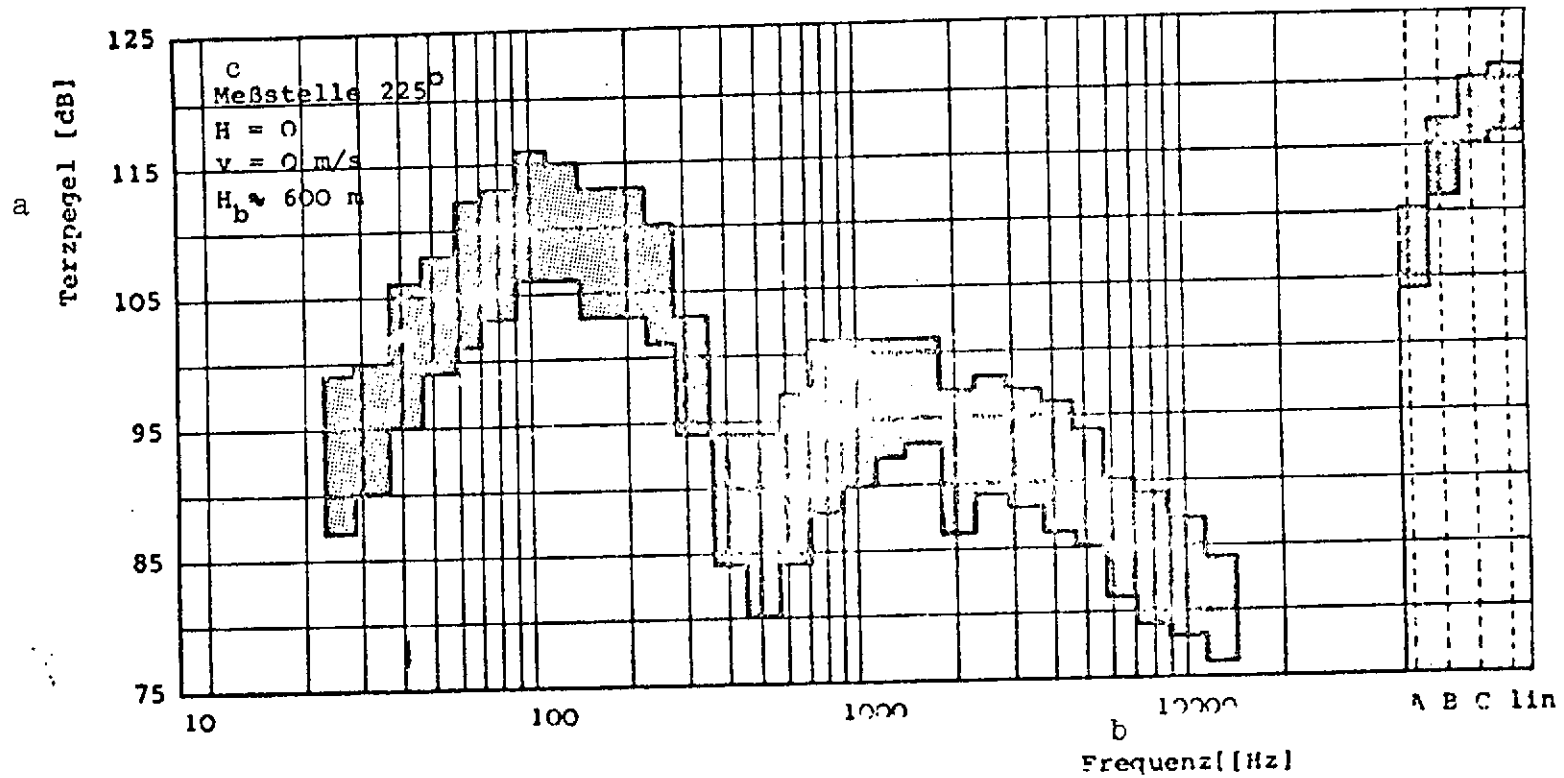


Fig. 3.2.1-6. Measured Do 31 El frequency spectrum at radius of 100 m (two cruising power plants at 89% n_F , nozzle setting -10°).

Key: a. 1/3 octave level
 b. Frequency
 c. Measurement point

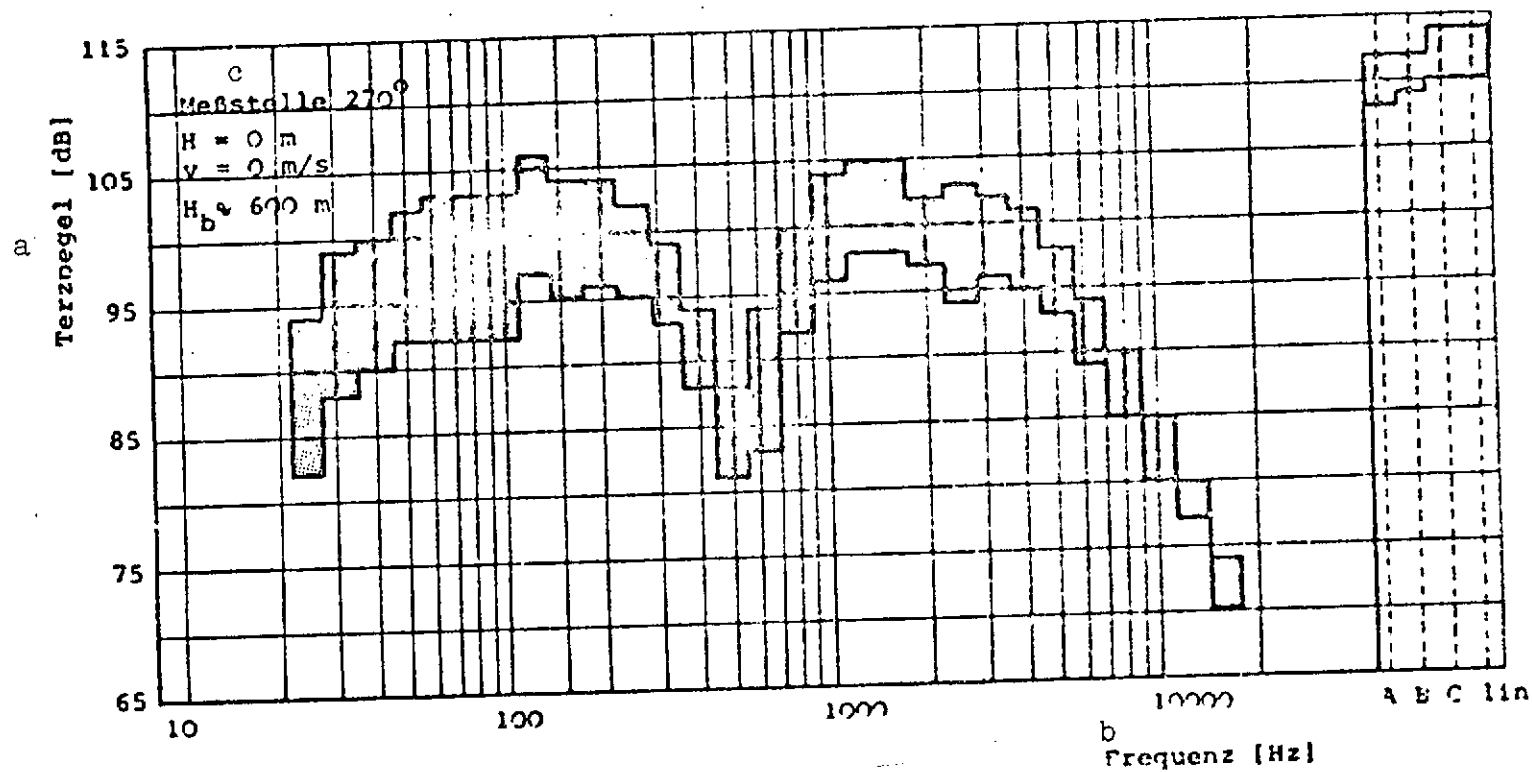


Fig. 3.2.1-7. Measured Do 31 El frequency spectrum at radius of 100 m (two cruising power plants at 89% n_F , nozzle setting -10°).

Key: a. 1/3 octave level
 b. Frequency
 c. Measurement point

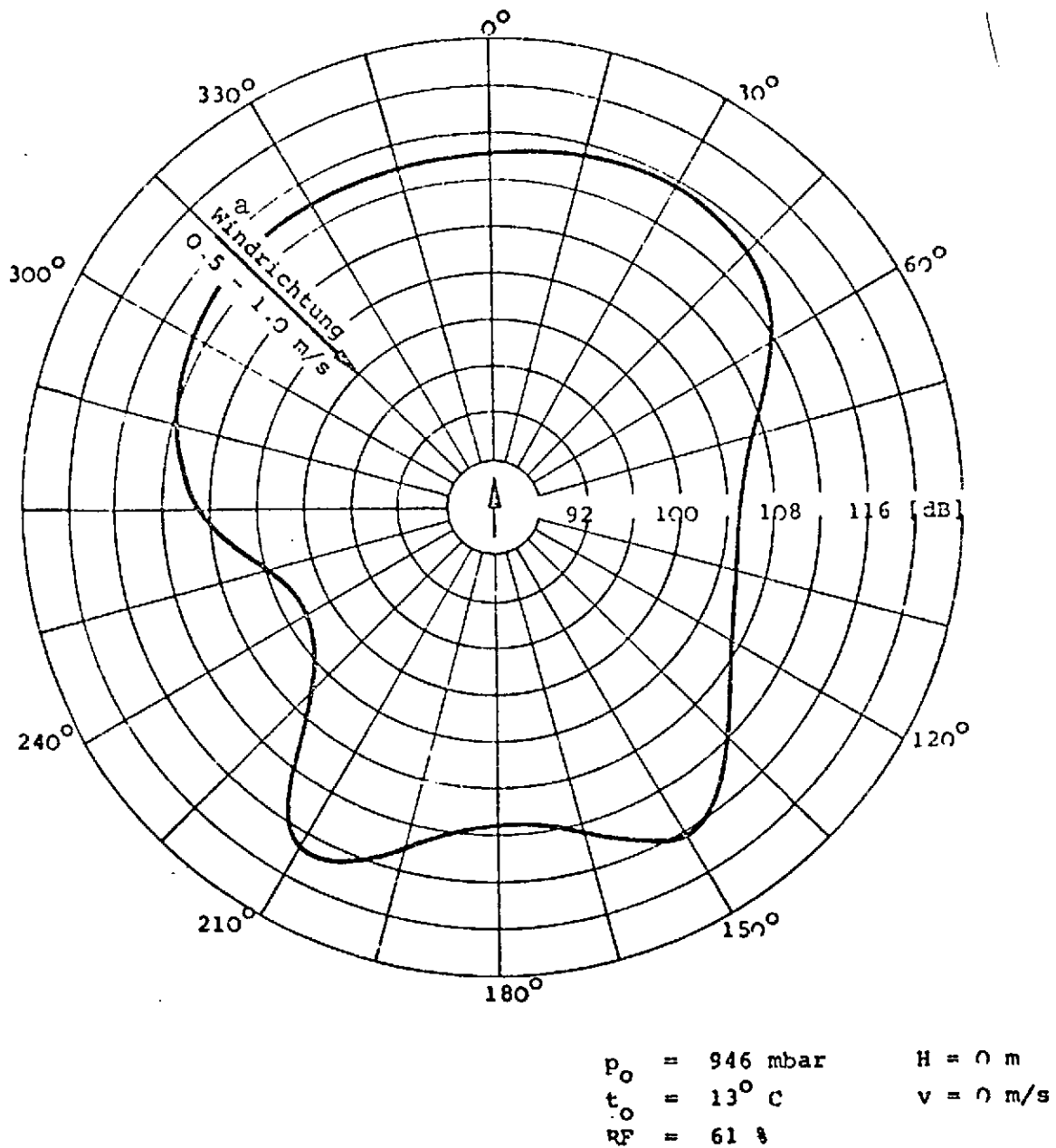


Fig. 3.2.1-8. Do 31 E3 maximum peripheral noise level contours [dB] at radius of 100 m (two cruising power plants at 86% nF, nozzle setting 74°, eight lift power plants at 11,600 - 11,900 rpm).

Key: a. Wind direction

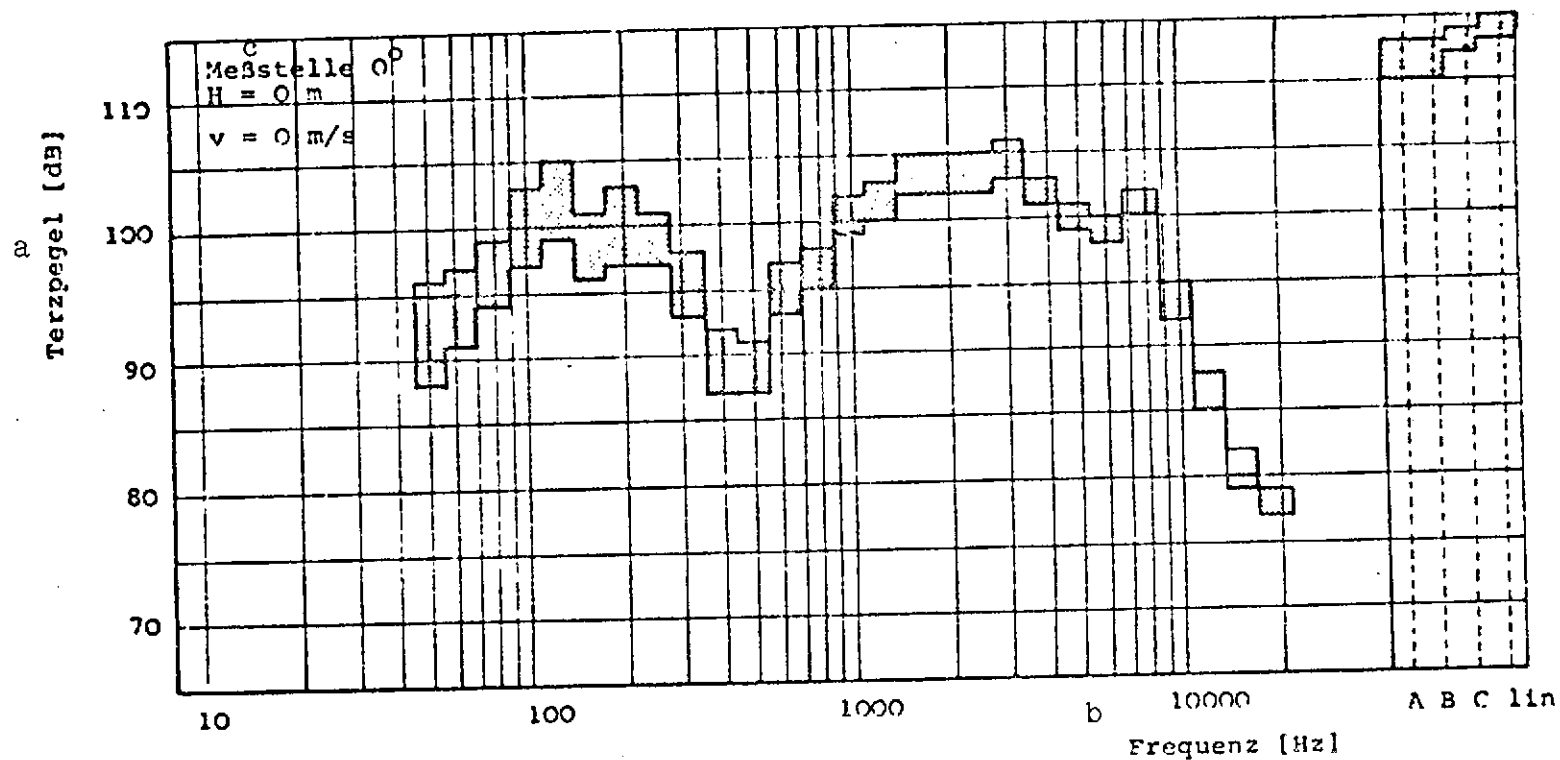


Fig. 3.2.1-9. Measured Do 31 E3 frequency spectrum at radius of 100 m (two cruising power plants at 86% n_F , nozzle setting 74° , eight lift power plants at 11,600 - 11,900 rpm).

Key: a. 1/3 octave level
b. Frequency
c. Measurement point

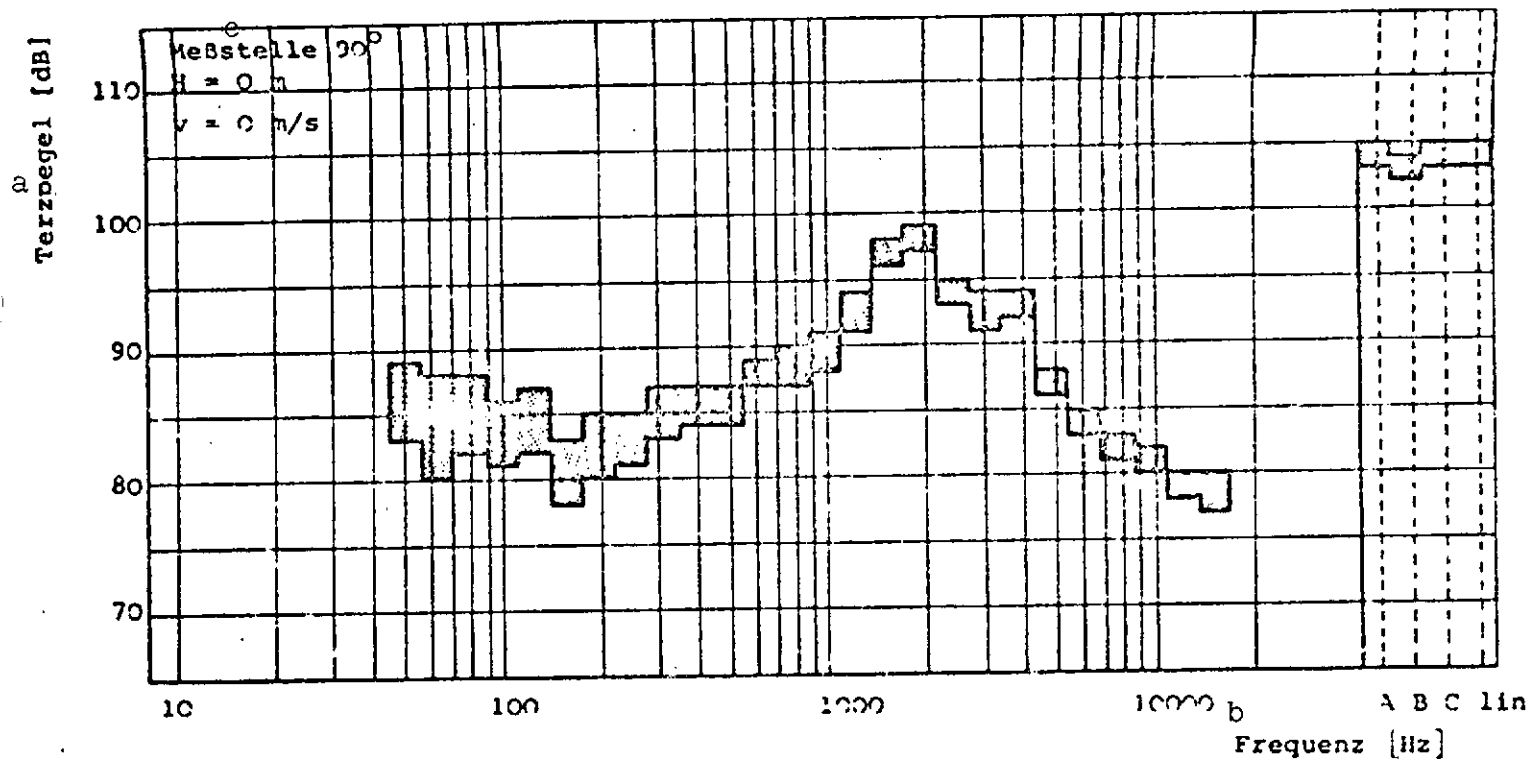


Fig. 3.2.1-10. Measured Do 31 E3 frequency spectrum at radius of 100 m (two cruising power plants at 86% n_F , nozzle setting 74° , eight lift power plants at 11,600 - 11,900 rpm).

Key: a. 1/3 octave level
 b. Frequency
 c. Measurement point

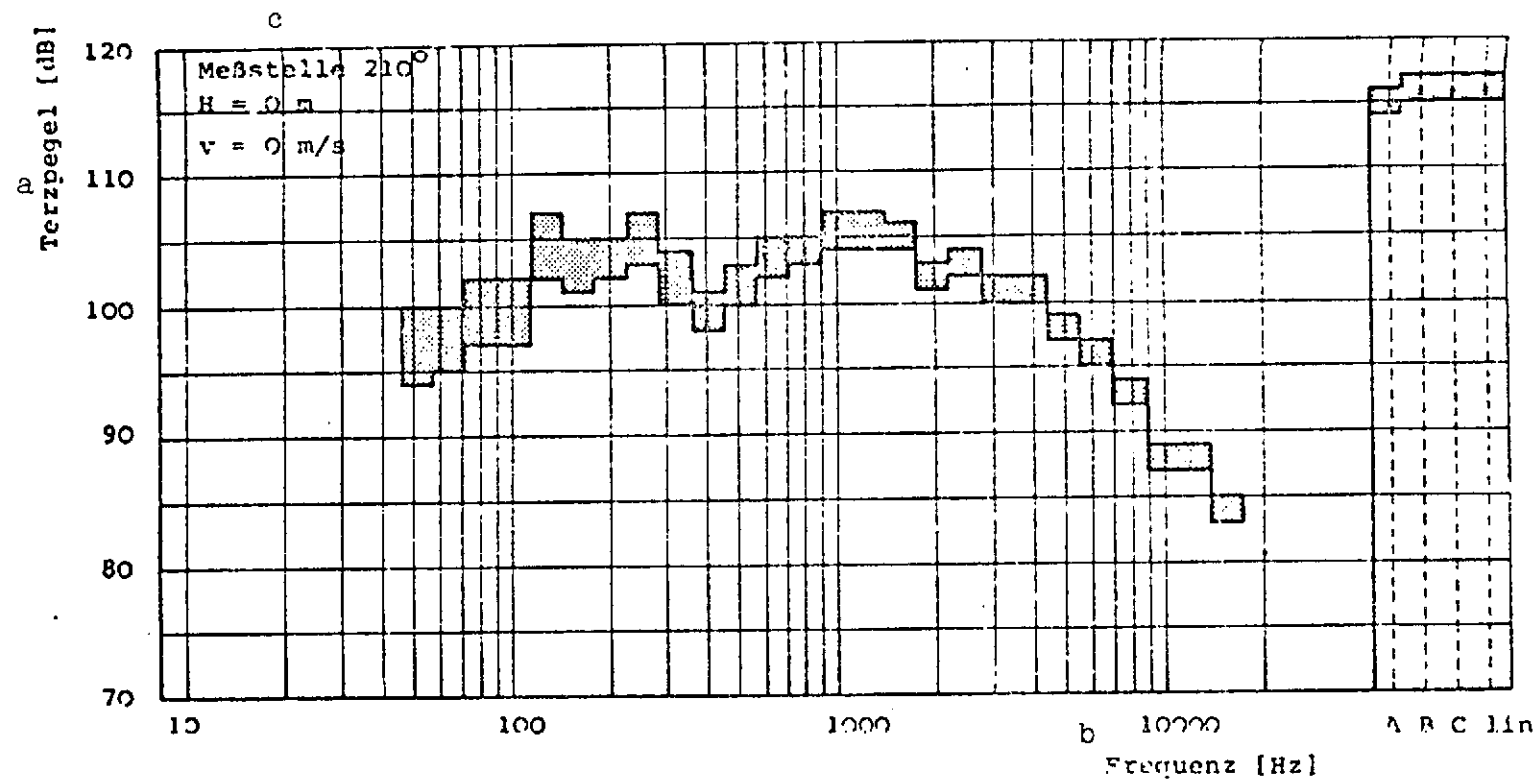
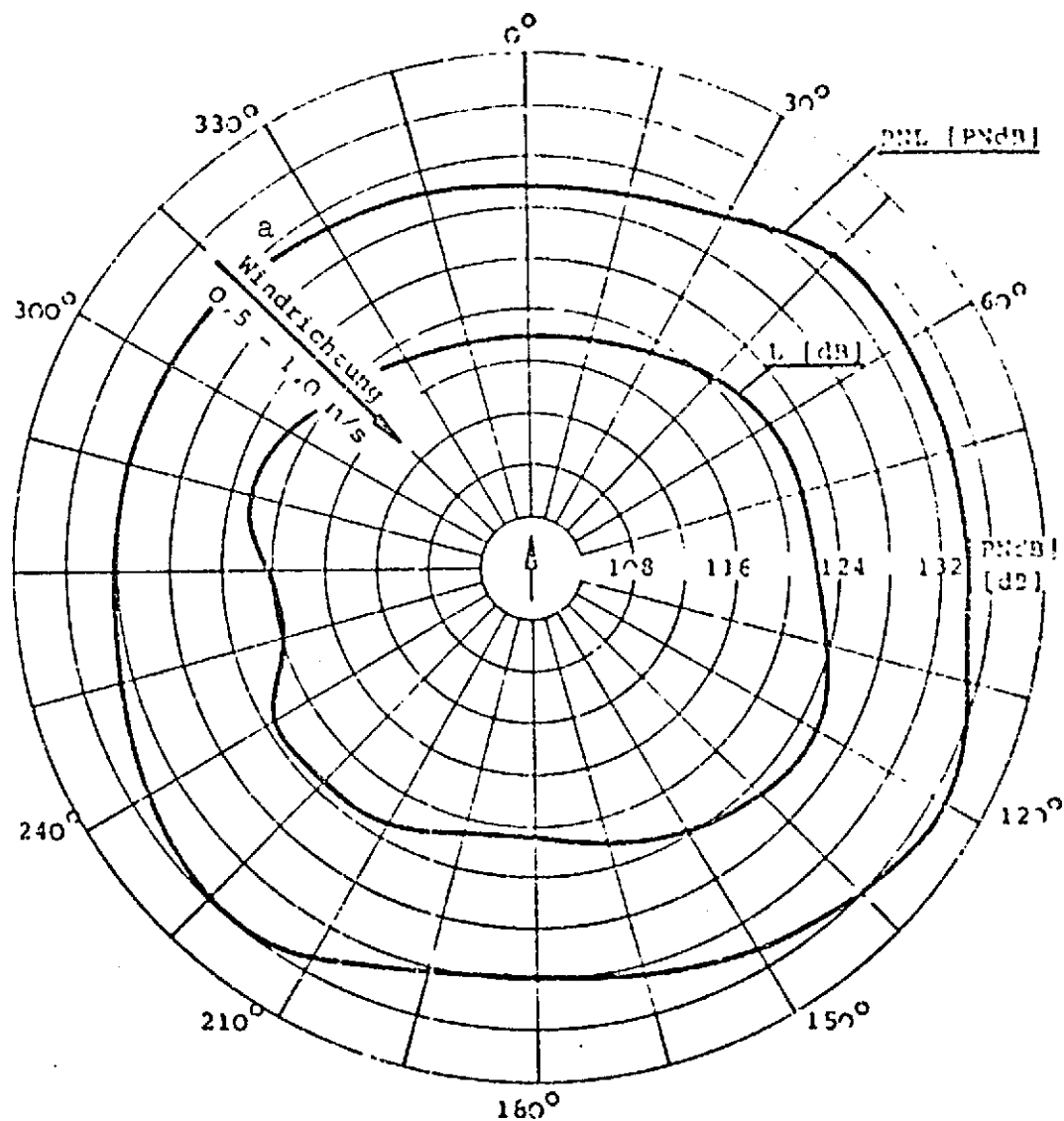


Fig. 3.2.1-11. Measured Do 31 E3 frequency spectrum at radius of 100 m (two cruising power plants at 86% n_F , nozzle setting 74°, eight lift power plants at 11,600 - 11,900 rpm).

Key: a. 1/3 octave level
b. Frequency
c. Measurement point



P_0	= 940 mbar	H	= 30,5 m
t_0	= 13°C	v	= 0 m/s
RF	= 61 s	R	= 100 m

Fig. 3.2.1-12. Do 31 E3 maximum peripheral noise level (hovering) (two cruising power plants at 72-78% n_F , nozzle setting 98°, eight lift power plants at 11,700 rpm).

Key: a. Wind direction

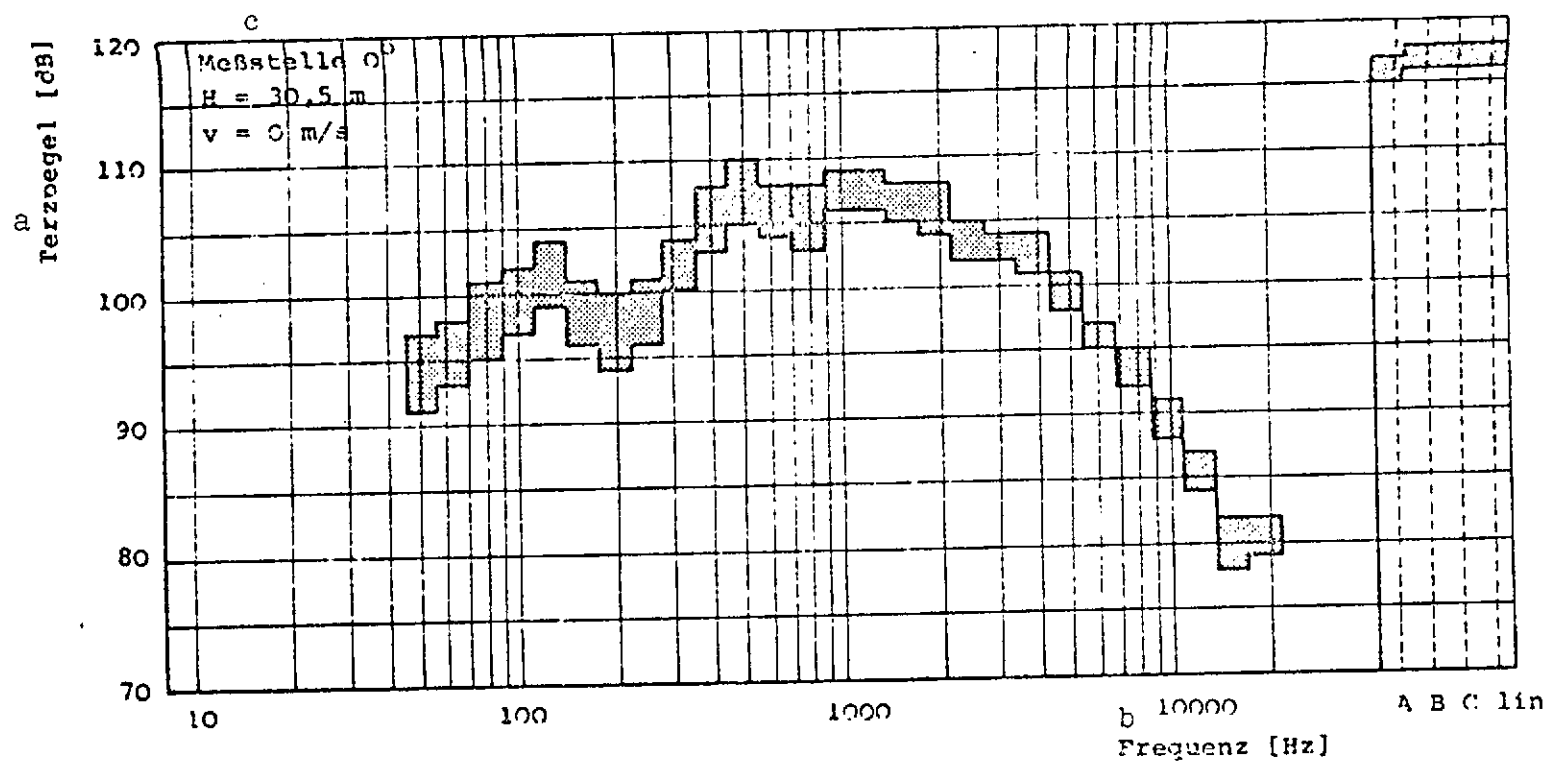


Fig. 3.2.1-13. Measured Do 31 E3 frequency spectrum at radius of 100 m (two cruising power plants at 72-78% n_F , nozzle setting 98°, eight lift power plants at 11,600 - 11,700 rpm).

Key: a. 1/3 octave level
 b. Frequency
 c. Measurement point

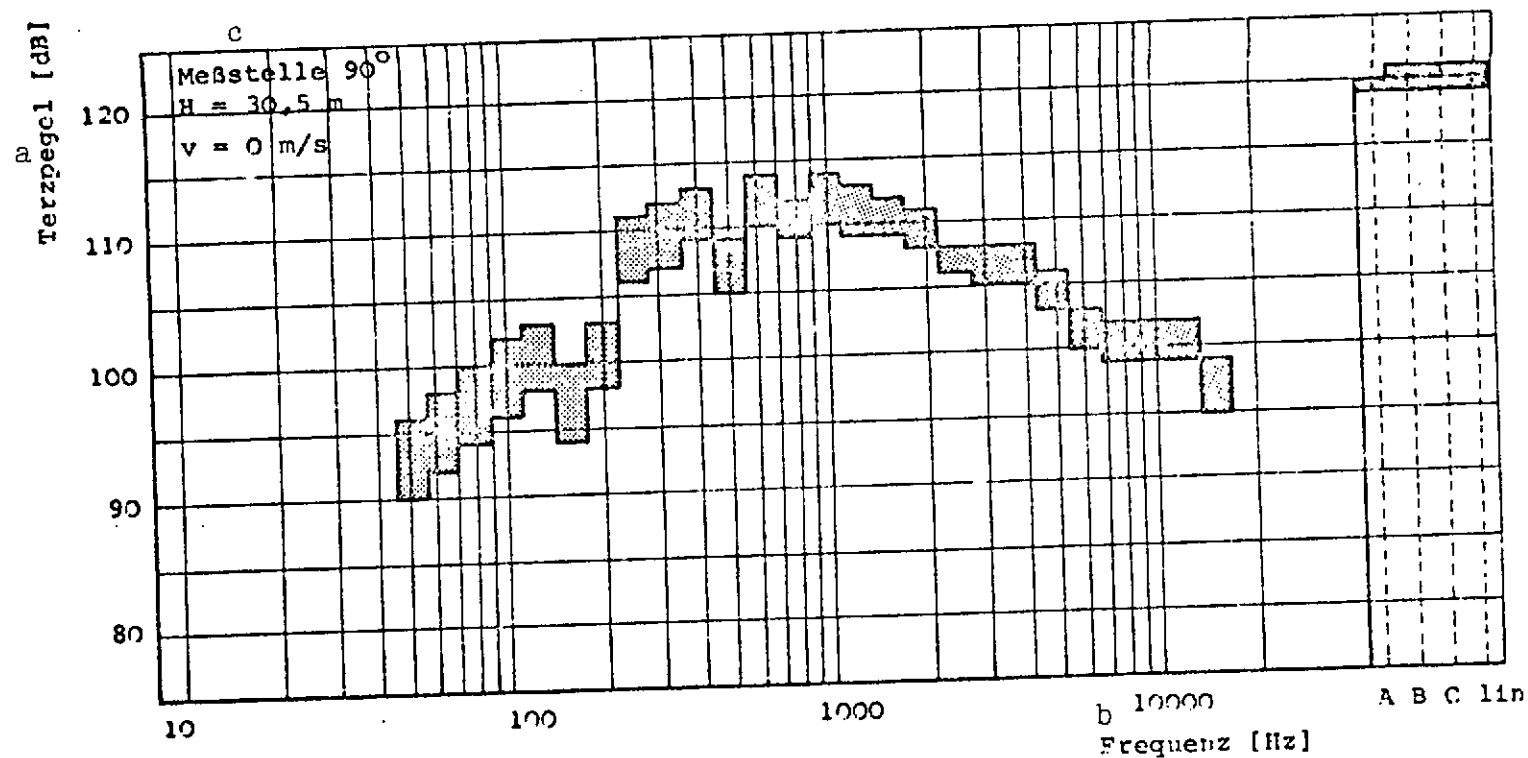


Fig. 3.2.1-14. Measured Do 31 E3 frequency spectrum at radius of 100 m (two cruising power plants at 72-78% n_F , nozzle setting 98°, eight lift power plants at 11,600 - 11,700 rpm).

Key: a. 1/3 octave level
b. Frequency
c. Measurement point

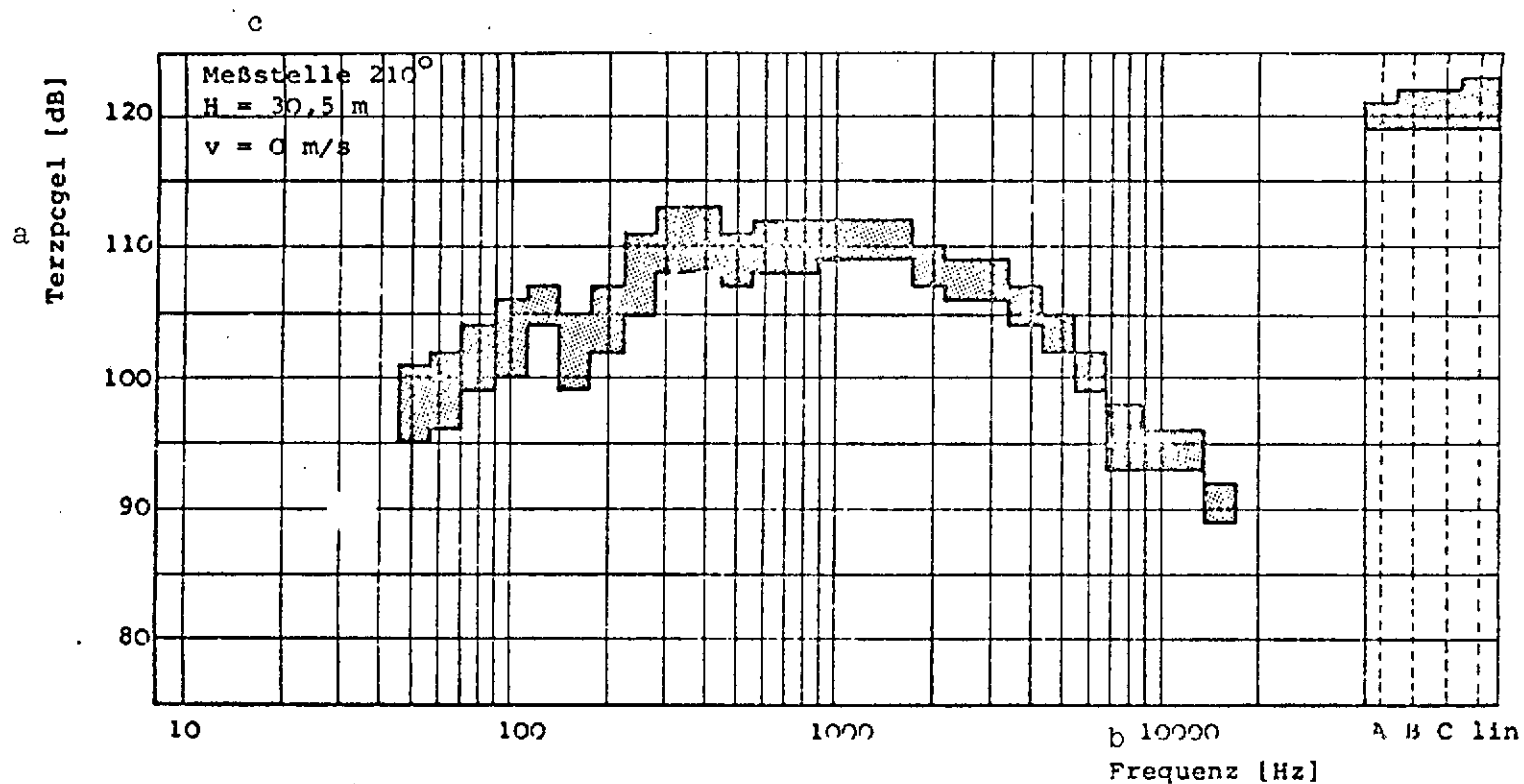


Fig. 3.2.1-15. Measured Do 31 E3 frequency spectrum at radius of 100 m (two cruising power plants at 72-78% n_F , nozzle setting 98°, eight lift power plants at 11,600 - 11,700 rpm).

Key: a. 1/3 octave level
b. Frequency
c. Measurement point

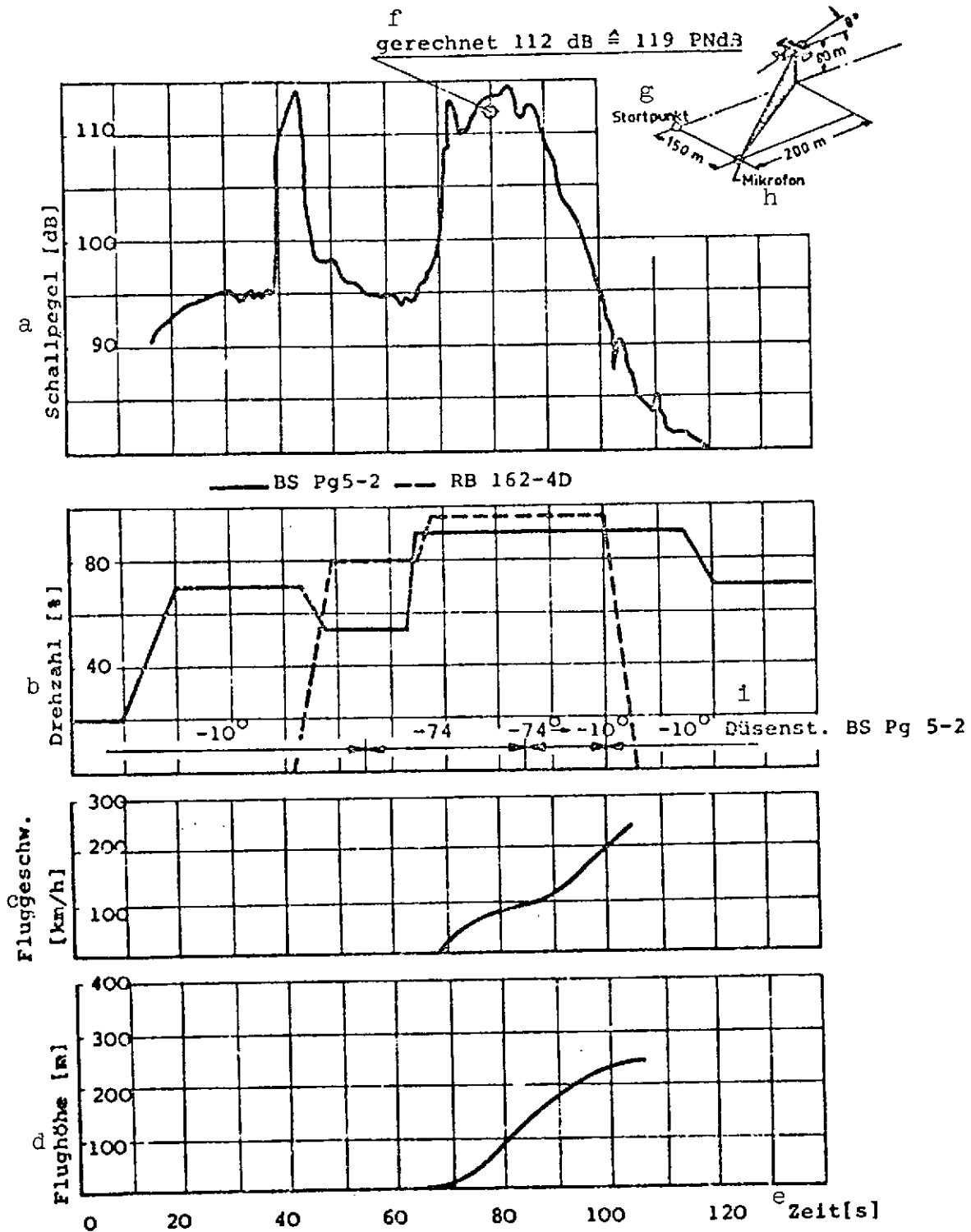


Fig. 3.2.2-1. Do 31 E3 noise level curves vs. time for a takeoff transition (trial 77) (microphone position 150 m to the side of takeoff point).

Key: a. Noise level; b. Engine speed; c. Aircraft speed; d. Altitude; e. Time; f. Calculated; g. Takeoff point; h. Microphone; i. Nozzle setting

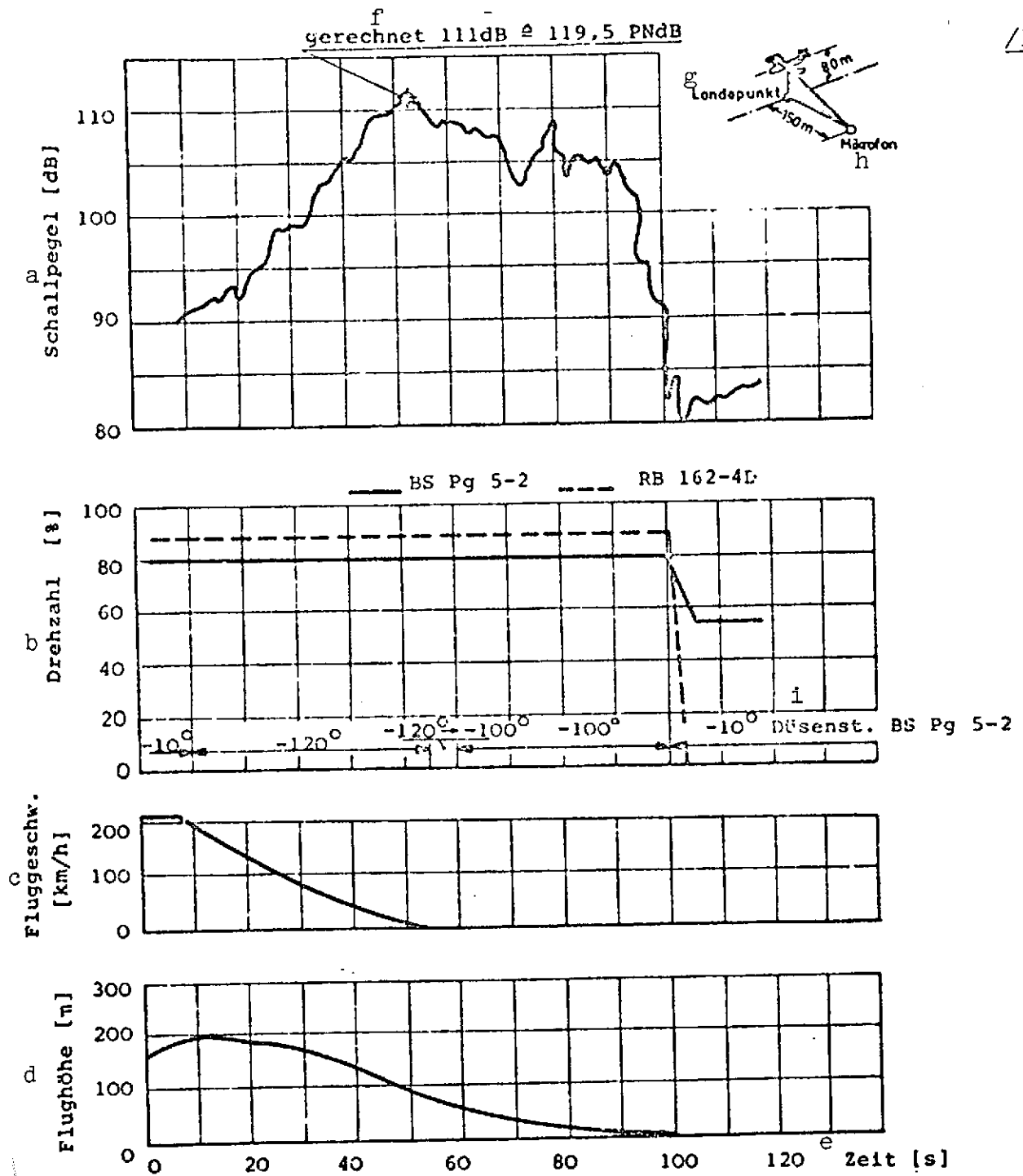


Fig. 3.2.2-2. Do 31 E3 noise level curves vs. time for a landing transition (trial 77) (microphone position 150 m to the side of takeoff point).

Key: a. Noise level; b. Engine speed; c. Aircraft speed; d. Altitude; e. Time; f. Calculated; g. Landing point; h. Microphone; i. Nozzle setting

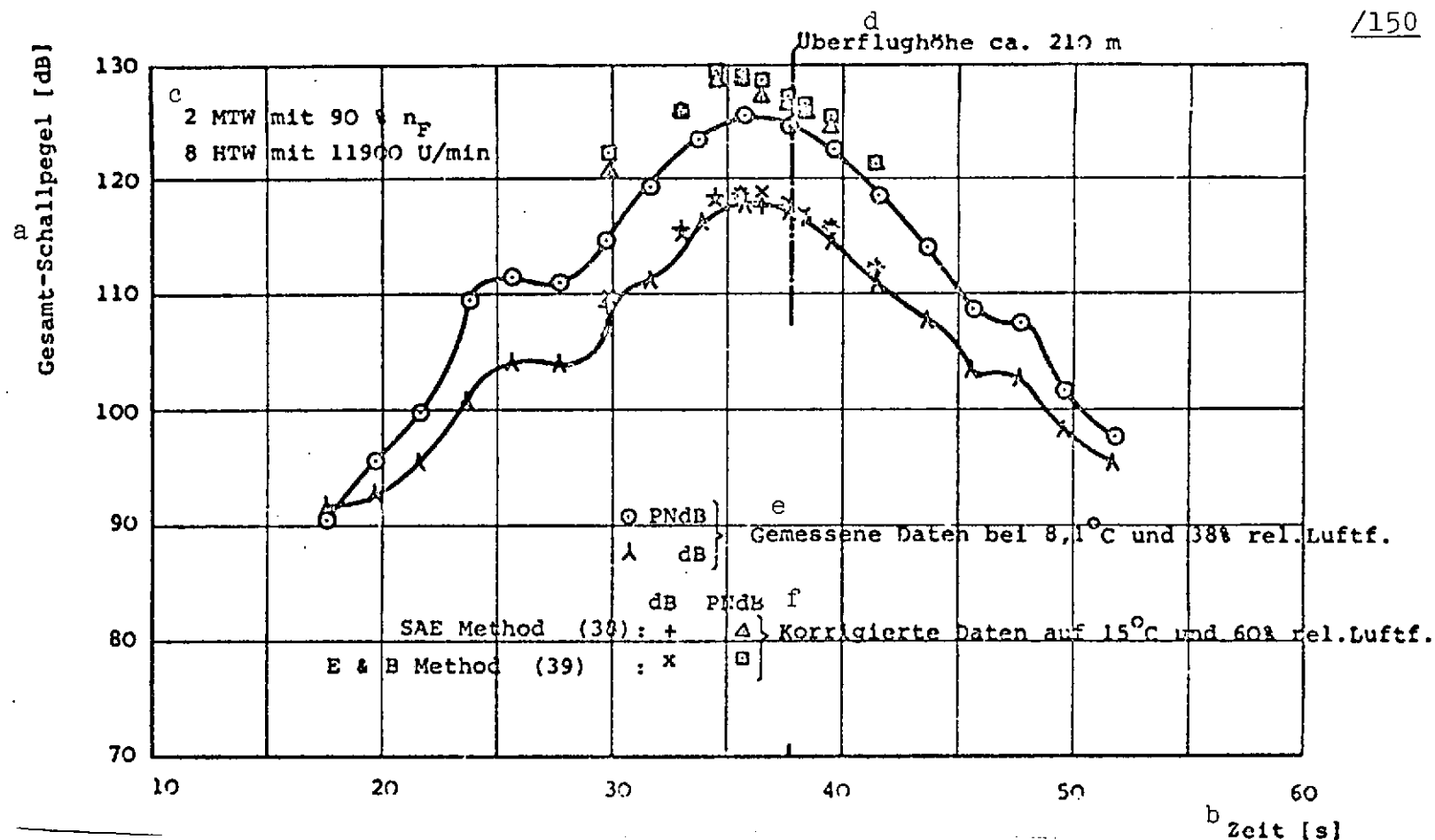


Fig. 3.2.2-3. Do 31 E3 noise level curves vs. time for a takeoff transition (trial 77) (microphone position 460 m from takeoff point, under flight path).

- Key:
- a. Overall noise level
 - b. Time
 - c. Two cruising power plants at 90% n_F ,
eight lift power plants at 11,900 rpm
 - d. Flyover altitude
 - e. Data taken at 8.1°C and 38% rel. humidity
 - f. Data corrected to 15°C
and 60% rel. humidity

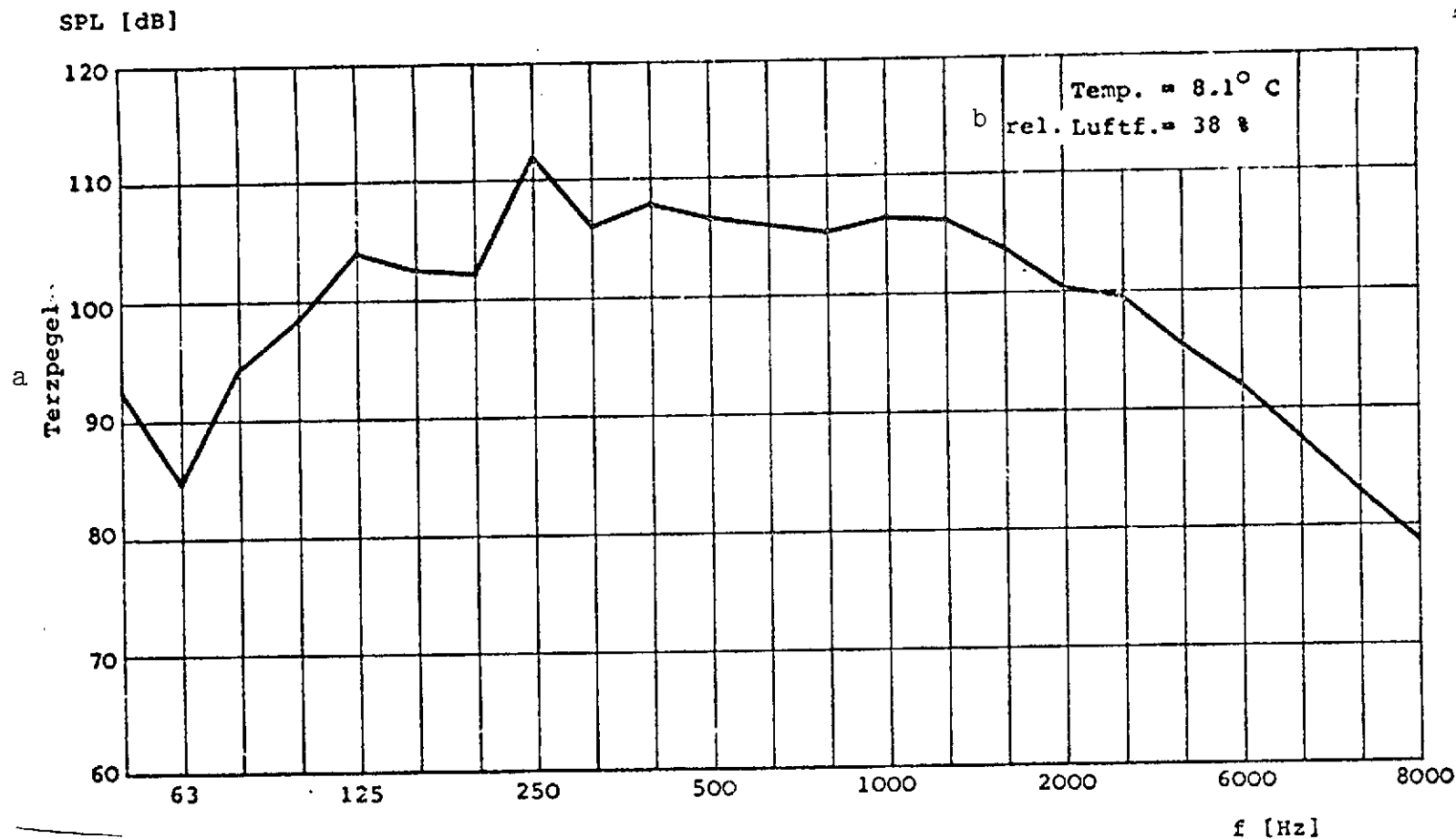


Fig. 3.2.2-4. Measured Do 31 E3 frequency spectrum at time of maximum noise level (takeoff transition, trial 77) (microphone position 460 m from takeoff point, under flight path; flyover altitude about 210 m).

Key: a. 1/3-octave level
b. Rel. humidity



Key: a. Overall noise level
b. Time
c. Two cruising power plants at 80% nP,
eight lift power plants at 11,000 rpm
d. Flyover altitude

- e. Data taken at 8.1°C and 38% rel. humidity
- f. Data corrected to 15°C and 60% rel. humidity

SPL [dB]

/153

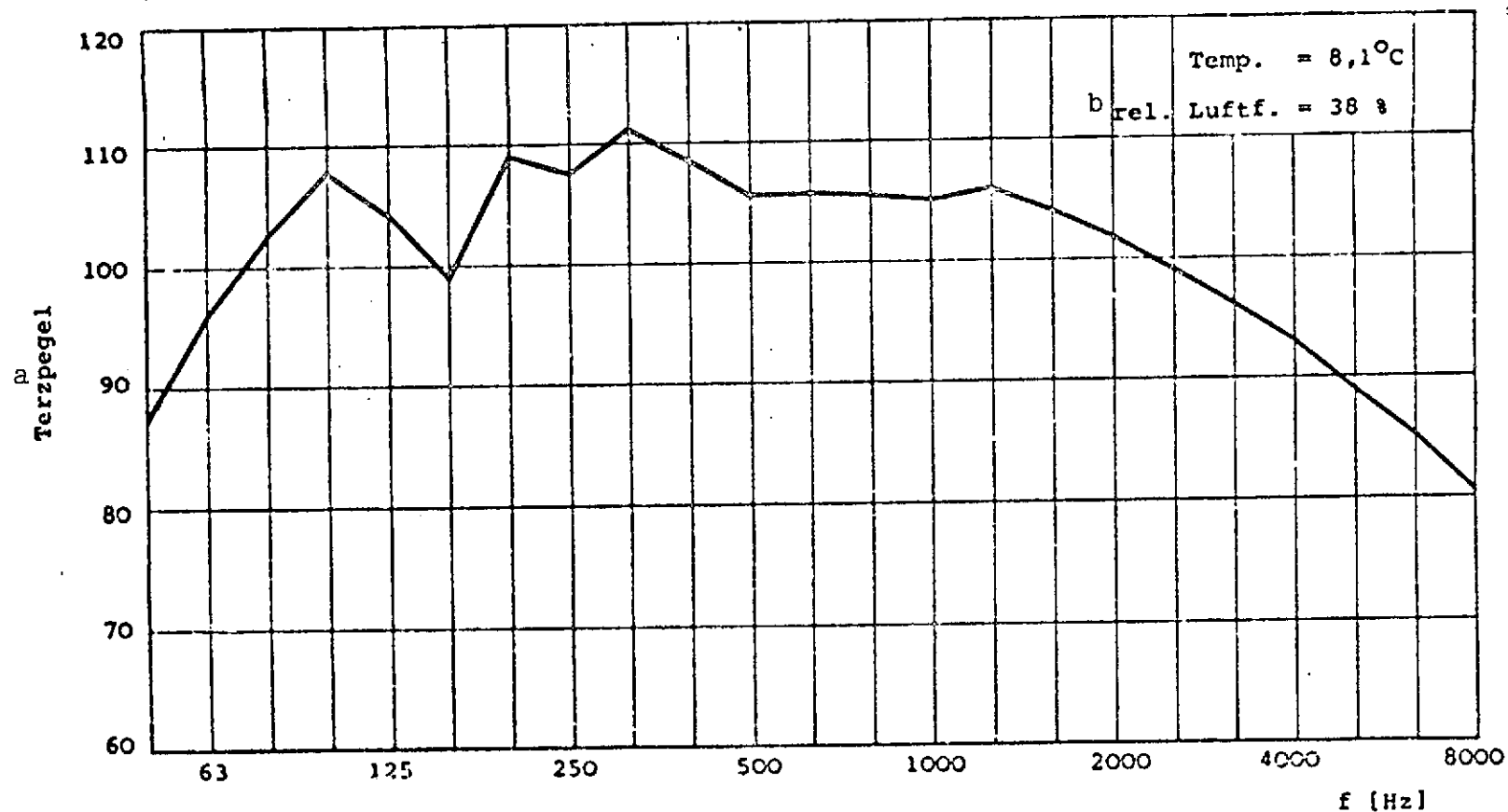


Fig. 3.2.2-6. Measured Do 31 E3 frequency spectrum at time of maximum noise level (landing transition, trial 77) (microphone position 460 m from takeoff point, under flight path; flyover altitude about 180 m).

Key: a. 1/3-octave level
b. Rel. humidity

REFERENCES

1. Smith, M. H.T., "The aero gas turbine noise problem: steps towards a solution," Rolls Royce, lecture to the Belgian Association of Aeronautic and Astronautic Engineers and Technicians (A.B.I.T.A.), Brussels, April 1968. /57
2. Rolls-Royce, "Three shaft turbofan proposals, RB 207-03, " Noise, P.D.S. 38 [sic], Vol. 2, January 1967.
3. Taylor, P. A., Some design considerations for a low noise, direct lift VTOL engine," DGLR Sympos., Munich, Oct. 1970.
4. Bartels, Burkhardt, Dittmar, Scholten, and Zink, "Studies on sound radiation from fan power plants and noise abatement measures," ZTL-Fag 4, final report, 1970, Do 4.01 b.
5. Bartels, P. and Burkhardt, H., "Generation of sound by fan power plants and its abatement," ZTL-Fag, 4, final report 1971, Do. 4.10.
6. Kryter, K. D. and Pearsons, K. S., "Modification of Noy Tables," JASA 36 (Feb. 1964).
7. Snaith, J., "Pegasus 5 noise levels," Rolls-Royce Memorandum, /58 February 12, 1968, Ref. SGH/JDV/26696, unpublished.
8. Denning, R. M., "Pegasus 5 exhaust noise," Rolls-Royce Memorandum, July 27, 1968, Ref. SGH/Dng/26778, unpublished.
9. "Pegasus 5 peak PNdB at 500 ft linear," Rolls-Royce T.E.D. 58590/1, October 7, 1968, unpublished.
10. Brooks, J. R, "Pegasus 5 in Dornier Do 31 aircraft," Rolls-Royce Memorandum, October 10, 1968, unpublished.
11. Greatrex, F. B., "Bypass engine noise," SAE Meeting, April 1960.
12. Szlenkier, T. K., et al., "Initial studies of jet lift systems with fan-like exhaust characteristics for V/STOL transport aircraft," AGARD CP 22, 1967.
13. Coles, W. D., et al., "Turbojet engine noise reduction with mixing nozzle-ejector combinations," NACA TN 4317, August 1958.
14. Large-scale ejector tests by Hawker Siddeley Aviation, unpublished results, 1969. /59

- 5. Bartels, P., Scholten, R., et al., "Determination of noise level contours in free flight field," Do Report 65/19, Nov. 1965, unpublished, study contract T I 3-56-403-K-402 from the Federal Ministry of Defense.
16. Lighthill, M. J., "On sound generated aerodynamically. II. Turbulence as a source of sound," Proc. Roy. Soc. A. 222 (1954).
17. Dornier AG, "Determination of the reflection effect of a shell on the level of sound in a free field," Test Report VD 508-B 1, 1966, unpublished.
18. Dornier AG, "Study of the thermal and acoustic stability of Do 31 airframe components," Test Report VS 382-B 1, Feb. 1964, unpublished.
19. Dornier AG, "Jet noise measurements taken during Do 31-2B tail control nozzle testing," Test Report VW 394-B 6, June 1965, unpublished.
20. Dornier AG, "Do 31 study of the rigidity of primary landing gear doors," Test Report VS 443-B 2, Feb. 1966, unpublished.
21. Dornier AG, "Do 31 sound transmission measurements performed on an isolated segment of fuselage skin," Test Report VS 452-B 1, July 1966, unpublished. /60
22. Dornier AG, "Study on V/STOL transport aircraft: sound transmission tests for designing the most desirable fuselage lining," Test Report VD 518-B 1, Sept. 1967, unpublished.
23. Dornier AG, "Do 31 near field and far field sound measurements," Test Report VS 571-B 1, May 1968, unpublished.
24. Noise level data from Deutsche Lufthansa AG relating to overall VTOL requirements of the Lufthansa/Bundeswehr request for bids, letter of July 30, 1969.
25. Bartels, P., Kaufmann, D., Scholten, R., and Wichert, B., "Calculation of sound levels for an airliner of the Trident type and the Do 31 E3 VTOL aircraft," Contract III B 4-420-01-5/68, Oct. 1968, from the Federal Minister of Public Health.
26. Coles, G. M., "Estimating jet noise," Aeron. Quarterly 14 (Feb. 1963).

27. Kobrynski, M., "General method for calculating the sound pressure field emitted by stationary or moving jets," Onera T.P. 578, 1968. /61
28. Bartels, P., Deschler, R., and Wichert, B., "Program for calculating sound propagation, weighting and ground level contours," Dornier AG computer program, unpublished.
29. Bishop, D. E., "Noise contours for short- and medium-range transport aircraft and business aircraft," Techn. Rep. FAA-ADS-35, March 1965.
30. "Land use planning with respect to aircraft noise," Air Force Manual No. 86-5, Oct. 1964.
31. Scholten, R. and Flemming, M., "Present and future noise problems in VTOL engineering with respect to experience obtained with the Dornier Do 31 VTOL jet transport aircraft," paper for conference on noise at Wiesbaden on March 18, 1969.
32. "VTOL boom throughout the world," Der Flieger 50(2/3) (Feb./March 1970).
33. Dornier AG, "Do 231 project study as part of Lufthansa/Bundeswehr request for bids for a V/STOL airliner/transport aircraft," Section 4.5: "Noise and Vibration."
34. Dornier AG, "Do 31 E1 far field (100 m) sound measurements," Memorandum EV-31/215, Jan. 1968, unpublished. /62
35. Dornier AG, "Do 31 near field and far field sound measurements," Test Report VS 571-B 2, August 1968, unpublished.
36. Bayerdörfer, G., "Do 31 E3 far field sound measurements," Dornier Memorandum EV-31-237, April 1968, unpublished.
37. "Installation noise report," INR. 90002, Rolls-Royce.
38. Society of Automotive Engineers, "Standard values of atmospheric absorption as a function of temperature and humidity for use in evaluating aircraft flyover noise," SAE ARP 866, August 1964.
39. Evans and Bazley, "The absorption of sound in air at audio frequencies," Acoustica 6 (1956).